THE ROLE OF INTEGRIN-LINKED KINASE IN GLIOBLASTOMA MULTIFORME AND ITS POTENTIAL FOR TARGETED THERAPY

by

LINCOLN A EDWARDS

B.Sc. (Hons),
York University, 1999

A THESIS SUBMITTED IN PARTIAL FULFILLMENT OF THE REQUIREMENTS FOR THE DEGREE OF

DOCTOR OF PHILOSOPHY

in

THE FACULTY OF GRADUATE STUDIES

(Pathology and Laboratory Medicine)

THE UNIVERSITY OF BRITISH COLUMBIA

September 2005

ABSTRACT

Integrin-linked kinase (ILK) is a serine/threonine kinase that has been shown to be involved or implicated in diverse disease processes ranging from Alzheimer's disease to cancer. The involvement of ILK in cancer has been associated with its uncontrolled activation within cells due to the loss of its regulator, the tumor suppressor gene *PTEN*. Cellular events are tightly regulated by the actions of PTEN which can inhibit ILK activity. The focus of my thesis is to evaluate the role of ILK in glioblastoma cell lines and *in vivo* models derived from these cell lines. Three key questions were addressed: (i) Does ILK play a role in cancer progression in PTEN null glioblastoma cell lines? (Chapter 3) (ii) Given that combination therapy will provide optimal therapeutic results, what rationally chosen agents could be used in combination with an ILK inhibitor? (Chapters 4) And (iii) Is ILK a possible therapeutic target for the treatment of glioblastoma multiforme? (Chapters 5). It was hypothesizd that ILK is constitutively active in glioblastoma multiforme due to the high frequency of *PTEN* loss within this cancer and that targeting ILK alone and in combination would result in either tumor growth delay or cell death. Results from Chapter 3 indicate that ILK activity is elevated with loss of *PTEN* and verify ILKs role as an intermediate between PTEN regulation and PKB/Akt activation in glioblastoma cancer cells. Targeting ILK with an antisense oligonucleotide *in vivo* resulted in a significant tumor growth delay or stable disease ($\leq$7% increase compared to a 100% increase of the saline treated control). Chapter 4 reveals that targeting ILK in combination with one other therapeutic agent (i.e. U0126) not only resulted in better therapeutic activity but that a synergistic combination could be achieved. Chapter 5 examined the effect of ILK targeting on tumor growth and the tumor micro-environment, suggesting that ILK inhibition may have anti-angiogenic, chemo and radiosensitizing effects.

These studies demonstrated the potential of ILK targeting in glioblastoma cancer, an important finding, given that this target had not been previously explored in GBM progression. In addition, the results offer key insights into the anti-tumor effects of targeting ILK alone and in combination as well as its role in the cell signaling pathogenesis in GBMs. These results also lay the foundation for pre-clinical data supporting the further exploration of ILK targeting for clinical use.

TABLE OF CONTENTS

*

LIST OF TABLES

LIST OF FIGURES

ABBREVIATIONS

BCA	Bicinchoninic acid
BSA	Bovine serum albumin
CI	Combination Index
DAPI	4',6-diamidino-2-phenylindole
DMEM	Dulbecco's modified Eagle's medium
DMSO	Dimethylsulfoxide
DNA	Deoxyribonucleic acid
EGFR	Epidermal Growth Factor Receptor
ELISA	Enzyme Linked Immunosorbent Assay
FBS	Fetal bovine serum
GBM	Glioblastoma multiforme
GW5074	(3-(3,5-Dibromo-4-hydroxy-benzylidene)-5-iodo-1,3-dihydro-indol-2-one
HBSS	Hanks balanced salt solution
HIF-1α	Hypoxia inducible Factor-1 alpha
ILK	Integrin-linked kinase
i.p.	Intraperitoneal
i.v.	Intravenous
IC_{50}	The concentration required to achieve 50% inhibition in cell proliferation
MAPK	Mitogen Activating Protein Kinase
MMAC1	Mutated in Multiple Advanced Cancers
MTD	Maximum tolerable dose
MTT	3-[4,5-dimethylthiazol-2-yl]-2,5-diphenyl tetrazolium bromide
MW	Molecular weight
ODN	Oligonucleotides
PAGE	Polyacrylamide gel electrophoresis
PBS	Phosphate buffered saline
PDGFR	Platelet Derived Growth Factor Receptor
PI3K	Phosphatidylinositol-3'-kinase

PI(3,4,5)P3	Phosphatidylinositol-3,4,5-triphosphate
PKB	Protein Kinase B
p.o.	per os (by mouth)
PS	Phosphatidylserine
PTEN	Phosphatase and Tensin Homologue
QD	quaque die (daily)
RAG-2M	Recombination Activation Gene
RPM	Revolutions per minute
S.D.	Standard deviation
SDS	Sodium dodecyl sulphate
S.E.M.	Standard error of the mean
TMA	Tissue Microarray
TUNEL	Terminal deoxynucleotidyl transferase-mediated biotinylated UTP Nick end labeling
VEGF	Vascular Endothelial Growth Factor
WT	Wild type

ACKNOWLEDGEMENTS

I would like to thank my supervisor, Dr. Marcel Bally, for taking a chance on me I couldn't have chosen a better supervisor. Who has shown me by example his passion for the work, and its importance. Your dedication and honesty about your work are truly motivating.

To my supervisory committee Dr.Shoukat Dedhar, Dr. Brian Thiessen, Dr. William Jia, for all your advice.

A special thanks to all those who have helped me and without which I would not have made it this far. To Yanping Hu, Gigi Chiu, Euan Ramsay, Gwyn Bebb, Spencer Kong, Ludger Ickenstein, Sharon Johnstone, Maggie Li, Nancy Dos Santos

Also special thanks to those who were there to make my experience so rewarding when I was here and in TO. Thank you-I really appreciated it. Sunil Varughese (The short list), Pantelis Elinas (the truth hurts), Laura Desjardines (what are you doing?), Sam Forrest, Jenny Forrest, Emerson Headley (From birth, almost impossible), Janet Columa (I don't know where to begin-but you were there), Janet Woo, Nancy Dos Santos, Richard Neufville (your never home), Annie Neufville (thanks for showing me how you did it), Malcolm Wilson, Aunt Beryl, Ian Wilson (wouldn't have be here without your friendship) Aunt Concie, Uncle Barry, Mrs Lewis and cousins (love those Christmas dinners with you guys), My sister and my wonderful nephews and neice. Tansel Kilijcarson (For telling me how to do this). Barbara and Sandra Harriot, Annie (you have no idea the example you set)

DEDICATION

To my Mom,

Estella Edwards

We did it Mom!

This would not have been possible without your love, support and belief in me,

and to one of my best friends Sam Forrest

Sam I wish you were here to see this (Sigourney)

CHAPTER 1

OVERVIEW

The ability of living cells to sense, process, respond and adapt to their surroundings is achieved by intricate cellular communication ranging from extracellular to intracellular to intercellular. Despite what is a complicated network of communication, these cell signals that are essential for movement, thought, behavior, development, and response to disease or injury are tightly regulated. This is no more evident than within the central nervous system. The brain is responsible for everything from movement to cognition and all of these activities require cell communication. It has been well established that cells are not only self sufficient entities, but they also function as "microsocieties" that require group coordination to elicit and emit precise cellular signals. Dysregulation of cell signaling pathways within the brain can ultimately result in brain cancer and death. To this end, it has become important to decipher cell signaling pathways in brain cancer to provide better insight into this disease process. Decoding the molecular basis for cell signals not only improves our fundamental understanding of normal biological functions, but also has the potential to offer new treatment options for diseases resulting from improper cell signal communication.

1.1. Brain Cancer

Brain cancer can exists in two forms, primary brain tumors or secondary brain tumors. Primary brain tumors originate *de novo* from central nervous system cells such as glioblastoma multiforme (GBM) with an overall incidence rate of gliomas per 100,000/year adjusted for the world population being higher in men (3.32) than women (2.24) [1]. In the US alone approximately 15,000 patients will die from primary brain tumors (CBTRUS 2002) per year.

Grade I or grade II astrocytomas classified by the World Health Organization (WHO), are primary brain tumors. Secondary brain tumors are the product of metastasis from a primary cancer elsewhere within the body (e.g. lung, breast cancer). Malignant astrocytomas (GBM), the most common subtype of primary brain tumors, are highly invasive and destructive tumors which can lead to significant neurological impairments such as paralysis, changes in cognition, vision, seizures and stroke. Signs and symptoms associated with a brain tumor largely depend on their location, size and biological growth rate. The symptoms are usually progressive unless the first symptom is a seizure. Patients with a primary brain tumor rarely undergo symptoms such as weight loss, fever, chills and night sweats common of other tumor types such as lymphoma [2]. Prognosis also appears to get worse with increasing age at time of onset (see Figure 1.1).

Initially, the field of neuro-oncology appeared hopeful with the first brain tumor surgery performed in the 19th century in 1884 by Rickman Godlee [3]. However, this quickly dissipated after it became clear that patients were not cured by surgery and survival was only marginally prolonged. In an attempt to improve patient outcome to surgery, Harvey Cushing, proposed a histological grading system, based on morphological differences between cancerous and normal cells within the central nervous system. Dr. Cushing, was able to correlate histological grade to clinical outcome [3].

Figure 1.1

Median Survival Time (MST) of Glioblastoma Multiforme Patients by Age.

Bar graph showing a study involving 677 patients diagnosed with glioblastoma multiforme that the MST (expressed in months) declines with increasing age from diagnosis.

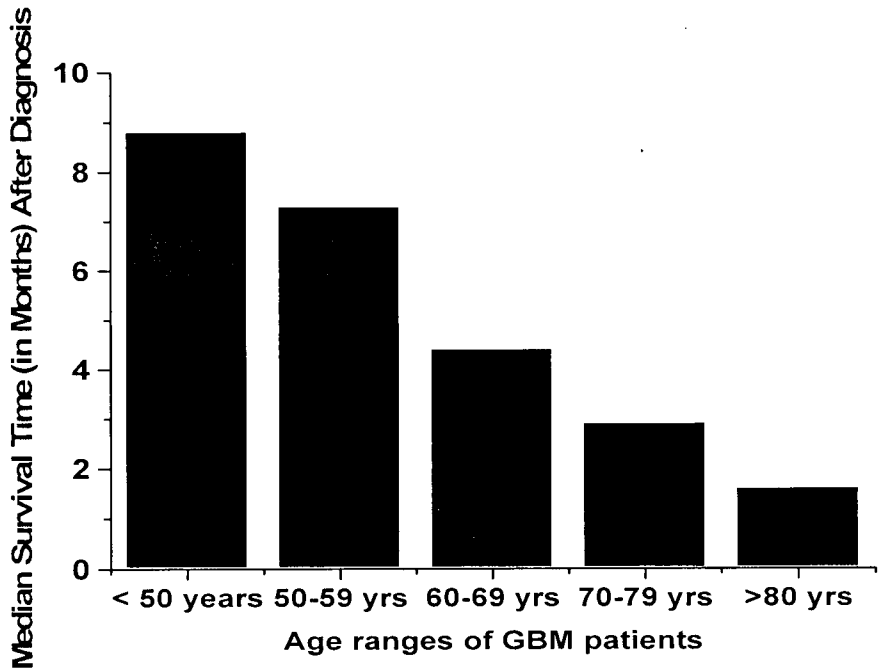

Adapted from Ohgaki et al., 2004 Can Res

At present, the most widely used classification and grading system is that of the WHO [4]. Gliomas are classified by the degree to which they display astrocytic, oligodendritic or chod plexus epithelium (cells that secrete cerebral spinal fluid for the brain and spinal cord) which are then graded on a scale of I to IV based on malignancy which is judged by histological features such as pleomorphism, high mitotic activity, microvascular proliferation and necrosis. Grade I tumors (i.e. pilocytic astrocytomas) are non-malignant tumors that can be removed completely if necessary. Grade II tumors are considered "low-grade" tumors that are malignant and, although can be deemed appropriate for surgical resection, do not generally lead to a cure. In addition, seventy percent of grade II gliomas ultimately turn into grade III and IV tumors within 5-10 years of diagnosis (reviewed in [5]). Grade III and IV tumors are defined by whether the tumor has necrosis which indicates a Grade IV astrocytoma (glioblastoma multiforme). However, due to tumor heterogeneity found within malignant astrocytomas sampling issues can make determinations of tumor grade for the pathologist difficult.. New molecular profiling techniques for tumor grading should allow for improved categorization of malignancy, as well as being helpful in guiding treatment options [6] (see section 1.3).

1.1.1. Origin of Gliomas

The etiology of gliomas is still in debate. Unlike other tumors such as retinoblastomas in which there is strong evidence of an inheritance pattern [7]. In glioma a familial pattern of inheritance is low. Similar to diseases that are associated with certain tumors such as Von Hippel Lindau's syndrome (hemangioblastoma) and tuberose sclerosis. The origin of gliomas may be rooted in the general mechanisms of cancer. One of the earliest concepts of cancer genesis was proposed by Cohnheim in 1889 who observed that the cells of malignant tumors

were very similar in appearance to developing cells. Cohnheim later suggested that malignant tumors arose from pools of embryonic cells [9]. However, the loss of embryonic cells after the age of 4 suggested that this was an unlikely source from which adult tumors arose [10]. Willis in 1967 suggested that cells were infected with cancer due to a carcinogenic stimulus of some kind and that this infection spread from the centre of the tumor mass to the periphery, where those cells at the periphery were less affected by the cancerous stimuli [11]. The debate of the origin of gliomas is now purely centred around whether glioblastoma multiforme's like other cancers are derived from transformed differentiated cells which are mature cells [12-13] or from transformed undifferentiated which are cancer stem cells [14-19]. Of the two theories of gliomagenesis the major theory has been that gliomas arise from adult differentiated cells [20]. This was largely due to the thought that glial cells were the only dividing cells, and therefore these cells would logically be the cells with transforming ability. Since the discovery of neural stem cells which are multipotent and self-renewing, in addition to glial progenitor cells, this has re-opened the possibility that gliomas arise from undifferentiated cells to become cancer stem cells [21]. Given the pluripotent nature of neural stem cells and the finding by Shoshan and colleagues that glial progenitor cells expressed antigens found in gliobastomas and other brain cancers, this has given further support for the undifferentiated cell transformation origin of gliomas, shifting the paradigm [22].

1.1.2. Brain Cancer and Viruses

Currently there is no definitive evidence that viruses are directly responsible for human brain tumors, and there is no comprehensive model [23]. Tadaro and Huebner [24] proposed that vertebrate DNA would contain viral genetic information which would only be activated in

light of environmental stimuli such as ionizing radiation, carcinogens or other viruses [24]. The interaction would result in brain tumors, and this is known as the viral oncogene hypothesis [24]. Suggestive evidence indicates that viruses are at least involved in causing neurological disorders such as progressive multifocal leucoencephalopathy (PML) which is a demyelinating disease and is seen in about 4% of AIDS or immunosuppressed patients, and is frequently associated with Hodgkin's disease and leukaemia [25]. Evidence in support of a viral etiology comes from the isolation of viruses from oligodendrocyte nuclei and JC virus isolated from polymonuclear lymphocytes of brains and then injected into hamsters which resulted in malignant gliomas [26]. More compelling evidence was obtained in a study conducted by Barbanti-Brodano et al., (1987) in which 40 human brain tumors and five normal human brains were analyzed for DNA sequences homologous to BK virus (this virus has already been shown experimentally to cause brain cancer). Recently, 225 brain tumor specimens in 2 independent laboratories were investigated for JC, BK and SV40 polyomaviruses and indicated that only 4% contained virus suggesting that a viral component is not the major cause of gliomas [27]. Although there have been isolated links between viruses and several brain tumor subtypes in addition to astrocytomas, the link is not confirmative.

1.1.3. Immune Surveillance and Privilege

It has been suggested that there is a significant latent period before tumor development due to the continuous elimination of malignant cells by the immune system [28]. Thus it has been proposed that when the immune system can no longer effectively handle tumor cell removal, tumor formation will occur [29]. Further investigation is needed to explore the possible roles of other immune cells and their involvement in immune surveillance. Immunologically

privileged sites were first recognized as such in light of their delayed response or lack of response from the immune system to tissue grafting compared to immune responses seen in non-privileged immune sites [30] this included the brain [31]. However, several transplantation studies for diseases such as multiple sclerosis, Parkinson's and Hunington's disease, have indicated that the brain does not enjoy absolute immune cell free status as lymphocytes can cross the blood-brain barrier (see section 1.4). The brain does however, enjoy and modified immune response such as deviance (re-direction of the immune response to another site), ignorance (absence of the immune response activation) or tolerance (acceptance or a threshold level before immune cell stimulation) [32]. It appears that the role of the immune system within the brain when a brain tumor is present is not well known, an approach to determining the extent of potential mechanisms of brain tumor formation may lie in the diagnosis or more specifically the tests used to determine malignant glioma. For example, a local increase in white blood cells in the early stages of a malignant glioma, may lend evidence to an immune surveillance mechanism. Diagnosis of brain tumors is not only important for possibly providing information on the etiology of brain tumors but also is a necessity for the treatment of malignant gliomas.

1.2 Diagnosis of Brain Tumors

The accuracy of diagnosis is critical to defining treatment options, where time may be the most critical factor in the effective treatment of glioblastoma cancer. In very rare cases glioblastoma tumors in conjunction with other tests can be diagnosed by spinal tap and subsequently identified by the cerebrospinal fluid (CSF) marker. Ideally, a brain scan followed by tissue biopsy where a frozen section is prepared and examined intraoperatively by a neuropathologist is used in making a diagnosis [2]. It is important to note that diagnosis through

biopsy material may be confounded by non-malignant cells causing a sampling error, resulting in a lower grade tumor diagnosis. Histological sections prepared from tumor samples give diagnostic information such as necrosis, endothelial cell proliferation and although rarely done mitotic index evaluation using MIB-1 (marker for determining cell proliferation) . Strong MIB-1 staining is an indicator of an aggressive tumor [2].

Diagnostic imaging is one of the most definitive methods and has advanced the ability to diagnose gliomas. Computed tomography (CT) and magnetic resonance imaging (MRI) are the common diagnostic imaging methods and less commonly used is positron emission tomography (PET). CT or MRI (see Fig. 1.2) are immediately considered in response to neurologic symptoms or in response to patient complications [2]. It is important to note that although there are several imaging modalities which detech gliomas, none of them can with absolute accuracy define the subtype or grade of the glioma. The origins of malignant gliomas are not well defined thus prevention strategies will be difficult to define. For this reason, it is critical to determine the biology of high grade gliomas and although biopsied material provide some information the molecular aspects of high grade glioma should also be considered consistent with the focus of this thesis, better treatment options are needed for patients burdened with brain cancer [33].

Figure 1.2
Diagnosing a Brain Tumor

Glioblastoma multiforme; axial CT scan of a mass the tumor regresses (scans from top left to right bottom) following treatment with Procarbazine, Lomustine (CCNU) and Vincristine, collectively called PCV. Initial tumor is seen in top left and treatment begins in top right panel with complete remission by the lower right panel.

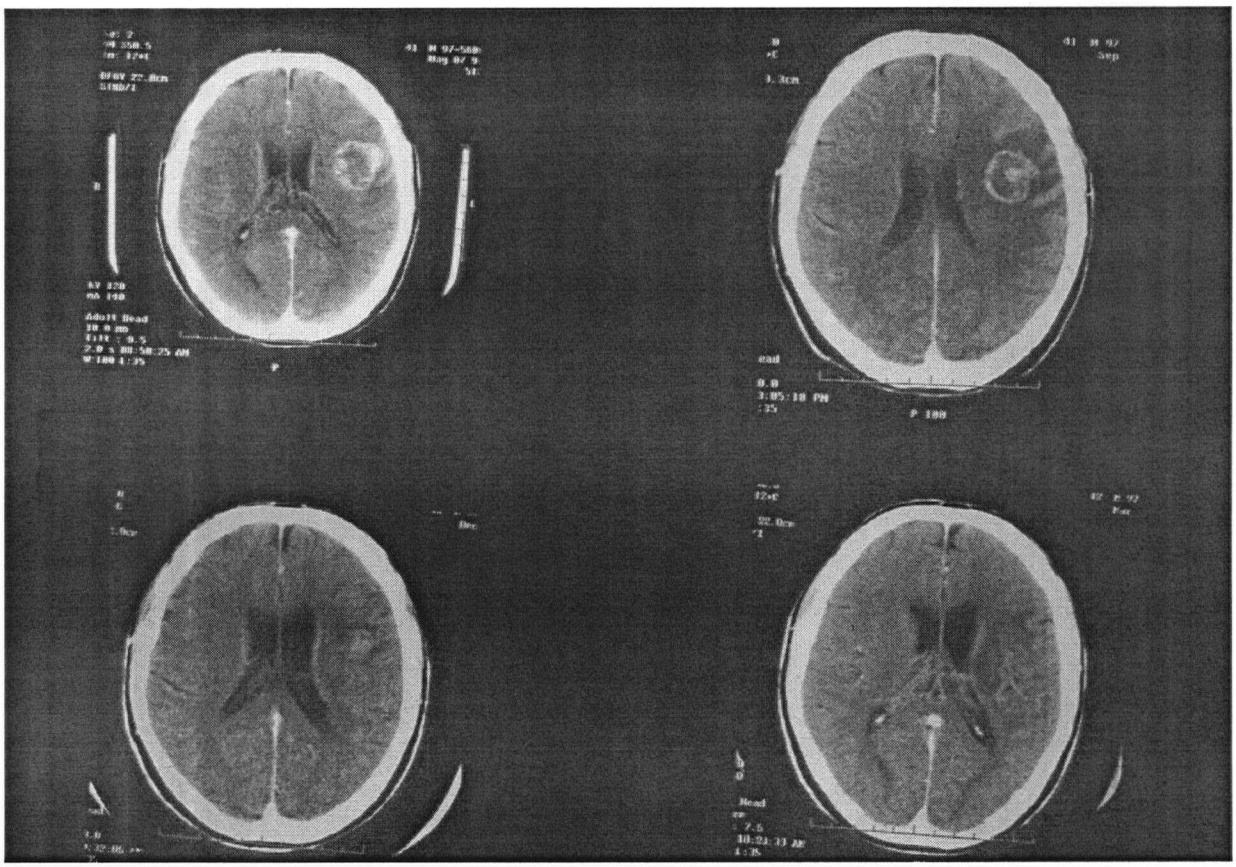

Courtesy of Dr. Brain Thiessen, BC Cancer Agency, Medical Oncology

1.3. Conventional Treatment of Glioblastomas

Surgical Intervention

Surgery is the principal means of treatment for accessible brain tumors particularly for high grade gliomas that can be approached without severe damage to the rest of the brain [34]. Surgery can achieve many things depending on the tumor type including (i) a definitive diagnosis, (ii) symptom relief and improve quality of life and (iii) reduce the amount of tumor that has to be treated. However, surgery is often hindered by tumor location, size and characteristics (tumor borders not well defined), which is especially true for GBM. Although GBMs do not spread beyond the brain, GBM is locally very invasive leaving these tumors surgically incurable [35]. This is when radiotherapy becomes useful and recently improved efficacy in the treatment of brain tumors has been seen with radiotherapy in combination with chemotherapy [34].

Radiotherapy

The most common form of radiotherapy is ionizing radiation. This type of radiotherapy is high frequency, short wavelength as opposed to visible light which is low frequency, long wavelength, essentially as energy is imparted to radiation the wavelength decreases resulting in greater penetration of biological material [35]. At the cellular level, ionizing radiation results in deoxyribonucleic acid (DNA) damage. The use of radiation can result in reactive oxygen species causing DNA damage [36], single and double strand breaks [37] and DNA-protein cross-linking [38-40]. DNA cross linking due to ionizing radiation also results in DNA replication arrest [38].

Radiotherapy encompasses many methods of using radiation to treat gliomas. Teletherapy involves using an external-beam from a source located at a distance from the patient, this is done using a machine known as an orthovoltage or supervoltage machine. A supervoltage machine is very useful for the treatment of gliomas because of its interaction with biological material. The maximum amount of energy is able to penetrate tissue to a specific depth depending on the energy of the photon [35][41]. Brachytherapy radiation is placed within close proximity of the patient, usually in the form of seeds or wafers. Brachytherapy usually involves the placement of seeds containing I^{131} which decays and kills the tumor. The criteria for the use of brachytherapy as a treatment option is dependent on tumor size, geometry and location of the tumor. Brachytherapy is however, rarely used currently because of evidence suggesting it is no more effective than other treatments and because of patient risk associated with the treatment. Approximately half the patients develop brain necrosis due to radiation (reviewed in [2]).

Although radiation therapy is a proven treatment for several cancers including brain tumors [42] there are or can be serious complications with the use of radiation therapy, particular with respect to how aggressively to treat the tumor. The tumor margins (where the tumor ends and the normal tissue begins) are at times hard to define even with today's advanced imaging methods (see section 1.2). The result of going beyond the tumor margins can lead to affects on the normal neurological structures. Even patients who do well with radiation treatment, may experience acute side effects during treatment such as fatigue and alopecia. Similarly, patients who do well during treatment may experience serious side effects sometime after the treatment has ended (see Table 1.2) that can affect various parts of the central nervous system, such as the cranial nerves [43]. Some of the major side effects of radiation therapy are

somnolence syndrome which is a disruption in the sleep-wake cycle. Patients with somnolence experience sleepiness, headache and sometimes anorexia. In some cases patients experience a severe sleep disorder, sleeping for 20hrs a day [44]. As early as two weeks after the end of radiation treatment patients may develop acute encephalopathy with symptoms ranging from nausea, headache, fever to herniation and death [45-46]. An unfortunate side effect of focal radiation treatment that commonly occurs in the treatment of primary brain tumors such as gliomas is a transitory loss of cognitive function [47]. A prospective study revealed five patients receiving focal cranial radiation for primary brain tumors all displayed memory deficits within the first six months of treatment [47]. Another study revealed that 17 patients treated with focal cranial radiation also had neurological deficits [48], in both studies the loss of cognitive function did resolve within a year. In addition to the side-effects of radiation therapy, which hinder its effectiveness, the two major reasons why radiation is not curative are (1) radiation resistance where radiation induced radicals which would damage DNA are converted to sulfhydrils due to the donation of hydrogen to the radical in the absence or low levels of oxygen resulting in less DNA damage. The power of hypoxia can not be understated as even a fraction of cells that are hypoxic can lead to radioresistance, simply because radiation would kill the radiosensitive tumor cells leaving the hypoxic fraction behind. [49]. (2) Radiation is less likely to be effective regardless of the modality i.e. brachytherapy or teletherapy) because of the deep penetration that would be required into the brain due to the infiltrative nature of high grade gliomas. In addition, there is apparently no real difference in patient survival between the radiotherapy approaches [50].

Table 1.1

Complications Associated with Radiation Therapy of a Neurological Nature

Region of CNS	Complications during Radiation Treatment	Complications after Radiation Treatment
Brain	-Loss of cognitive function -Solmnolence syndrome -Acute brain inflammation -Exacerbation of pre-existing symptoms	-Cerebral radionecrosis -Dementia leukoencephalopathy -Radiation induced Brain tumors
Cranial Nerves	-Hearing loss -Loss of smell (Anosmia) -Loss of taste (Ageusia)	-Visual loss -Cranial nerve paralysis

Adapted from Behin et al., 2004 Sem Neurol

Chemotherapy

The goal of treating cancer is cure. Although chemotherapy has had an impact on some cancers in which cures are possible such as testicular cancer and Hodgkin's disease it is clear that chemotherapy of malignant intracranial lesions such as glioblastomas is viewed as an adjunct to other treatment options such as radiation (see previous section) or surgical intervention (section 1.3). Several reasons account for the poor performance of chemotherapy. Primarily, factors related to drugs crossing the blood-brain barrier and to mechanisms of drug resistance are of greatest concern. Like radiation therapy, there can be serious side effects associated with chemotherapy (see Table 1.2) and like radiation, there is chemoresistance with respect to gliomas, resistance is also associated with hypoxia where chemotherapeutic drugs are ineffective simply because of a lack of blood-flow and therefore a lack of transport of chemotherapeutic agents to the tumor. In addition, hypoxia has a significantly decreased metabolic rate, which makes chemotherapy less effective on hypoxic and essentially dormant cells than on highly proliferating cells [51-53]. Chemotherapy can also be employed where there is evidence suggesting recurrence of a tumor after previous tumor surgery or radiotherapy. Recurrence can occur within a few months after initial treatment [54-56]. Thus chemotherapy remains an important component of glioblastma treatment. Ideally such chemotherapy would be relatively non-toxic and, as indicated in section 1.4, it would be ideal if such chemotherapy targeted key molecular defects known to be associated with glioblastoma progression, resistance and tumor cell survival.

For chemotherapy to be effective, drug efficacy is of major concern, however, there are several variables that play an important role in determining if chemotherapy will be effective.

Table 1.2

Main Complications Associated with Chemotherapy for the Treatment of Brain Tumors

Agent	Route of Admistration	Side Effects	Drug Considerations	Brain Tumor Type
Carmustine (BCNU)	I.V.	Nausea Myelosuppression Pulmonary fibrosis	Cumulative Myelosuppression Leukemogenesis	Malignant glioma
Lomustine (CCNU)	P.O.	Nausea Myelosuppression Pulmonary fibrosis	Cumulative Myelosuppression Leukemogenesis	Malignant glioma Oligodendroglioma
Temozolomide	P.O.	Nausea Fatigue Headache Constipation Myelosuppression		Malignant glioma
Vincristine	I.V.	Peripheral neuropathy Constipation	Blisters (vesicant)	Malignant glioma Oligodendroglioma
Cisplatin	I.V.	Nausea Renal insufficiency Peripheral neuropathy Myelosuppression	Nephrotoxicity Ototoxicity	Malignant glioma PNET
Irinotecan	I.V.	Severe diahrrhea Nausea Myelosuppression		Malignant glioma

Adapted from Mcallister et al., 2002 Practical Neuro-Oncology

Such factors include age, neurologic status and the extent of disease at diagnosis [57]. As indicated above, chemotherapeutic response rates on average are low for patients with brain tumors and this seems to correlate with neurologic status and elderly patients (reviewed by LaSala [58]). Aside from clinical variables to drug efficacy, there are also biological variables such as the blood-brain barrier.

1.4. Biological Barriers to Brain Tumor Treatment

The Blood Brain Barrier (BBB), as recently as 5 years ago, has been a point of controversy with regards to its importance in achieving effective treatment of brain tumors [59]. Despite this, most reports suggest that the BBB is a major obstacle in the delivery of various drugs identified for use in the treatment of brain tumors [60]. The BBB inhibits the delivery of greater than 98% of all therapeutics that target the brain, including anti-cancer agents [61]. The BBB essentially separates the brain from circulating blood. The BBB consists of 3 major cells, pericytes, astrocytes and endothelial cells. The endothelial cells are the major road block presented by the BBB due to expression of numerous tight junctions [62]. In addition, there is a lack of pinocytosis in the capillary endothelium inhibiting solutes from crossing the BBB unlike what is observed in other tissues. The only access to the brain is restricted to a lipid-mediated pathway (i.e. lipid-soluble molecules), carrier-mediated transport, or receptor-mediated transport. The latter two pathways are associated with nutrient and peptide transport, respectively.

In addition to the BBB, the existence of a blood-tumor barrier (BTB) exacerbates the problem of effective delivery. The BTB is comparable to the BBB, except that this barrier is found within the tumor. The BTB is a microvascular network consisting of either

nonfenestrated or fenestrated capillaries or interendothelial gaps, the presence of these microvessel properties is dependent upon tumor grade [63]. Similar to other tumors, glioblastoma growth is dependent on stimulating blood vessel formation (angiogenesis) in order to provide sufficient nutrients for the tumor cells to proliferate.

The constant metabolic demands of tumor cell proliferation and survival result in a tumor microenvironment that is both hypoxic and pro-angiogenic. This tumor microenvironment is important in brain tumor formation and is associated with high grade gliomas. Low-grade astrocytomas can hijack the blood supply of normal tissues in their surrounding environment without instigating angiogenesis making them non-angiogenic tumors, even though these tumors can grow to sizes that rival angiogenic tumors [64]. As tumor grade increases, from a grade II to a grade III or IV GBM the presence of hypoxia becomes apparent and significant necrosis is typically observed [64]. A possible explanation into how hypoxia and necrosis develop, is that a highly proliferative tumor cell population eventually outgrows or exhausts the existing blood supply resulting in hypoxic and necrotic conditions [65]. Another proposed mechanism is a blockage of blood-vessels or a degeneration of blood vessels leading to discreet areas of hypoxia and necrosis [66]. It is a treatment dilemma knowing that hypoxia is associated with radiation resistance and the lack of blood vessels or blockage of blood vessels, along with the BTB act in a coordinated fashion to limit the effectiveness of systemic treatment options. Two approaches have been proposed to address these concerns, including the use of regional chemotherapy (e.g. wafers containing cytotoxic drugs or infusion pumps) and strategies designed to effect the stability of the BTB, through the use of anti-vascular agents.

One of the key markers of hypoxia is hypoxia inducible factor 1 (HIF-1), which is a transcription factor consisting of a HIF-1α and HIF-1β subunit. HIF-1 expression has been

correlated with tumor grade [67] and can be activated or upregulated with loss of such tumor suppressors as *TP53* and *PTEN* molecular markers commonly associated with glioblastomas [68] (see Chapter 5). HIF-1 expression has been shown to be under the control of the PI3-kinase/Akt pathway, key pathways associated with tumor cell survival, proliferation and invasion [69]. The presence of hypoxia ultimately leads to angiogenesis as does changes in developmental and physiological states [70]. This involves vascular endothelial growth factor (VEGF) which is a principle mediator in angiogenesis. HIF-1 can mediate the activation of VEGF through binding to a hypoxia responsive element (HRE) located within the VEGF promoter region to increase VEGF transcription [71-72]. VEGF appears to be vital as even the loss of one allele in mice led to embryonic lethality [73-74]. Both hypoxia and angiogenesis have been associated with tumor cell invasion [75-76]. Although these features have been well studied and have long been understood to adversely affect treatment options, basic research into the factors that regulate hypoxia and angiogenesis will aid in the development of targeted agents where hypoxia and angiogenesis are considered in the treatment of cancer. This will prove to be particularly important in the development of effective treatment options for malignant glioma where hypoxia and angiogenesis are prominent.

1.5. Brain Cancer and Targeted Therapy: The New Strategy- ILK Targeting

Cancer, in general, is a complex multi-step process involving the activation and/or abrogation of signal transduction pathways resulting in a variety of cellular activities. Cancer, in effect, is the loss or disregard of normal cell communication, which engenders unregulated cell proliferation, migration, and an inhibition of apoptotic arrest. Although the complexity of cellular communication is intimidating, knowledge of cell signal communication is at a stage

where strategies designed to specifically augment or inhibit these pathways in a reasonably specific manner can be considered. At the root of this effort is knowledge that cellular communication is dictated by protein kinases, and the possibility that small molecules can be identified to block kinase activity and/or molecular strategies can be used to block or elicit production of these enzymes. While chemotherapy remains one of the primary ways to treat cancer, conventional chemotherapeutic agents are rather blunt instruments that are easily circumvented by rapid drug metabolism and tumor drug resistance. This problem is further exacerbated by the lack of specificity of chemotherapy and the associated systemic toxicity on the cancer patient. Specific and selective inhibitors of kinases offer a more "surgical" approach to management of cancer, particularly when the role of the enzyme is well understood in normal and diseased cells. For these reasons there has been a concerted effort into gaining a better understanding of protein kinases, not only for the intimate role they play in proliferative diseases, but also as molecular targets in cancer therapy. The PI-3-kinase pathway protein Integrin-linked kinase (ILK) defines such a molecular target and its potential as a therapeutic target can be highlighted by the observation that with loss of *PTEN* , overexpression of ILK leads to tumorigenicity [77].

1.5.1. ILK and its Importance in Brain Cancer

Integrin linked kinase (ILK), was first discovered by yeast two hybrid screening trying to identify proteins that interact with the cytoplasmic domains of the cell surface receptors known as integrins [78]. Co-immunoprecipitation studies verified that ILK interacts with the β1 integrins and was later found to interact with the β3 components of integrins [78]. Integrins are a large family of receptors that exist as heterodimers composed of α and β subunits that can

interact with extracellular matrix proteins such as collagen and fibronectin [79]. The result of an integrin-ILK interaction identifies not only how signaling proteins connect and communicate with the extracellular matrix, but also how intracellular cytoskeletal proteins are connected. Evidence of intracellular cytoskeletal activity can be seen with several proteins that interact with ILK and connect to the actin cytoskeleton (Fig. 1.3). Yeast two hybrid analysis with ILK as bait led to the identification of CH-ILKBP also known as α-parvin (found in mice) and actopaxin. CH-ILKBP, which contains two calponin homology (CH) domains, and mediates ILK association through its CH2 domain, at ILKs COOH terminal domain, [80] and also connects to the actin cytoskeleton. Similarly, two other proteins, affixin (the human orthologue of mouse β-parvin) which shares significant sequence similarity to CH-ILKBP within the CH2 domain, can interact with ILK at ILKs COOH terminal domain and paxillin, which interacts with ILK at ILKs COOH terminal domain through an LD1 motif can, like CH-ILKBP, connect to the actin cytoskeleton [81-82]. This new class of ILK binding proteins which consists of CH-ILKBP-actopaxin-α-paxin, affixin-β-parvin and paxillin are thought to act as one of the major bridging molecules, linking ILK to the actin filaments. Overexpression of the CH2 binding domain of CH-ILKBP-actopaxin-α-parvin in cells results in loss of actin stress fiber formation and cell shape change [82][80]. In addition, *C. elegans* with mutations in either ILK or CH-ILKBP-actopaxin-α-paxin show defects in the assemblage of muscle dense bodies that attach actin filaments to sarcolemma (Lin, X., and B.S.Williams. 2000. 40th American Society for Cell Biology Annual Meeting. 2666 [Abstr.]). The regulated interaction of these proteins with ILK mediates the dynamic interaction of integrins with the actin cytoskeleton during cell attachment, spreading and migration.

ILK can initiate a signal transduction cascade from its interaction with integrins, and it is more than likely that ILKs ability to phosphorylate β1 integrins at Ser790 regulates localization of β1 integrins to focal adhesions [83]. ILK has also been shown to localize to fibrillar adhesions [84]. ILKs involvement in both focal adhesions and fibrillar adhesion is consistent with a role of ILK in cell adhesion, spreading and fibronectin matrix assembly [77][85]. In addition, ILKs interaction with integrins at its C-terminus leading to cell signaling is only part of ILKs ability to initiate cell communication. The N-terminus of ILK, along with having a phosphoinositide-binding motif, contains four ankyrin repeats that allow for protein-protein interactions [86-87]. PINCH is a LIM domain-only protein, that can interact with ILK at the ILK N-terminus, through the LIM1 domain of PINCH [88]. The adaptor protein Nck-2 (also known as Nckβ or Grb4), interacts with PINCH through the PINCH LIM4 domain and the Nck-2 SH3 domain, Nck-2 can then be recruited by growth factor receptors such as EGFR [89]. Moreover, Nck-2 could conceivably bring other components of the growth factor and small GTPase signaling pathways into proximity [89]. The coupling of ILK to integrins and growth factor receptors indicates that ILK has a role in both integrin and growth factor receptor signaling, making ILK very versatile and potentially able to initiate other cell signaling cascades. ILK appears to be deeply rooted in the PI3K pathway, as ILK is positively regulated by PI3K and negatively regulated by the protein phosphatase PTEN [90]. Specifically, through its phosphoinositide binding motif at its N-terminus, ILK can bind PIP_3 resulting in ILK activation, PTENs ability to dephosphorylate PIP_3 can therefore inhibit ILK activity. Similarly, PKB/AKT is known to be an important regulator of cell cycle progression and cell survival, which is also affected by PIP_3 levels regulated by PTEN [91]. ILK has been shown to regulate the cell cycle by increasing expression of cyclin D1 and cyclin A [92-93], and increased ILK activity corresponds with

increased PKB/AKT expression in a PI3K dependent manner [94][95]. Full activation of PKB/AKT is dictated by phosphorylation of PKB/AKT at two sites: Thr-308 and Ser473. The phosphorylation of Thr-308 is carried out by phosphatidylinositol 3-kinase dependent kinase-1 (PDK1) and for complete activation of PKB/AKT, ILK stimulates phosphorylation at the Ser473 site [96]. It should be noted that several other kinases can phosphorylate PKB/AKT on Ser473 such as DNA protein dependent kinase [97], at least 9 other kinases have been identified [98] There is little doubt that ILK can regulate PKB/AKT phosphorylation however, the precise mechanism remains unclear. Lynch et al., [95] have suggested that ILK causes PKB/AKT phosphorylation via an indirect mechanism. On the other hand, ILK has been shown to directly phosphorylate several proteins *in vitro* including PKB/AKT and myosin phosphatase [96][99]. Recently, RNA interference (siRNA) targeted at ILK resulted in a significant decrease in phosphorylation on Ser473 of PKB/AKT that could be rescued by kinase-active ILK. Further, conditional knock-out of ILK using the Cre-Lox system resulted in inhibition of phosphorylation on Ser473 of PKB/AKT [100]. Since the activity of ILK and PKB/AKT is positively regulated by PI3K and is negatively regulated by PTEN, and ILK mediates PKB/AKT activity, ILK appears to occupy a nodal position in the regulation of PKB/AKT activity (see Fig 1.4). In the context of this thesis, given ILK's critical role in regulation of several cell signaling pathways, it was anticipated that ILK expression and activity would play a role in cancer development and progression. This would be particularly true in tumors where *PTEN* is frequently mutated, such as GBM.

Figure 1.3

Structure of ILK and its relationship to various interacting molecules in the PI3K cell signaling pathway

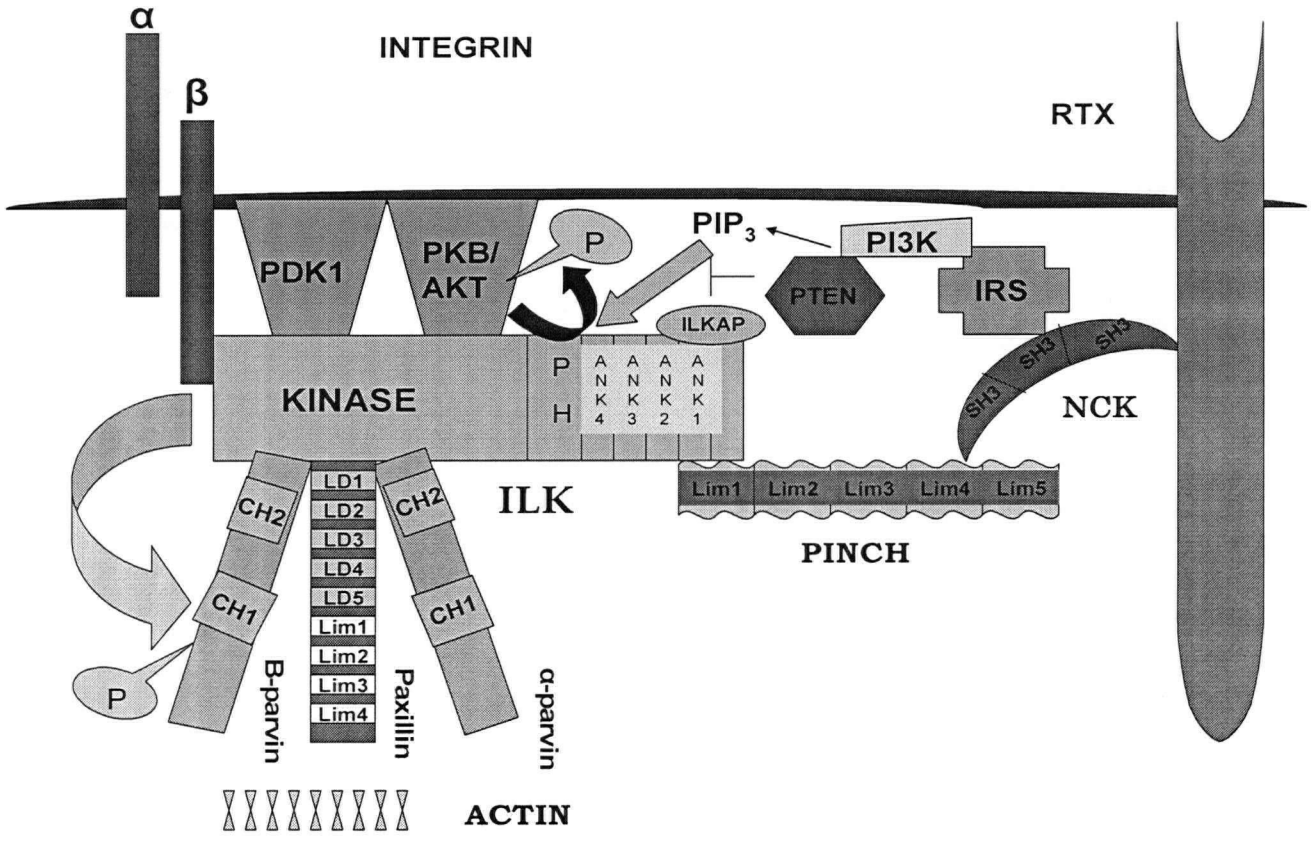

Adapted from Wu & Dedhar J Cell Biol. 2001 155(4):505-10

1.5.2. The Role of ILK in Tumorigenesis and Invasion

The downstream targets of ILK, the most prominent being PKB/AKT, appear to be involved in several oncogenic related processes including anchorage-independent growth, invasion, migration and prolonged cell survival when ILK is overexpressed or constitutively active. Wu and colleagues showed that ILK can act as a proto-oncogene by demonstrating that overexpression of ILK in epithelial cells induces tumorigenicity in nude mice [101]. Reduced sensitivity to anoikis is also observed when ILK is overexpressed in anoikis-sensitive SCP2 cells causing inhibition of apoptosis in these cells. On the other hand, downregulation of ILK activity by dominant-negative ILK or dominant negative PKB/AKT reverses anoikis sensitivity in SCP2 cells, indicating again ILKs role in the regulation of PKB/AKT [102]. Prolonged cell survival results from ILKs activation of PKB/AKT leading to the inactivation of downstream pro-apoptotic factors such as BAD [103] and caspase-9 [104]. ILKs ability to induce an invasive phenotype is observed with ILK overexpression in mammary and intestinal epithelial cells (IECs). ILK overexpression is associated with increased expression of matrix metalloproteinase (MMP-9). Soft agar studies of IECs with ILK overexpression revealed cell growth, essentially promoting anchorage-independent growth [105]. Further, ILK overexpression leads to the loss of cell-cell adhesion due to suppression of E-cadherin expression via activation of the E-cadherin repressor Snail, again promoting a migratory/invasive phenotype [106]. The activities of ILK in tumorigenesis and cell invasion are not limited to just the *in vitro* setting. Transgenic mice that overexpressed ILK via a mouse mammary tumor virus (MMTV/ILK) were associated with the development of papillary adenocarcinomas and spindle cell tumors [107].

Figure 1.4

ILK Signaling: Cell signaling pathways activated by ILK. ILK is a major effector serine/threonine kinase that links integrins and receptor tyrosine kinases to the cytoskeleton and downstream signaling molecules.*

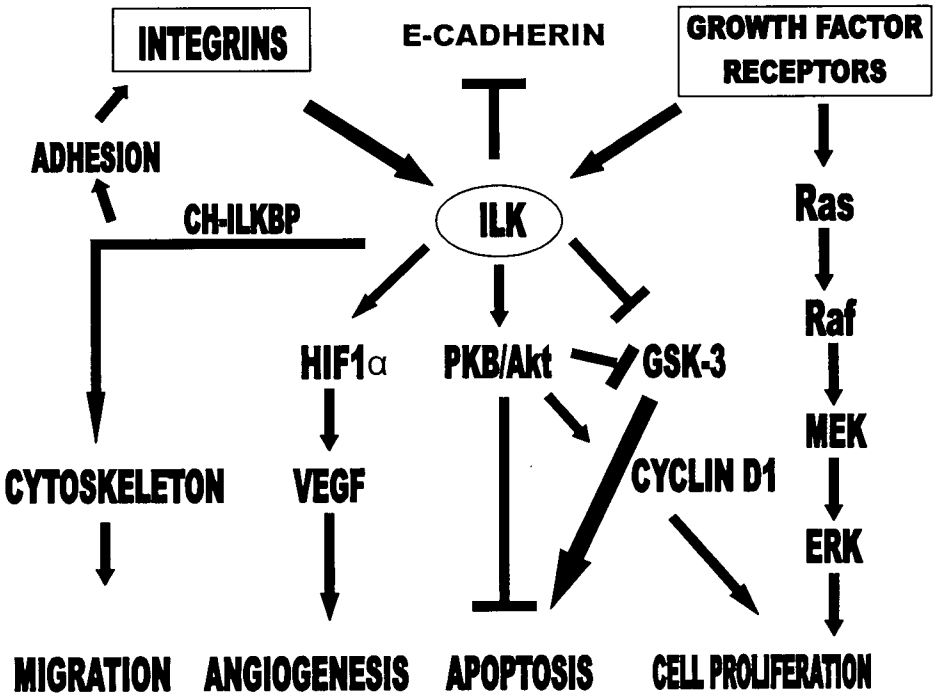

* Published in Cancer Treatement Reviews Edwards et al., 2004 119:59-75

As summarized in section 1.4.3. ILK expression is becoming increasingly identified with patient survival and is a potential prognostic indicator of cancer [92]. Tissue microarray and immunohistochemistry of 67 primary melanomas, for example, showed that ILK expression was found to increase with melanoma invasion and progression and that 5-year patient survival was inversely correlated to ILK expression [108].

1.5.3. Relevance of Integrin-linked kinase to human cancer

Evaluation of ILK in primary prostate tumor tissue revealed that ILK expression increased in high grade tumors (i.e. prostatic adenocarcinoma) but did not increase in benign prostatic hyperplasias and low-grade prostatic adenocarcinomas [110]. Importantly, ILK expression was also inversely related to 5-year patient survival, 81% of patients whose tumors overexpressed ILK failed to survive beyond 5 years [110]. This suggests that ILK could be a prognostic marker for prostate cancer. The consistency of ILK expression and its potential as a prognostic marker is even greater in Ewing's Sarcoma and primitive ectodermal tumors, as 100% of the cases analyzed showed ILK expression that indicated 100% mortality beyond 5 years [108]. The activity of ILK in several cancers and its potential as a prognostic marker is further seen in ovarian cancer where recently seventy-three tissue samples (10 normal, 10 benign, 14 borderline, 17 grade I/II, and 22 grade III) were analyzed for ILK expression by immunohistochemistry. Immunoreactive ILK was detected in 53 specimens where intensity of ILK staining correlated with tumor grade. Normal ovarian tissue showed no immunoreactive ILK [109]. In addition, peritoneal tumor fluid increased ILK expression in ovarian cancer cell lines, but had no effect on normal ovarian surface epithelial cell lines, indicating that peritoneal tumor fluid may contain factors that sustained ILK expression in ovarian cancer cell lines [109].

Although interest in ILK activity has been focused on PKB/AKT, ILK is involved in the phosphorylation of other cell signaling proteins that are associated with a cancerous phenotype. One such cell signaling protein is glycogen synthase kinase-3 (GSK-3). ILK overexpression regulates a phosphorylation mediated inhibition of GSK-3. Inactivation of GSK-3 results in a loss of cell-cell adhesion due to loss of E-cadherin expression. Since metastasis requires the separation of tumor cells from the bulk tumor this evidence suggests the involvement of ILK, GSK-3 and E-cadherins in metastatic activity. Further, loss of E-cadherin expression is highly correlated with breast cancer invasion and metastasis [111]. ILK expression has also been demonstrated to be highly elevated in precancerous colon polyps from patients with familial adenomatous polyposis and colon carcinomas [112]. Mutations in proteins that act in a PI3K dependent manner could potentially, like PTEN, be associated with cancer progression.

Recently, besides PTEN, two potential tumor suppressor proteins, disabled homolog 2/differentially expressed protein 2 (DOC-2) and stomach cancer-associated protein-tyrosine phosphatase-1 (SAP-1) have been shown to negatively regulate ILK activity and are associated with breast and stomach cancer respectively [113-114]. Another negative regulator of ILK has been identified, ILKAP, a protein phosphatase which selectively inhibits ILK activity on the Wnt signaling pathway [115], however, evidence of tumor activity has yet to be associated with ILKAP mutation. An increased understanding of the cellular pathways controlling cancer cell proliferation, survival and metastasis has opened new avenues for cancer treatment. However, the pathways that govern the features of cancers are complex as revealed by ILK signaling. Thus, efforts in this thesis are concerned with glioma treatment strategies that target ILK sigaling, but there is an understanding that optimal therapeutic results will depend on agents

targeting ILK used in combination with existing anticancer drugs as well as combination with other targeted agents.

1.6. Rationale for Combination Approaches

The increased genetic instability typically exhibited by cancer cells predisposes them to acquire numerous molecular alterations or mutations, and indeed the vast majority of cancers contain multiple molecular alterations. Consequently, therapies directed against a single cellular or molecular target are unlikely to result in a significant response. Combinations of conventional chemotherapy drugs have been used as one approach; however, the emergence of drug resistance remains a considerable limiting factor. Since cell signaling is largely responsible for the apoptotic and cytostatic effects of conventional chemotherapy and radiation-based therapeutics, the addition of molecular target inhibition to these established treatment approaches has the potential to enhance the effectiveness of both established and emerging therapies. Combination strategies that attack multiple cellular targets and/or signaling in parallel or sequential pathways known to contribute to the overall transformed state will likely yield the most dramatic therapeutic benefit.

1.6.1. Why Molecular Targeting Involving ILK?

ILK has been identified as a plausible target for the treatment of cancer in which the PI3K pathway is involved. In addition, the Ras/Raf/MAPK pathway has also been shown to be involved in several cancers. Although these pathways in cancer are typically presented as separate entities, the reality is that there is a great deal of cross-talk between these pathways, including at the level of ILK regulation. Molecular combination therapy could exploit

approaches that target specific pathways in conjunction with established treatment practices or approaches that target multiple independent pathways each known to influence cancer progression and survival. Before any attempt can be made to discuss molecular drug combinations however, it is reasonable to test whether the combinations have the potential to interact in a synergistic, additive or antagonistic manner as judged by cell based screening assays. These data provide evidence that support further evaluations of selected drug combinations but typically provide no information on mechanisms governing the combined drugs or, importantly, how to use the drugs *in vivo* in a manner that insures optimal synergistic effects are maintained. The Chou and Talalay median-effect approach **[116]** is one of the most prevalent methods to assess drug combination effects. The median effect principle (approach) allows for an easy to use method of analyzing dose-effect relationships in *in vitro* and *in vivo* systems with single or multiple drug agents, which can then be used to determine the drug-drug interactions (e.g. synergy). Other methods include the use of isobolograms, the fractional product method and the parametric response surface approach. The isobologram has been the longest running method to determine additivity, synergy and antagonism **[117]**, it allows for the evaluation of a drug combination at a desired effect level. Problems with this method arise in having to make a large number of measurements in order to have accurate analysis of single and drug combination effects and analysis is only accurate for drugs with a similar mode of action. The fractional product method is an equation that determines the additive value of a drug combination. If the value calculated from the equation is larger or smaller than the equation then the drug combination is synergistic or antagonistic respectively. Unfortunately, this method is only valid if the two drugs used in combination have completely different mechanisms of action. The parametric response surface approach uses highly sophisticated models and calculations and

is not widely used most likely because of the complicated nature of this model [118]. For a comprehensive review of approaches to assess drug interaction effects, please refer to the excellent review by Greco et al.[117].

1.6.2. The Evaluation of Targeted Molecular Drug Combinations *(in vitro)*

To evaluate drug combinations the multiple drug effect equation (Eq 1) of Chou was introduced [119-120]. The multiple drug effect equation that defines the additive effect only, indicates that any effect greater than the additive effect is a synergistic one.

$$f_a/f_u=(D/D_m)^m \qquad \text{Eq 1}$$

From equation 1, where D= the dose of drug, D_m= the median-effect dose indicating the potency (determined from the x-intercept of the graph of the median effect plot), f_a=the fraction affected by the dose, f_u=the fraction unaffected, where $f_u=1-f_a$ and finally m=an exponent representing the shape of the dose-effect curve determined by the median effect plot. The median effect plot determines the slope of the line from a plot of the log f_a/f_u (y-axis) and the log D (x-axis) to determine the D_m. In otherwords the median effect plot determines the median dose e.g. IC_{50} or LD_{50}. From equation 1 the combination index (CI) equation was formed [116]. The benefit of the CI equation for drug combinations in the treatment of cancer is that the CI gives a quantitative determination of synergy, antagonism and additivity (see Eq 2). Chou and Talalay proposed that a CI value of 1 represents an additive effect, CI < 1 indicates a synergistic effect and that a CI > 1 indicates an antagonistic effect [116].

$$CI = (D)_1/(D_x)_1 + (D)_2/(D_x)_2 \qquad \text{Eq 2}$$

For each combination dose, and single drug alone the data can be plotted as the percent of cells inhibited (i.e. the fraction affected-Fa) and the CI value determined for each combination (D), using the single drug alone (D_x) (Eq 2) which results in a Fa versus a CI plot. Equations 1 and 2 and the graphs that can be generated from drug combination data have been used in the development of a user friendly software program CalcuSyn (BioSoft, Ferguson MO, USA). A representative graph generated by CalcuSyn is shown using the conventional chemotherapy combination of BCNU and Carboplatin, which are used in the treatment of malignant glioma The results shown in Fig. 1.5 suggest that these agents exhibit a synergistic relationship (Fig 1.5). These data illustrate an important point when considering combination effects by this approach. CI varies as a function of the fraction of affected cells, a parameter that is obviously related to the drug dose (Eq 1). Thus CI values indicating antagonism are estimated at doses inducing a measured effect (e.g. % cytotoxicity) of less than 20% while the CI is indicative of synergistic interactions when these drug doses used achieve effect levels of >0.5.

The point of molecular targeted drug combinations is not only to limit monotherapy failure, as has been indicated in some Gleevec ™ patients [121-122], but also to increase the therapeutic benefit of the drug combination. This can occur at dose levels less than that required by either one of the agents used alone. Provided that toxicity to normal cells is not enhanced by the use of the combination, then the synergistic combination should achieve improved therapeutic results. In addition, a multi-targeted attack on cell signaling proteins should reduce or limit the emergence of drug resistance [123]. Although *in vitro* assays can be used to define

synergistic interactions, these assays provide little information as to how this synergy can be obtained *in vivo*.

Figure 1.5

Representative plot showing a synergistic effect of the conventional chemotherapeutic alkylating agents BCNU and Carboplatin on U87MG glioblastoma cells exposed for 48 h. Note that each data point (open circles) moving from left to right is an increasing ratio of the drug combination of BCNU and Carboplatin the drug to drug ratio used was 3.9 to 6.9 for BCNU and Carboplatin respectively. The data points that fall below the dotted horizontal line which represents the CI value 1 indicates a synergistic relationship the line running through most of the points is generated by Calcusyn, and only runs through points that are synergistic. *

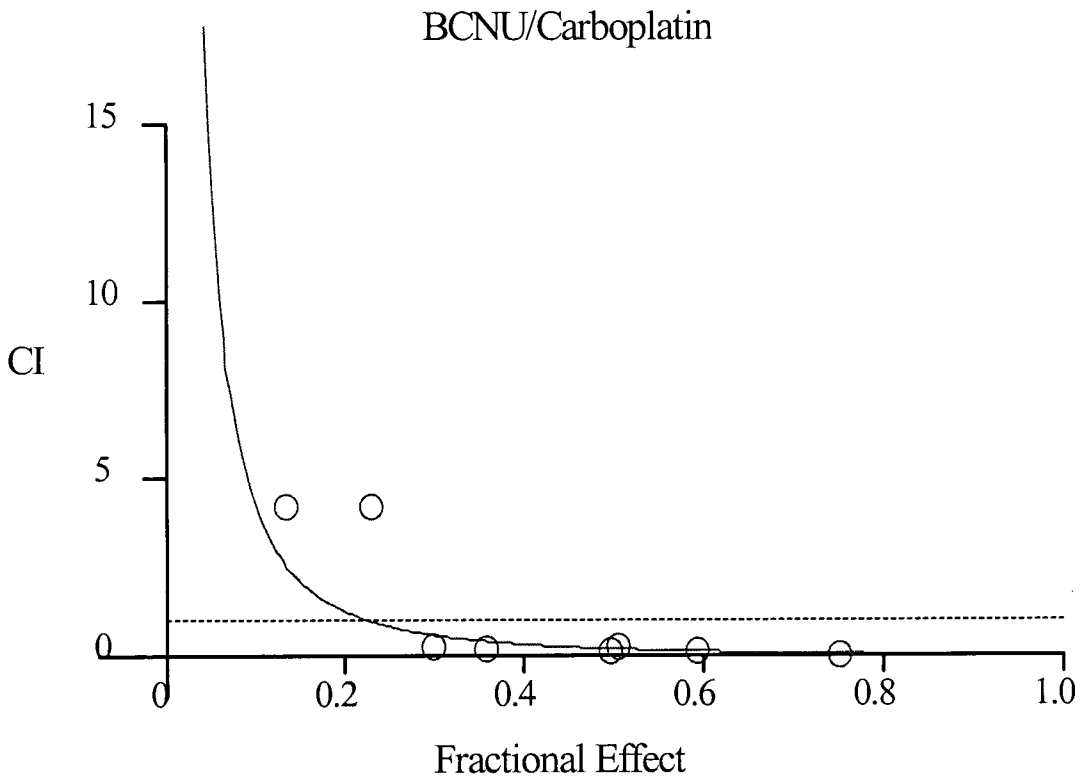

* Published in Cancer Treat Rev Edwards et al., 2004 119:59-75

It can be argued that an approach to achieving synergy *in vivo* could be developed on the basis of the ED_{50} concentration of each drug and in combination and then relating this information to pharmacokinetic parameters. Moreover, it should be noted that in any drug combination approach there will be a balance between efficacy and toxicity. For example, targeting ILK and MEK1/2 protein may provide a good response with an acceptable level of toxicity, while targeting ILK and the EGFR may give a better efficacy response with comparable toxicity. The importance of choosing the "right" targets will, therefore, be only one of the parameters that must be considered when developing drug combinations for clinical use. Other issues such as those effecting biodistribution, metabolism and toxicity must also be considered to define effective means to prevent cancer cells from circumventing the targeted pathways.

1.6.3. Rationalized Molecular Drug Combinations

Cell signaling gone awry in cancer allows not only for the unregulated cellular activities that define cancer, but also allow cancer cells to evade or escape attempts at single agent therapy. For example, the G-protein Ras stimulates the Ras/Raf/MAPK pathway, (a cell proliferation pathway) however, this stimulation can be inhibited by wortmannin, which is a PI3K pathway (a cell survival pathway) inhibitor. In contrast, stimulation of the Ras/Raf/MAPK pathway via receptor tyrosine kinases such as EGFR is insensitive to wortmannin [124]. However this is subjective as the effects of wortmannin may be cell type dependent. Further, EGFR overexpression which has been implicated in breast and ovarian cancer, was inhibited by the EGFR inhibitor CI-1033 in MDA-MB-435 breast cancer cells. Even though reduced levels of PKB/AKT were seen in the MDA-MB-453 breast cancer cells, this was not sufficient to induce

apoptosis in these cells. In addition, exposure of gemcitabine to MDA-MB-453 cells resulted in the activation of Erk1/2 with low levels of apoptosis. However, the combination of CI-1033 and gemcitabine 24hrs later in the MDA-MB-435 cells resulted in the suppression of PKB/AKT and Erk1/2 with a significant increase in apoptosis over either of the two agents alone [125]. These examples illustrate the importance of knocking out multiple targets especially in light of the cross-talk that can exist between intracellular pathways. In the context of drugs targeting ILK, studies have demonstrated that the combination of the EGFR inhibitor PD153035 and an ILK inhibitor (KP392) and the combination of PD153035 and the ILK inhibitor (KP307-2) [108] can result in an additive and synergistic drug combination effect on SF-188 and U87MG glioblastoma cells respectively (see Fig 1.6). Interestingly, studies have also shown a synergistic interaction can be obtained with an ILK inhibitor and the EGFR inhibitor PD153035 when tested *in vitro* against U87MG cells. This is illustrated in Figure 1.7 through the use of a dose reduction index (DRI) plot obtained from data generated by CalcuSyn. The dose reduction index determines how much of each drug in a synergistic combination may be reduced at a given effect level versus the doses for each agent alone. In this case the plot was generated at an effect level in which 90% cell kill is achieved i.e. Fa=0.9 (see Fig 1.7). The same level of cytotoxicity can be achieved by using a drug combination at a dose that is 5-fold lower for the ILK inhibitor and 6-fold lower for the EGFR inhibitor. The DRI really highlights one of the primary outcomes associated with use of a synergistic drug combination; where reduced amounts of drug in combination will achieve the same effect (an affect on cell viability) but at a lower dose. It can be argued that this synergy may, in turn, lead to effective control of tumor growth at dose levels that would exhibit reduced toxicity.

Figure 1.6

(A) Fraction affected (Fa) versus combination index (CI) plot where the dotted horizontal line represents CI=1, indicating an additive effect of the EFGR inhibitor PD153035 and the ILK inhibitor KP392 in combination against SF-188 glioblastoma cells exposed to drug(s) for 48 h. The drug to drug ratio was 1 to 5 for KP392 and PD153035 respectively *(B)* dose-effect curve showing that the effect of the two drugs is equal to the effect of the greatest single agent, PD153035. The doses used are as follows PD153035 (0,5,7.5.10,12,14,16,18,20uM) KP392 (0,30,40,50,60,70,80,90,100uM) CI, combination index, Effect (x-axis) Fraction effect, Effect (y-axis) cell viability. Both graphs were generated using the software program CalcuSyn. *

A

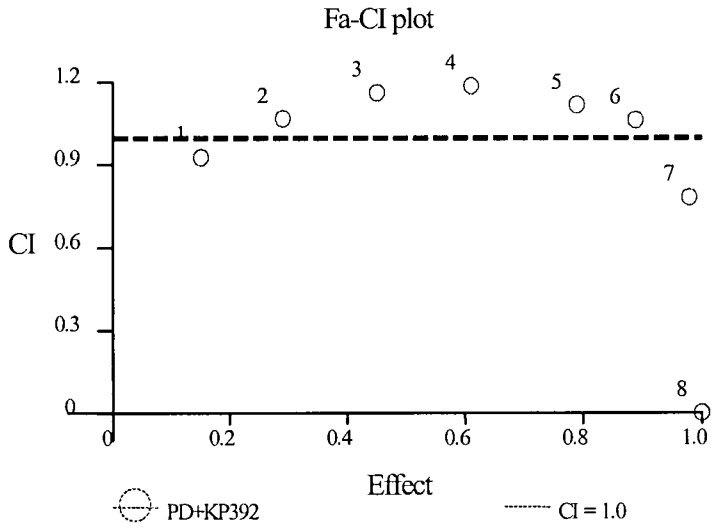

B

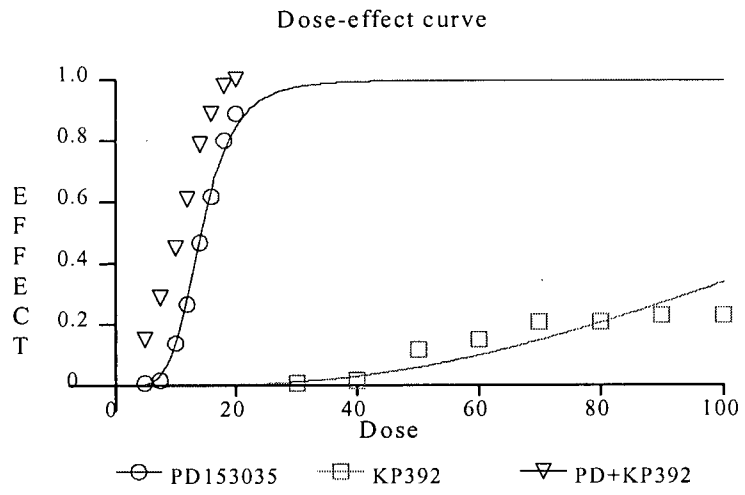

* Published in Cancer Treatement Reviews Edwards et al., 2004 119:59-75

Figure 1.7

The DRI of the ILK inhibitor KP307-2 and the EGFR inhibitor PD153035 that results in a synergistic drug combination upon exposure (48 h) to the U87MG glioblastoma cells. The drug to drug ratio was 1 to 1 for KP307-2 and PD153035 respectively. *

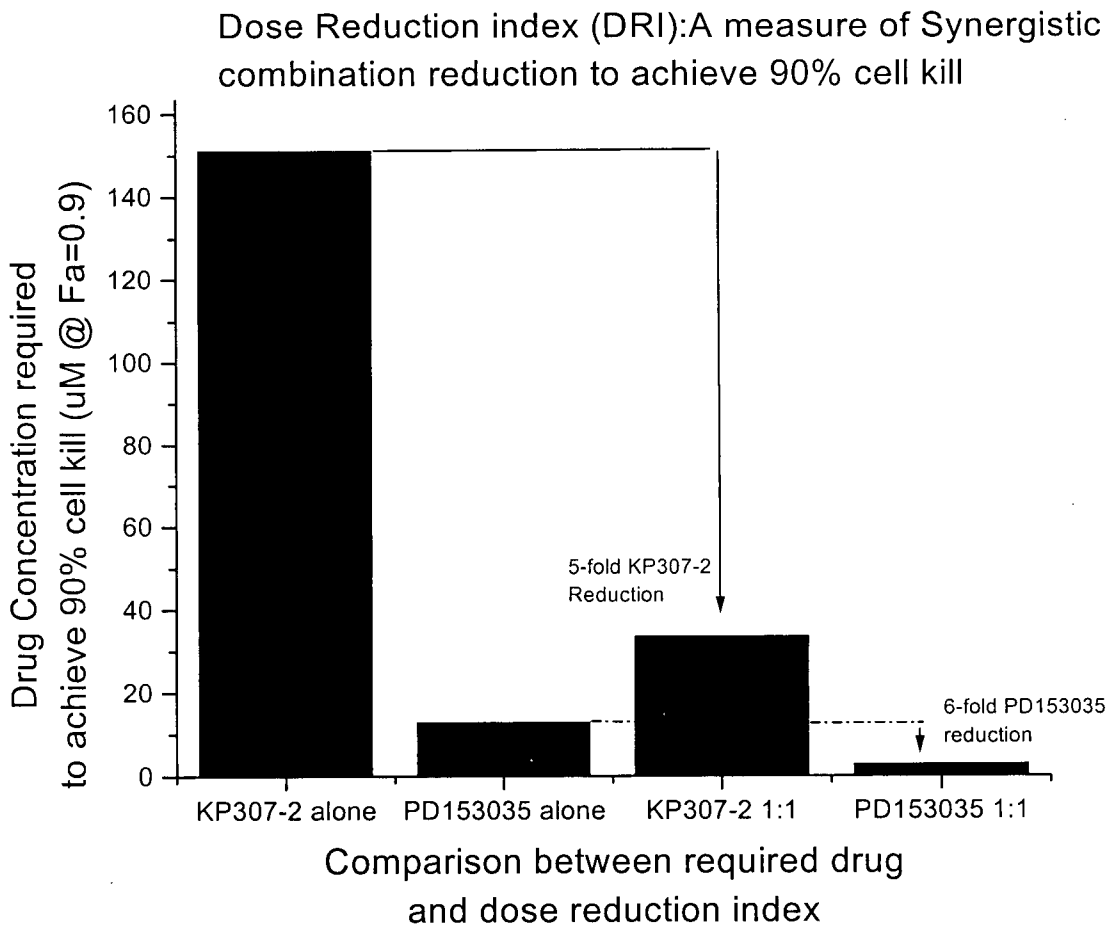

* Published in Cancer Treatement Reviews Edwards et al., 2004 119:59-75

1.7. Thesis Rationale and Hypothesis

It is clear that overexpression of ILK results in malignant progression [106][112]. In normal cells, overexpression leads to tumorigenicity, anchorage-independence, cell cycle progression and tumor invasiveness [77][92][93]. Inhibition of ILK activity has also been shown to suppress the growth of human colon carcinoma cells in SCID mice [106]. In human colon cancer, increased ILK activity has been associated with effects on downstream cell signaling molecules such as GSK-3 and as much as a 9-fold increase in myelin basic protein (MBP) phosphotransferase activity [126]. In addition, ILK overexpression is observed in malignant crypts from both primary and metastatic lesions. Marotta and colleagues relate that selective inhibition of ILK alone or in combination would be an effective means of treating this cancer [127]. Studies in prostate cancer have demonstrated a critical role of ILK in tumor angiogenesis, whereby ILK regulates VEGF expression in tumor cells and VEGF mediated vascular morphogenesis [128]. Since the function of ILK surrounds the activation of key downstream PI3K regulators such as PKB/AKT, GSK-3 [102][126] and various cellular functions including angiogenesis, apoptosis, and cell proliferation, (see Fig 1.3) and given that inactivation of ILK by dominant negative ILK, kinase deficient ILK, and ILK siRNA can block ILK activity and cell transformation, ILK is a very good candidate for drug targeting. ILK activity and the subsequent downstream activity of PKB/AKT has been associated with the loss of *PTEN*. It has further been shown that the loss of *PTEN* is frequently observed in the brain cancer glioblastoma multiforme on the order of 80% [129]. Furthermore, PKB/AKT expression has been correlated to poor prognosis in glioma patients [130-131]. It is therefore proposed that targeting ILK in glioblastoma cancer would result in a therapeutic effect. In addition it would be

anticipated that targeting ILK in combination with another agent that is involved with a cell signaling pathway apart from ILK may enhance this therapeutic benefit.

CHAPTER 2

MATERIALS AND METHODS

2.1. Tumor Cell Lines and Transfections

In vitro experiments were perfomed with glioblastoma cancer cell types. *PTEN* negative U251, U87MG glioblastoma cells and *PTEN* positive SF-188 glioblastoma cells were obtained from ATCC repository. Cells were cultured in Dulbecco's Modified Eagle medium (DMEM) containing 10% fetal bovine serum with 1% L-glutamine and 1% penicillin/streptomycin at 37°C in a humidified atmosphere containing 5% CO_2. For all experiments cells were used in exponential growth phase. U87MG cells were transiently transfected with ILK antisense (ILKAS) using Lipofectamine 2000 ™ reagent (Invitrogen, MD, USA) according to the manufacturer's guidelines using 1-4 μg (optimally 2 μg) antisense, and 12 μl Lipofectamine 2000 ™ reagent in 10 cm^3 tissue culture dishes. Retroviral constructs with either *PTEN* empty vector (U87EVG) or with an inducible *PTEN* construct (U87.23) were generously provided by Dr. Michael Wigler (Cold Spring Harbour). U87 cells with the various vector constructs were maintained with hygromycin selection at 50 μg/ml. Muristirone A (Invitrogen, Burlington, Ont) was reconstituted in 100% ethanol prior to adding to cells for induction. Cells were harvested 24-48 hrs later.

Drugs and Antisense Sequences

3-(3,5-Dibromo-4-hydroxy-benzylidene)-5-iodo-1,3-dihydro-indol-2-one (GW5074) was purchased from Sigma-Aldrich (St. Louis, MO, USA). The raf-1 inhibitor GW5074 was prepared fresh by dissolving in sterile 100% DMSO at a stock concentration of 1038 μM and

protected from light. The drug was diluted with serum free DMEM prior to use. MEK inhibitor U0126, purchased from Promega (Madison, WI, USA), was prepared by dissolving in sterile 100% DMSO to a stock concentration 10 mM. In all of the *in vitro* experiments, the final DMSO concentration did not exceed 0.3%. A patented library of over 80 antisense sequences affecting *ILK* was obtained from ISIS Pharmaceuticals Inc (Carlsbad, CA, USA). Sequence ID no 37 (5'-GAGATTCTGGCCCATCTTCT-3') was used and is designated here as ILKAS. ILKAS is a 20mer antisense oligonucleotide (ODN) with a phosphothioate backbone, 5'-methylcytidines with the first 5 nucleotides (at the 5'-end) 2'O-methyls and the last 5 nucleotides (at the 3' –end) 2'O-Methyls. The ILKAS affects the 635 "coding region" or open reading frame (ORF) which lies between the translation initiation codon and the translation termination codon of human *ILK*. A non-silencing antisense sequence was also obtained, designated SCRAM2, and a reverse polarity antisense (RILK) was also used with the same modifications as those of ILKAS. Note that all transfection experiments were done in serum-free media using the Lipofectamine 2000 ™. Growth factors contained in serum refeeding were added exogenously, however, EGF was added 20 min prior to transfection in serum-free media. after transfection Antisense sequences for *in vitro* use were generated at the University of British Columbia Nucleic Acid Protein Service Unit (Vancouver, BC, Canada). Antisense sequences were ammonia-butanol purified. Antisense sequences for *in vivo* use were generated at Eurogentec (Philadelphia, PA USA).

2.2. Cell Viability/Cytotoxicity Assays

MTT assay and drug combination effects with U0126, GW5074, ILK antisense, QLT0254 and QLT0267

Growth inhibition of U87MG, U251 and SF-188 cells was determined by the colorimetric (3-[4,5-Dimethylthiazol-2-yl]-2,5-diphenyl-tetrazolium bromide) MTT assay [132]. In brief, cells were plated at 3000/100 µl in 96-well plates and allowed to adhere overnight before exposure to antisense and/or inhibitors were incubated for 24 or 48hrs at 37°C, ILKAS (1-16 µM), GW5074 (2-32 µM) and U0126 (10-80 µM). Plates were assessed using the microtiter plate reader (Dynex Technologies Inc, Chantilly, VA), measuring absorbance at a wavelength of 570nm. The percentage of viable cells following treatment was normalized to untreated controls. All assays were performed in triplicate at least two times. The MTT data obtained following treatment of cells with the indicated agents alone or in combination, was combined so that the number of samples analyzed for each drug or drug ratio concentration was equal to or greater than 6. Effective concentrations were analyzed using the CalcuSyn software (Biosoft, Freguson, MO). CalcuSyn program provides a measure of the combined drug interaction by the generation of a combination index (CI) value. The CI value is based on the multiple drug-effect equation of Chou and Talalay [119-120], and defines the drug interactions as synergistic, (which is more than the expected activity effect or greater than an additive interaction) or antagonistic, (which is less than the expected activity effect or less than an additive interaction). Chou and Talalay defined the CI value as <1 for synergism, =1 for additive, >1 for antagonism.

Growth inhibition of U87MG, U251 and SF-188 cells was determined by the colorimetric MTT assay [132]. In brief, cells were plated at 10,000/100 µl in 96-well plates and allowed to adhere overnight before exposure to the ILK inhibitor QLT0254 or QLT0267 and incubated for 24 or 48hrs at 37°C. Plates were read using the microtiter plate reader (Dynex Technologies Inc, Chantilly, VA) at a wavelength of 572nm. The percentage of viable cells following treatment was normalized to untreated controls. All assays were performed in triplicate.

Clonogenic Assay

Colony formation was evaluated using a soft agar colony forming assay. Briefly, cells were exposed to drug for 5 hrs. Cells were washed with serum free DMEM. Subsequently, 2000 cells/well were mixed with DMEM containing 15% FBS and 0.5% agar and plated on 6-well plates (three wells/condition). The plates were then transferred to a 37°C incubator with 5% CO_2. After 12-14 days of incubation, colonies were scored in 2 colony grids (Epicentre, Madison, WI) per well using a Zeiss ID02 microscope (Don Mills, Ontario). Colony formation for each condition was calculated in relation to values obtained for untreated control cells.

Nuclear Morphology

Untreated and treated cells were incubated a minimum of 12 hrs in medium at 37°C without additional drug treatment. Cells were then harvested and stained with 0.10μg/ml DAPI (4',6-diamidino-2-phenylindole) for 30 min at room temperature. Cells were cytospun onto a glass slide, and viewed with a Leica microscope (Germany) with a 40X objective lens under UV fluorescent illumination. Images were captured using DC100 digital camera and Image database V. 4.01 Software (Leica, Germany).

Flow Cytommetric Assay of Apoptosis following treatment with QLT0254 and QLT0267

5 X 10^5 cells were cultured with or without drug treatment and later incubated for a minimum of 12 hrs in culture media at 37°C without additional drug treatment. Control cells were untreated or treated with the vehicle control PTE (PEG300/Ethanol/Tween 80/citrate (63:29:7.8:0.2 w/v/w/w). Cells were then harvested and fixed with cold 70% ethanol stored overnight at -20°C and stained with propidium iodide (PI) staining buffer (1mg/ml RNase A, 0.1% Triton X-100,

50 μg/ml PI in PBS) to determine the apoptotic/necrotic cell population (the sub G_1/G_0 cell fraction).

Flow Cytometric Assay of Apoptosis following treatment with ILK antisense.

5 X 10^5 cells were cultured with or without antisense and later incubated for a minimum of 12 hrs in culture media at 37°C without additional drug treatment. Cells were treated with ILKAS. Control cells were untreated or treated with reverse ILK antisense sequence (RILK) and these data were compared to cells treated with ILKAS. Note, a liposomal vector control was also included in the experiment which had no effect. Cells were then harvested and fixed with cold 70% ethanol stored overnight at -20°C and stained with propidium iodide (PI) staining buffer (1mg/ml RNase A, 0.1% Triton X-100, 50 μg/ml PI in PBS) to determine the apoptotic/necrotic cell population (the sub G_1/G_0 cell fraction). In order to evaluate the early stages of apoptosis, treated cells were stained with Annexin V-FITC (CALTAG) in Annexin V staining buffer for 15 min at room temperature and counter stained with 50 ug/ml propidium iodide in Hank's Balanced Salt Solution (Stem Cell Technologies) with no phenol red and analyzed with a FACSCalibur flow cytometer (Becton Dickinson, San Jose, CA) for the induction of apoptosis.

Flow Cytometric Assay of Apoptosis following use of specified drug Combinations

Cells (5 X 10^5) were cultured with or without drug and later incubated for a minimum of 12 hrs in culture media at 37°C without additional drug treatment. Camptothecin (32 μM) was used as a positive control for induction of apoptosis which was measured by Annexin V-FITC/PI staining. Cells were treated with ILKAS, GW5074 or the combination of ILKAS and GW5074. Control cells were untreated or treated with RILK in combination with GW5074. A liposomal vector control was also included in the experiment. Cells were then harvested and fixed with

cold 70% ethanol stored overnight at -20°C and stained with propidium iodide (PI) staining buffer (1mg/ml RNase A, 0.1% Triton X-100, 50 μg/ml PI in PBS) to determine the apoptotic/necrotic cell population (the sub G_1/G_0 cell fraction). In order to evaluate the early stages of apoptosis, treated cells were stained with Annexin V-FITC (CALTAG) in Annexin V staining buffer for 15 min at room temperature and counter stained with 50 μg/ml propidium iodide in phenol red-free Hank's Balanced Salt Solution (Stem Cell Technologies) and analyzed with a FACS Calibur flow cytometer (Becton Dickinson, San Jose, CA) for the induction of apoptosis.

2.3. Protein Analysis

Preparation of Cell Extracts

Adherent cells (5 X 10^6) were plated in 100 x 20mm tissue culture treated plates. Cells were washed initially with Hanks' Balanced Salt Solution (HBSS) and then trypsinized with Trypsin-EDTA (1X) (Invitrogen, Gibco, Burlington, Ont). Cells were then collected in Dulbecco's modified Eagel's medium (DMEM) containing 10% fetal bovine serum (FBS) and 1% L-glutamine with 1% penicillin/streptomycin. Cells were centrifuged at 10, 000 rpm for 5 minutes and the pellet resuspended in 10ml of phosphate buffered saline (PBS) and centrifuged again at 10, 000 rpm and the pellet resuspended in 1ml of PBS and transferred to microcentrifuge tubes. PBS was removed and the cell pellets were placed on ice where they were treated with 1ml of ice-cold lysis buffer (50 mM Tris, 150 mM NaCl, 2.5 mM EDTA, 0.1% SDS, 0.5% sodium deoxycholate, 1% NP-40, and 0.02% sodium azide) containing protease inhibitors (Complete-Mini protease inhibitor tablets: Boehringer Mannheim GmBH,

Mannheim, Germany). Lysates were centrifuged for 10 min at 15,800 x g at 4°C. Supernatant was then aliquoted into new microcentrifuge tubes and stored at -70°C until further analysis.

Western Blot

The following antibodies were used: anti-ILK (affinity purified rabbit polyclonal, Upstate Biotechnology, Virginia, USA); anti-ILK, anti-P-Akt-Ser-473, anti-P-Akt-Thr-308, anti-Akt, anti-MAPK, anti-P-MAPKp42/p44, anti-MEK1/2, anti –P-MEK1/2-Ser217/221 (New England Biolabs, Canada); anti-human β-actin (Sigma St. Louis, MO); anti-HA (Roche, Mannheim, Germany); Anti-HIF-1α (Santa Cruz Biotechnology, CA); and anti-VEGF (Calbiochem, CA). The secondary antibodies used were horseradish-conjugated anti-mouse or anti-rabbit IgG (Promega, Madison, WI). Densitometric analysis was done and then normalized to control or time 0 samples.

For *in vivo* ODN treated and untreated tumors, the tumor tissue was homogenized (using a mortar and pestle) with ice-cold lysis buffer (50 mM Tris, 150 mM NaCl, 2.5 mM EDTA, 0.1% SDS, 0.5% sodium deoxycholate, 1% NP-40, and 0.02% sodium azide) containing protease inhibitors (Complete-Mini protease inhibitor tablets: Boehringer Mannheim GmBH, Mannheim, Germany). After incubation for 30 min on ice, samples were centrifuged at 10,000 rpm for 15 min, and stored at -20°C. Protein content in the lysed extracts was determined using a detergent-compatible Bio-Rad assay (Bio-Rad Labs, Hercules, CA). Similarly, for *in vitro* studies, involving ODN treated cells and untreated cells, protein content was determined using Bio-Rad assay. Cell lysates samples were incubated for 15 min on ice, samples were centrifuged at 5,000 rpm for 10 min. Samples were loaded with 2X SDS buffer-(2 X 0.064 M Tris-HCl pH 6.8, 1.28% SDS, 12.8% glycerol, 1.28% 2-mecaptoethanol, 0.25% bromophenol

blue) and then boiled. Cell lysates were size fractionated through SDS-PAGE and transferred onto nitroceullulose membranes as described [133]. Proteins were detected by enhanced chemiluminescence (ECL; Amersham Pharmacia Biotech, Buckinghamshire, England) and visualized after exposure to Kodak autoradiography film. Equivalent amounts of protein (30 μg determined by Bradford assay) were resolved by 12% SDS-polyacrylamide gels or 4-15% gradient SDS-polyarcylamide pre-made gels (BioRad).

ILK Kinase Assays.

ILK kinase activity was determined in cell extracts by immunoprecipitation in vitro kinase assays, as detailed elsewhere [90] [126]. In brief, myelin basic protein (MBP) was used as a substrate for ILK, [^{32}P]-ATP was used as the phosphate donor in the kinase assay and [^{32}P]-MBP was detected by phosphoimage analysis of the gels.

VEGF ELISA

U87MG glioblastoma cells transfected with a retroviral construct with a PTEN inducible promoter (designated here as U87.23) were seeded into 60-mm dishes at a density of 2 X 10^5 cells/dish and incubated in regular media overnight and then placed in serum-free media for 24 h. 24 hrs later, control untreated U87.23 cells or cells treated with Muristirone A to induce PTEN, were treated with LY294002 or QLT0254 or QLT0267. The conditioned media was removed 24 h later and stored at -70°C until VEGF concentration was determined by ELISA (R&D Systems). U87MG glioblastoma xenograft tumors were homogenized using a mortar and pestle in NP-40 lysis buffer containing complete-mini protease inhibitor cocktail tablet (Roche,

Mannheim, Germany) and the tumor lysate removed and stored at -70°C until VEGF concentration was determined by ELISA (R&D Systems) as described above.

2.4. Animal Xenograft Models and Anti-Tumor Activity

Male Rag-2M mice (7-9 weeks old, 20-27g) were obtained from British Columbia Cancer Agency Joint Animal Facility breeding colony, and housed in an aseptic environment. A solid tumor model of SF-188, U87MG and U251 cells in Rag-2M mice was established by subcutaneous injection of 5 X 10^6 cells derived from tissue culture, resulting in tumor formation on the back of mice. All of the animal protocols were approved by the University of British Columbia Animal Care Committee and the studies were conducted in accordance with the guidelines of the Canadian Council of Animal Care. Efficacy experiments were conducted in male Rag-2M mice bearing U87MG tumors (6 mice per group). Treatments were initiated on day 22-post cell inoculation. Saline control, ILKAS or scrambled control (SCRAM2) oligonucleotides (ODNs) were administered using a treatment schedule of i.p. injections given (QD) for 5 days, followed by two days off, for a 3 week period at a dose of 5 mg/kg. Mice were observed daily and body weight measurements and signs of stress (e.g. lethargy, ruffled coat or ataxia) were monitored. Having previously determined the maximum tolerated dose exceeded 20 mg/kg in Rag-2M mice none of the mice treated with ILK antisense showed any indication of toxicities at the 5 mg/kg dose of the ILK antisense. Electronic calipers (Mitutoyo corp., Japan) were used to measure tumors and the mean tumor size (mm^3) was determined using the formula ½[length (mm)] x [width (mm)]^2. The tumor size per mouse was used to calculate the group mean tumor size ±SE (n=6 mice) the results are a representative graph of at least three experiments.

Animal Xenograft Models and Antitumor Activity of QLT0254 or QLT0267.

Male Rag-2M mice (7-9 weeks old, 20-27g) were housed in an aseptic environment. Efficacy experiments were conducted in male Rag-2M mice bearing U87MG tumors (6 or 18 mice per group). Note that groups containing 18 mice were designated as harvesting groups and mice were sacrificed and tumor tissue was taken for various analysis (i.e. tissue microarray, western blot, immunhistochemistry and ELISA). Treatments were initiated when tumors reached at least 15 mg. Saline control, or a vehicle control of PTE or the ILK inhibitor QLT0254 or QLT0267 were administered by oral gavage given (QD) for 7 days, for a 4 week period at a dose of 100 or 200 mg/kg. Mice were observed daily and body weight measurements and signs of stress (e.g. lethargy, ruffled coat or ataxia) were monitored. Having previously determined the maximum tolerated dose did not exceed 200 mg/kg in Rag-2M mice none of the mice treated with either ILK inhibitor showed any indication of toxicities at the 100 or 200 mg/kg dose. Electronic calipers (Mitutoyo corp., Japan) were used to measure tumors and the mean tumor size (mm^3) was determined using the formula ½[length (mm)] x [width (mm)]^2. The tumor size per mouse was used to calculate the group mean tumor size ±SE (n=6 mice). The results are a representative graph of at least two experiments.

2.5. Analysis of Isolated Tumor Tissues

Note that for BrdUrd, Hoechst and EF5 labelling mice were injected either i.v., or i.p. either 20 minutes, 1.5 or 3 hrs before sacrifice. Mouse tumors were collected at the indicated time points (e.g. 1 day after the final treatment) approximately 1/4 of the tumor was fixed in formalin. Paraffin-embedded tissues (1/4 of the tumor) were sectioned using a microtome and were stained using hematoxylin & Eosin (H&E). The other half was used for TUNEL (see next

section), and/or tissue microarray (TMA) analysis (Dr. Huntman, Ashish Rajput) and/or immunohistochemistry (Criterion labs) for floating sections was performed using anti-ILK, anti-phospho-PKB/Akt Ser473 and anti-PTEN, anti-IgG was used as a negative control (New England Biolabs, Canada) antibodies according to the manufacturers instructions. All tissue sections and subsequent staining was carried out by Criterion Laboratories (Vancouver, BC).

Terminal deoxynucleotidyl transferase-mediated biotinylated UTP nick end labeling (TUNEL)

For the terminal deoxynucleotidyl transferase-mediated biotinylated UTP nick end labeling (TUNEL) experiments, a Promega in situ Apoptosis kit was used according to the manufacturer's instructions and immunocytochemical analysis was performed.

Tissue Microarray (TMA) Construction.

Formalin-fixed, paraffin-embedded U87MG xenograft glioblastoma cancer tissue blocks were used to construct a TMA as described previously [134-135]. Briefly Core cylinders (0.6 mm diameter) were punched from initial formalin-fixed paraffin embedded blocks of U87MG xenograft tumors and deposited into smaller "microarray" paraffin blocks using a specific arraying device (Beecher Instruments, Silver Spring, MD) to create TMA blocks. Sections from the TMA blocks were then transferred onto glass slides for immunohistochemical analysis. TMAs contained, on average, 28 tissue cores per slide, with a total of 3 slides, 1 slide per marker.

TMA Immunohistochemistry, Scoring, and Analysis.

TMA sections were blocked with 3% hydrogen peroxide and incubated with mouse monoclonal or rabbit polyclonal antibodies against human integrin-linked kinase (ILK), vascular endothelial growth factor (VEGF) and hypoxia inducible factor-1 alpha (HIF-1α) followed by detection with the Envision system (Dako, Carpinteria, CA) and hematoxylin counterstaining. Note that TMA construction and staining were performed by Dr. David Huntsman.

CD31 and EF5 Immunohistochemistry.

Tumor cryosections (10 μm thick) were cut with a Cryostar HM560 (Microm International GmbH, Walldorf, Germany), and either air dried for 24 hours, then fixed in a 1:1 mixture of acetone-methanol for 10 minutes at room temperature, and blocked with 3% H_2O_2. Vasculature was stained using a platelet/endothelial cell adhesion molecule/CD31 antibody (1:100 dilution; BD PharMingen, San Diego, CA). An Alexa 546 goat anti-rat secondary (1:50 dilution; Molecular Probes) was used to detect CD31. Serial sections of tumors were fixed with ice-cold acetone for 5 minutes, air-dried, and stained with ELK3-51-CY3 antibody to detect EF5 adducts according to procedures described elsewhere [136]. Slides then were mounted with PBS and imaged (see Image Acquisition).

BrdUrd Immunohistochemistry.

After the slides were imaged for Hoechst and CD31 they were rinsed in PBS, placed in distilled water for 10 minutes, and then treated with 2 mol/L HCl at room temperature for 1 hour, followed by neutralization for 5 minutes in 0.1 mol/L sodium borate. Slides then were washed in distilled water and transferred to a PBS bath. Subsequent steps were each followed by a 5-

minute wash in PBS. Incorporated BrdUrd was detected using a monoclonal mouse anti-BrdUrd (1:200 dilution, clone BU33; Sigma), followed by an anti-mouse peroxidase conjugate antibody (1:100 dilution; Sigma) and a metal enhanced DAB substrate (1:10 dilution; Pierce, Rockford, IL). Slides then were counterstained with hematoxylin, dehydrated, and mounted using Permount (Fisher Scientific, Hampton, NH) before imaging.

Image Acquisition.

A motorized stage allowed for tiling of neighboring microscope fields of view. Images were captured with a fluorescence microscope (III RS; Zeiss, Oberkochen, Germany) with a cooled monochrome charge-coupled device video camera (model 4922; Cohu, San Diego, CA), frame grabber (Scion, Frederick, MD), a custom-built motorized x-y stage, and customized NIH Image software (http://rsb.info.nih.gov/nih-image/) running on a G4 Macintosh computer (Apple, Cupertino, CA). Serial sections were imaged for Hoeschst, and labeled with EF5 and Hematoxylin , whereas all other sections were stained with CD31, Hoechst and BrdUrd. Once immunostained for CD31, slides were imaged under PBS using a 510- to 555-nm excitation filter and a 575- to 640-nm emission filter. The slides then were immunostained for BrdUrd, and bright field images of BrdUrd positive staining were obtained. Once the images were acquired, the layers were stacked; the CD31 and Hoeschst and BrdUrd layers were thresholded; and a composite color image was produced with the grayscale BrdUrd/tissue layer.

Image Analysis.

Using the NIH Image software application and algorithms which were generously provided by Dr. Andrew Minchinton, images of EF5 fluorescence, CD31 fluorescence, and BrdUrd/tissue

staining from each tumor section were overlaid, and areas of necrosis and staining artifacts were removed. Hoeschst 33442 positive regions were identified by selecting all pixels that were 12 SD above the tissue background. For CD31 and BrdUrd images positive staining were selected for all of the pixels that were 5 and 2.5 SD above background levels respectively. Threshold levels were kept constant for all sections. CD31-positive regions that were <5 μm^2 in size were considered artifacts and removed from the analysis. The fraction of perfused vessels was determined by comparing CD31 and Hoeschst labeling of vasculature, CD31-positive vessels were considered perfused if >2% pixels of each CD31 positive object were also Hoechst 33342 positive.

2.6. Statistical Analysis

All of the statistical analyses were performed using the STATISTICA software program. For multiple comparisons, Post-hoc analysis using the Tukey-Kramer test was performed. Data were considered significant for P value < 0.05. The *in vivo* experiments were performed using an n of 6 mice per group and represent the mean ±SEM._Outcome variables such as tumor size, semi-quantitative analysis involving immunhistochemistry were in some cases expressed as 95% confidence intervals.

CHAPTER 3

INHIBITION OF ILK IN PTEN-MUTANT HUMAN GLIOBLASTOMAS INHIBITS PKB/AKT ACTIVATION, INDUCES APOPTOSIS, AND DELAYS TUMOR GROWTH*

3.1. Introduction

Glioblastoma multiforme (GBM) is the most common malignant brain tumor of adults, and has the distinction of being one of the most lethal with a median survival of 9 to 12 months [71]. The poor prognosis associated with GBM are due in large part to a lack of treatment options that consider the basic cancer biology that make GBM resistant to current therapies. In recent years, more attention has been given to signal transduction pathways that play key roles in the molecular pathogenesis of low grade astrocytomas in their progression to GBM.

PTEN/MMAC (phosphatase and tensin homologue on chromosome 10/mutated in multiple advanced cancers) is a tumor suppressor gene located on chromosome 10q23 [137-138] that is mutated at a high frequency in glioblastomas [139] and is known to regulate the phosphatidylinositol-3'-kinase (PI3K)/AKT pathway [140]. A homozygous disruption of *PTEN* results in embryonic lethality in mice, and germ-line mutations in *PTEN* are associated with the development of Cowden's disease and Bannayan-Zonana syndrome [141-143]. The frequency of *PTEN* mutation in glioblastomas, which has been shown to be as high as 80% [113], results in constitutive activation of PKB/AKT. PKB/AKT is a cell survival protein kinase that mediates its activity through various downstream effectors resulting in cell migration, cell cycle progression and an inhibition of apoptosis. In addition, *PTEN* mutation and increased PKB/AKT activity have been correlated with poor prognosis in glioma patients [144-145].

* A version of this chapter has been published. Edwards, L., Thiessen, B., Dragowska, V., Bally, M., Dedhar, S. (2005) Inhibition of ILK in PTEN-mutant human glioblastomas inhibits PKB/Akt activation, induces apoptosis, and delays tumor growth. Oncogene 24: 3596-3605. All work presented here is my work with indicated contributions.

Integrin linked kinase (ILK) is a serine -threonine protein kinase containing four ankyrin-like repeats [86] which are found at the NH_2 terminus of ILK with a pleckstrin homology (PH)-like motif, and a catalytic kinase domain at its COOH terminal domain. ILK is a key component of cell-extracellular matrix (ECM) adhesion and has been shown to anchor to integrins by interacting at its C-terminal domain to the cytoplasmic domain of β1 and β3 integrin subunits [86]. ILK also appears to interact with growth factor receptors via an adapter protein called PINCH (particularly interesting new cysteine-histidine-rich protein) which binds to Nck-2, a Src homology 2(SH2) and SH3 domain-containing adapter protein [146]. Since ILK can mediate signal transduction activity through its binding to β1 and β3 integrins, and the bridging of growth factor receptors via PINCH, ILK plays a key role in facilitating various cell signaling pathways. For example, ILK is involved in cell migration [147], cell cycle progression [92], growth and inhibition of apoptosis [90]_-_essentially the same cellular activities mediated by PKB/AKT. ILK therefore serves as an intermediate between PTEN regulation and PKB/AKT activation. ILK has also been shown to have a potential oncogenic role giving rise to mammary tumors in transgenic mice [101], to be expressed in neuroblastoma cells, and may play a role in Alzheimer's disease by controlling tau phosphorylation [148]. Knock-down of ILK protein by dominant-negative ILK and wild type PTEN has resulted in the inhibition of PKB/AKT activity and apoptosis in prostate cancer cells [90]. Recently, ILK regulation by PTEN has been shown in glioblastomas *in vitro* [149]. Studies here confirm that ILK and PKB/AKT are constitutively activated in human glioblastoma cells lacking PTEN expression. In addition, transfection of ILK antisense or wild-type PTEN into these cells dramatically inhibits serum independent PKB/AKT-Ser-473 phosphorylation as well as PKB/AKT kinase activity, and leads to apoptosis or apoptosis sensitivity. Inhibition of ILK activity by a small molecule ILK inhibitor also

inhibits serum-independent PKB/AKT-Ser-473 phosphorylation. Treatment of U87MG xenograft tumors with an antisense oligonucleotide that targets ILK results in tumor growth delay. These data demonstrate that ILK is critical for the PTEN-sensitive regulation of PKB/AKT-dependent cell cycle progression and cell survival, and is likely a valuable molecular target for the treatment of glioblastoma multiforme.

3.2. Hypothesis

Loss of *PTEN* has been associated with several cancers [150]. The molecular pathway that is, in part, responsible for this is the PI3-kinase pathway, where loss of *PTEN* results in constitutively active ILK which facilitates PKB/AKT phosphorylation at Ser473. This pathway has been shown to exist in prostate cancer. Due to the high rate of *PTEN* loss in the brain cancer glioblastoma multiforme, we propose this pathway is important in glioblastoma progression and inhibiting ILK activity will decrease cancer progression.

The research objectives are the following:

1) To examine the regulatory role of ILK in glioblastomas with respect to PTEN
2) To investigate the relationship between ILK and PKB/AKT activation
3) To determine the effects of ILK inhibition *in vitro* and *in vivo* on tumor growth and cell death
4) To investigate ILK as a potential therapeutic target in glioblastoma multiforme

3.3. Results

3.3.1. ILK Activity and PKB/Akt-Ser-473 Phosphorylation in *PTEN*-Mutant Human Glioblastoma Cells

There is now extensive evidence that mutational inactivation of the tumor suppressor *PTEN* occurs frequently in glioblastomas [130][131][144]. *PTEN* mutation leads to elevated levels of the PI3-kinase product phosphatidylinositol-3,4,5 triphosphate [$PI(3,4,5)P_3$] and increased phosphorylation of PKB/AKT on both Thr-308 and Ser-473 [91]. The purpose of these studies was to examine whether ILK regulates PKB/AKT in glioblastoma cells. Three glioblastoma cell lines were used, two *PTEN* negative, U251 and U87MG, and a *PTEN* positive cell line, SF-188, as shown in Fig 3.1A. PKB/AKT-Ser-473 phosphorylation levels are high in glioblastoma cell lines [151], in association with *PTEN* inactivation. In order to determine if ILK, in accordance with its role as an upstream regulator of PKB/AKT activation was also highly active with *PTEN* mutation, we examined ILK activity in these cell lines. This was measured by an ILK kinase assay which used myelin basic protein (MBP) as a substrate. ILK activity was assessed in the *PTEN* positive cell line SF-188 (Fig. 3.1B) and the *PTEN* negative cell line U251 (Fig. 3.1C) cultured under serum starved and serum re-feeding conditions. Incorporated

[^{32}P]-ATP on MBP was detected by phosphoimaging and quantified by densitometry (Fig. 3.1B and 3.1C), IgG controls for each cell line (first column) are provided for comparisons. ILK activity was elevated in the *PTEN* positive SF-188 cells when cultured in serum containing media (Fig. 3.1B). This increase in ILK activity was associated with PKB/AKT phosphorylation (gel, Fig 3.1B). ILK activity was low in the absence of serum

Figure 3.1

(A) Expression of endogenous PTEN in SF-188, U87MG and U251. Evaluation of ILK activity and PKB/AKT-Ser473 phosphorylation under serum starved and serum refeeding conditions in SF-188 *(B),* U251 *(C)* glioblastoma cells. To evaluate stimulation of ILK activity, cells were serum starved for 24 hrs, re-fed with serum for the indicated time period, and then analyzed for ILK activity by using myelin basic protein (MBP) (B & C bar graphs).

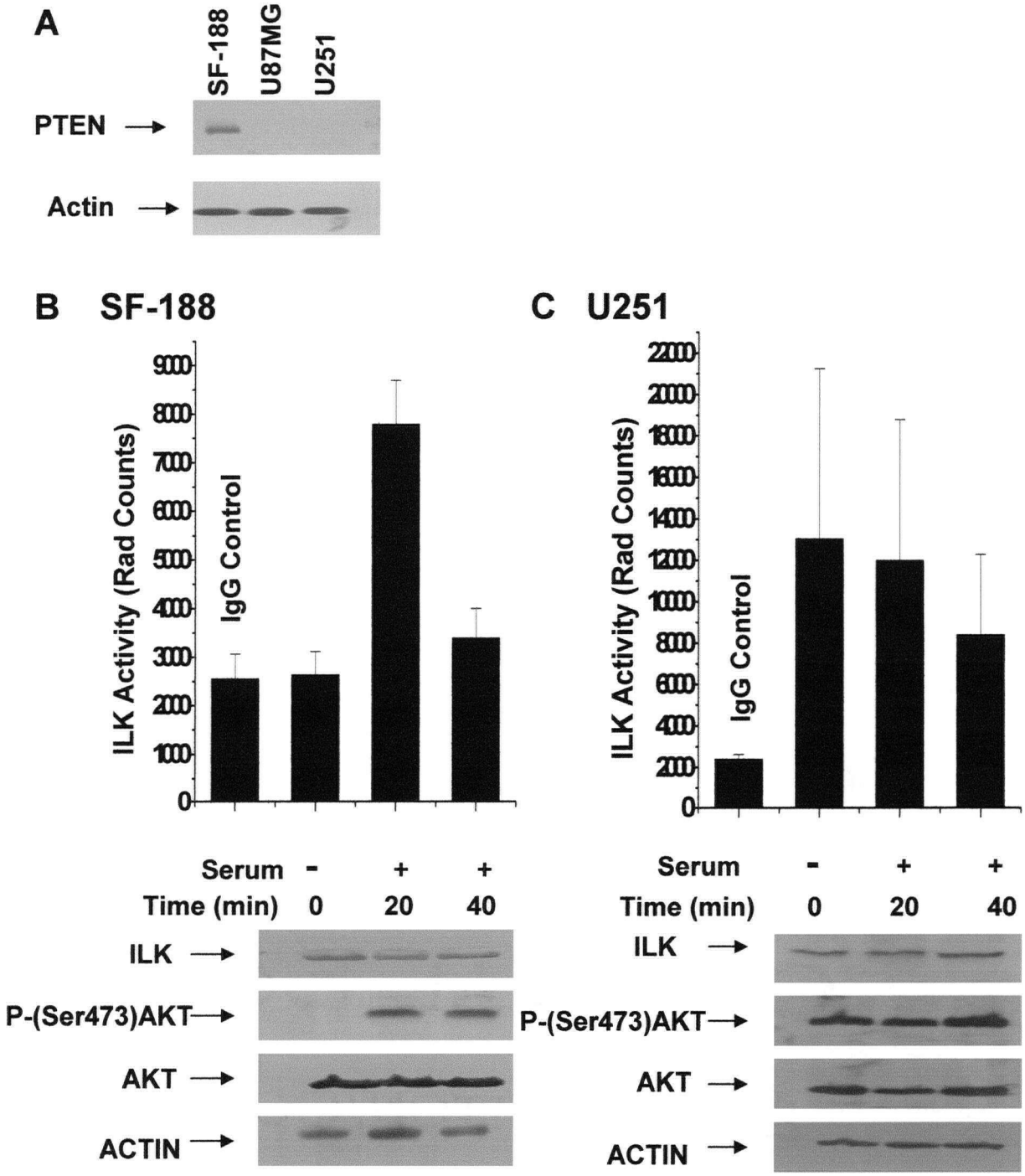

and there was no measurable PKB/AKT phosphorylation as determined by Western blot analysis. Total ILK and PKB/AKT levels did not change regardless of whether cells were cultured in the absence or presence of serum (Fig. 3.1B). ILK activity is rapidly stimulated by serum and then starts to decrease after 40 minutes to basal levels, consistent with previous studies showing rapid ILK activation and decreasing activity to basal levels after 40 min while maintaining the cell survival activity of PKB/AKT [87] (Fig. 3.1B). In contrast, ILK activity was high in the *PTEN*-negative U251 cells obtained from cultures in the presence or absence of serum (Fig. 3.1C). High ILK activity was associated with the presence of phosphorylated (Serine473)AKT (Fig. 3.1C). Consistent with the SF-188 cells, total ILK and PKB/AKT were not affected by the culture conditions. These data demonstrate that with the loss of *PTEN*, regulation of ILK and PKB/AKT activity is independent of the culture conditions (starved vs re-feeding). To determine the causal relationship between the regulatory loss of *PTEN* and the resulting ILK activity and subsequent PKB/AKT activity, *PTEN* negative U87MG cells transfected with an ecdysone-inducible [152] wild-type-*PTEN* retroviral construct (designated here as U87.23) were obtained. The ecdysone-inducible expression system allows the expression of the *PTEN* gene in the presence of muristirone A. Consistent with previous reports, a concentration of 0.5 μM of muristirone A allows for the full expression of *PTEN* (Fig. 3.2). The ILK and PKB/AKT activity of U87.23 with inducible *PTEN* was compared to that of the empty vector U87EVG retroviral construct in the presence and absence of muristirone A. When evaluating ILK activity (histogram), the vector control exhibited increased activity relative to the IgG control. Assessing the ILK activity in the *PTEN* transfected cell line in the absence of muristirone showed an increase in ILK activity, albeit not as high as that observed in the vector control.

Figure 3.2

The affects of PTEN induction on U87 cells transfected with various PTEN constructs. U87 empty vector (U87EV) and U87.23 (with wild-type PTEN) were induced with muristirone A where full PTEN expression (48 h) was achieved at 0.5 μM. Decreasing ILK activity (see bar graph) corresponds to increasing HA-tagged PTEN expression and decreasing PKB/AKT activity(see Western analysis). Total PKB/AKT, actin and ILK were also measured as loading controls. It should be noted that ILK levels appear to vary somewhat and may affect ILK and PKB/AKT activity. This may be due to retroviral transfection.

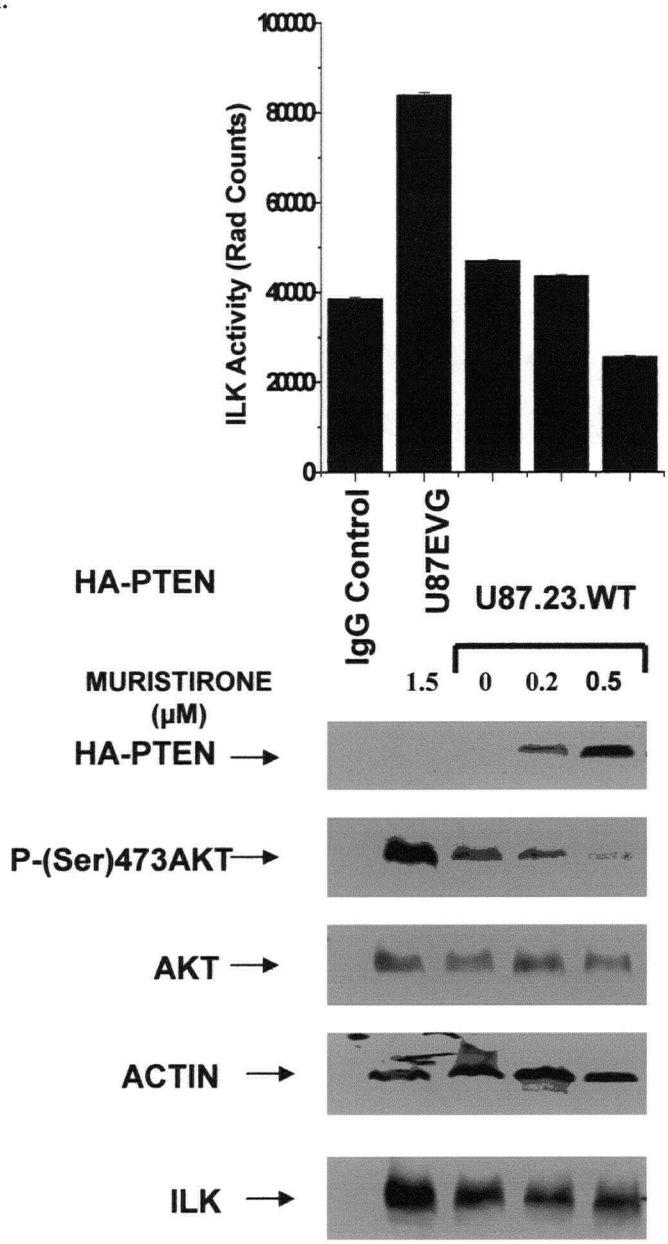

This may be due to a low level of expression of PTEN, which was not detected using the immunoblot analysis methods described. The ILK activity was reduced significantly in U87.23 cells cultured with 0.5 μM muristirone. Decreasing ILK activity engendered by muristirone was associated with increased PTEN expression and decreased AKT phosphorylation expression (Fig. 3.2 gels). Total AKT protein levels did not change significantly regardless of whether PTEN was expressed or not. It should be noted that ILK levels appear to vary somewhat and may affect ILK and PKB/AKT activity. This may be due to retroviral transfection.

These data demonstrate the regulatory effects of PTEN on ILK activity and subsequently on PKB/AKT activity in glioblastoma cells.

3.3.2. The effect of ILK inhibition on glioblastoma cell survival

Since PKB/AKT is constitutively phosphorylated on Ser-473 in *PTEN*-mutant cells [90][151], and having shown that ILK activity correspondingly decreases with AKT phosphorylation with or without PTEN induction (Fig. 3.2) the next step was to determine if inhibiting ILK activity would result in inhibition of AKT phosphorylation. Two strategies were used to achieve ILK inhibition. A small molecule inhibitor QLT0267 (QLT, Vancouver, BC, Canada) was used and previous generations of this inhibitor have shown therapeutic activity in a variety of tumor models [123][128][153]; alternatively, an antisense molecule was used that we have shown to down regulate ILK expression effectively in glioblastoma cells [154]. As shown in Fig. 3A, increasing concentrations of the ILK inhibitor QLT0267 (i.e. 0-100 μM) resulted in decreased AKT phosphorylation on Ser473 in U87MG glioblastoma cells. We also assessed the impact of U87MG cells treated with an ILK targeted antisense oligonucleotide (ILKAS). The

first studies evaluated the impact of the ILKAS on ILK expression in comparison to various controls including untreated cells (Fig 3.3B; CNT), liposomal vector alone (Fig 3.3B; VEC) and a reverse ILK antisense sequence (Fig 3B; RILK). These data demonstrate that treatment with the ILK antisense (Fig 3.3B; ILKAS) inhibits ILK protein expression, as judged by ILK protein levels determined 24 hours post-transfection. A time course study suggested that ILKAS mediated suppression of ILK was greater at 24 hrs than at 12 hours and that ILK down regulation was associated with decreased (~60%) phospho-AKT at Ser-473 activity (Fig. 3.3C). Importantly, transfection of the U87MG cells (*PTEN* negative) with the ILK targeted antisense did not affect phospho-Akt at Thr-308, consistent with the conclusion that ILK specifically phosphorylates PKB/AKT at Ser473.

3.3.3. Inhibition of ILK induces apoptosis in *PTEN*-negative glioblastoma cells

It has previously been shown that ILK activity can be suppressed by non-steroidal anti-inflammatory drugs (NSAIDs), such as a COX-2 inhibitor, which can result in decreased glioblastoma cell viability [149]. Given that ILK inhibition leads to decreased activity of the cell survival kinase AKT, an examination into whether ILK inhibition would induce apoptosis was carried out. For this purpose, Annexin V-FITC/PI staining of ILKAS treated glioblastoma cells (U87MG and U251) was completed (Fig. 3.4A). U87MG cells were treated with ILKAS. Camptothecin, a known inducer of apoptosis, was used as a positive control. The results indicated that there were very few PI positive and Annexin-V positive cells in the U87MG control cultures (Fig. 4A, Top 1st panel). Our positive control (Fig. 4A top 4th panel), camptothecin treated U87MG cells indicated 56% labeling (lower right and upper right quandrants representing early and late apoptosis respectively).

Figure 3.3

(A) U87MG cells exposed to increasing concentrations (0, 5, 20, 50100 μM) of the ILK kinase inhibitorQLT0267 resulted in decreased PKB/Akt phosphorylation at Ser473 as detected by Western blot analysis. *(B)* Western blotanalysis of U87MG cells untreated (CNT, lane1) or transfected with liposomal vector (VEC, lane 2) or transfected with reverse ILK antisense (RILK, lane 3) or with ILKAS (ILKAS, lane 4) *(C)* Transfection of ILKAS into U87MG cells abrogated ILK protein levels over 24 h, with decreased phospho-PKB/AKT at Ser473 levels. Numbers indicated below each band represent a densitometric analysis where the proteins under investigation were normalized against the time 0 treated samples.

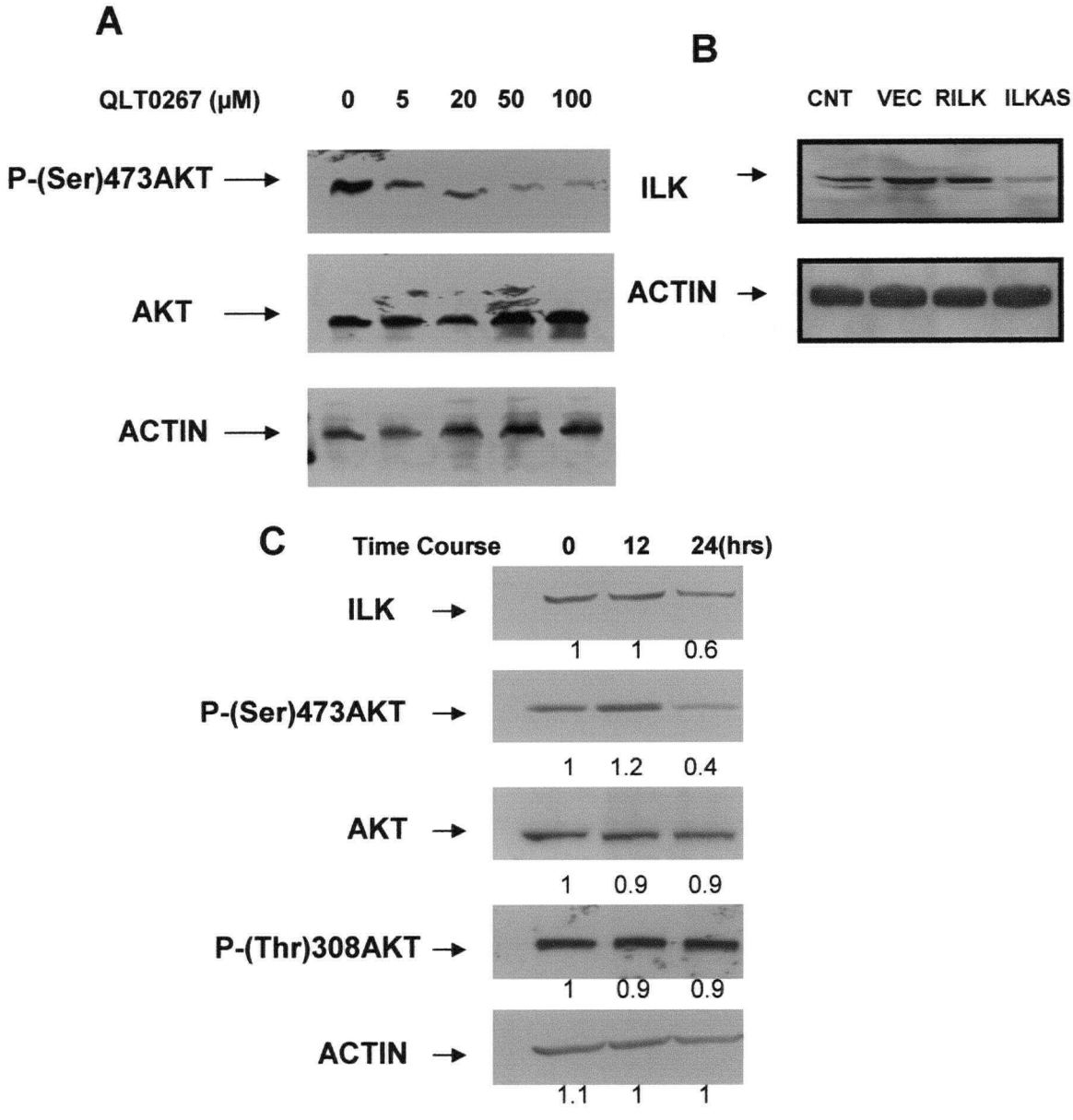

Figure 3.4

(A) In vitro assessment of apoptosis in U87MG (top panels) and.U251 (bottom panels) glioblastoma cells. FACs analysis via Annexin V-FITC/PI staining was used to observe the induction of apoptosis. Camptothecin was used as a positive control for Annexin V-FITC and PI staining. The induction of apoptosis was determined by flow cytometric analysis of Annexin V-FITC and PI-staining. Cells in the lower right quadrant indicate Annexin-positive, early apoptotic cells. The cells in the upper right quadrant indicate Annexin-positive/PI-positive, late apoptotic cells. Cells in the upper left quadrant PI-positive-necrotic cells, cells in lower left quadrant are Annexin/PI negative-live cells. Untreated cells (Control), reverse polarity ILK antisense treated cells (RILK), ILK antisense treated cells (ILKAS). *(B)* Flow cytometric/propidium iodide analysis revealed transfection of ILKAS into U87MG cells induced a greater degree of apoptosis than the RILK or the untreated U87MG cells. *(C)* Morphological changes associated with U87MG cells treated with ILKAS, reverse polarity antisense or untreated controls. Cells showing characteristic apoptotic morphology, nuclear DNA condensation or fragmentation can be seen (arrows) in the ILKAS treated cells and fewer cells are in the field than for the untreated and reverse polarity ILK antisense as shown by arrows. Note that U87MG cells were exposed to antisense oligonucleotides for a minimum of 12 h.

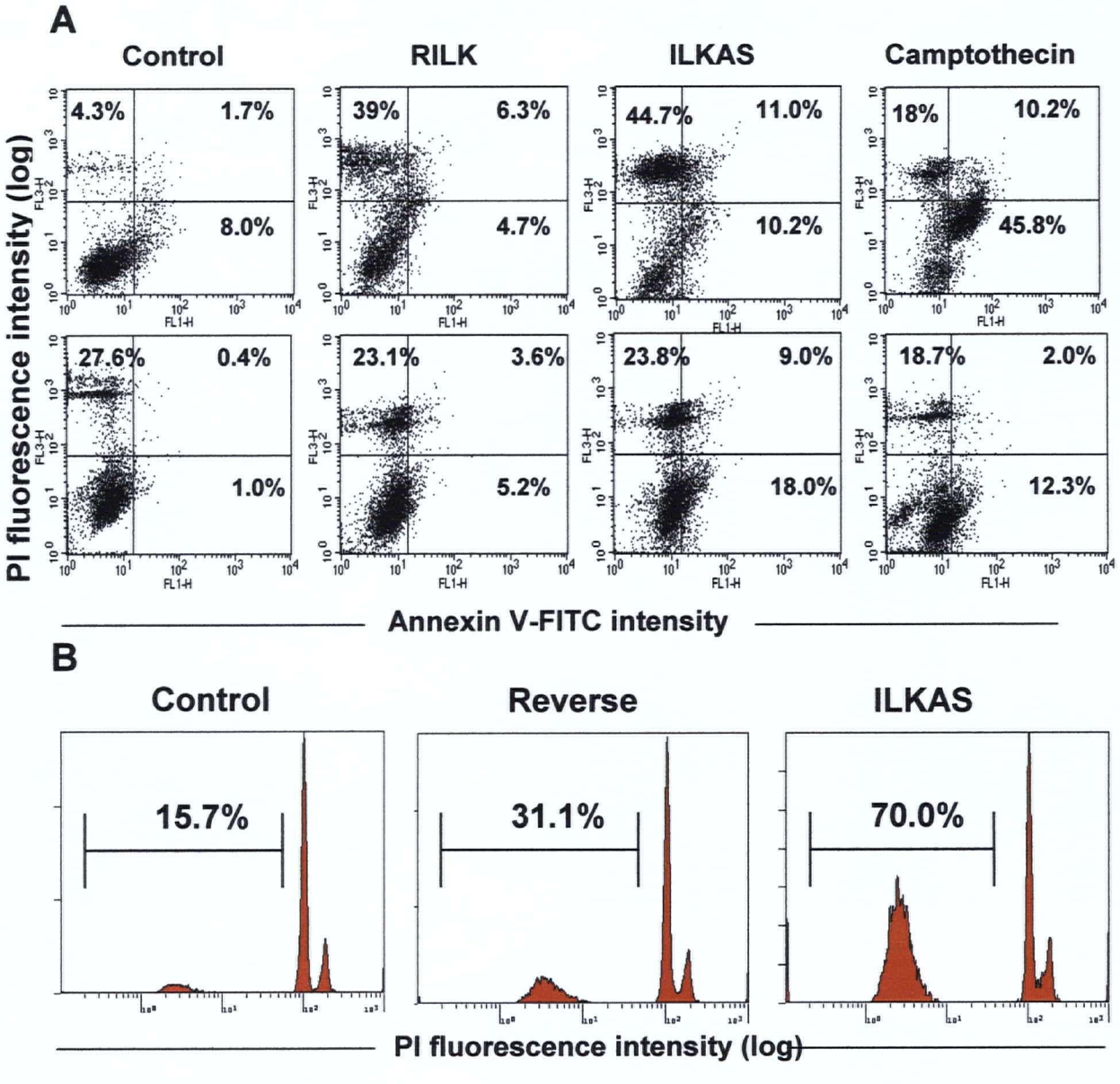
A
Control
RILK
ILKAS
Camptothecin
4.3%
1.7%
8.0%
39%
6.3%
4.7%
44.7%
11.0%
10.2%
18%
10.2%
45.8%
27.6%
0.4%
1.0%
23.1%
3.6%
5.2%
23.8%
9.0%
18.0%
18.7%
2.0%
12.3%
PI fluorescence intensity (log)
Annexin V-FITC intensity
B
Control
Reverse
ILKAS
15.7%
31.1%
70.0%
PI fluorescence intensity (log)
C

In comparison, approximately 21% of the U87MG cells treated with ILKAS were positive for Annexin-V labeling (Fig. 3.4A top 3rd panel). Less than 12% labeling was observed for the reverse polarity ILK (RILK) antisense treated U87MG cells (Fig. 3.4A top 2nd panel). Annexin V-FITC/PI staining was also completed for the U251 glioblastoma cells with 1.4% and 8.8% positive cells observed for untreated (Fig. 3.4A bottom 1st panel) and RILK (Fig. 3.4A bottom 2nd panel) treated cells respectively, while greater than 25% positive cells were noted for U251 cells treated with the ILKAS (Fig. 3.4A bottom 3rd panel), greater than our camptothecin positive control 14.3% (Fig. 3.4A bottom 4th panel).

To determine what the effects of antisense-mediated ILK inhibition were on the glioblastoma cells, we also examined U87MG cells by propidium iodide (PI) and DAPI staining (Fig. 3.4B-C). PI was used to stain the nuclear DNA content of control and ILKAS treated U87MG cells. Cells undergoing apoptosis and necrosis were identified as a population with decreased DNA content (the sub G_1/G_0 population). The sub G_1/G_0 U87MG treated with ILK antisense (Fig. 3.4B, far right panel) was compared to U87MG cells treated with a reverse antisense (Fig. 4B, middle panel) and U87MG untreated control cells (Fig. 3.4B, far left panel). The ILK antisense showed a 70% sub G_1/G_0 cell fraction of DNA by PI staining which is indicative of apoptosis, compared to a 15.7% sub G_1/G_0 population observed in untreated U87MG control cells. The sub G_1/G_0 cell fraction observed following treatment with the reverse antisense was higher than the untreated cell fraction (31.1% vs 15.7%). This is likely due to toxicity associated with the transfection method used. Regardless, the sub G_1/G_0 cell fraction observed when cells were treated with the reverse antisense was still substantially lower than that observed following treatment with of the ILK antisense.

To confirm whether transfection of glioblastoma cells with ILK antisense resulted in apoptotic cell death, we assessed the morphological changes of DAPI-stained U87MG cells (Fig. 3.4C). Nuclear fragmentation and chromatin condensation was seen in U87MG cells treated with the reverse antisense (Fig. 3.4C, middle panel) and to a lesser extent in untreated U87MG control cells (Fig. 3.4C, far left panel). Substantially more cells with fragmented nuclei and condensed chromatin were observed in U87MG cells treated with ILK antisense, indicative of late apoptosis (Fig 3.4C far right panel).

3.3.4. Antitumor efficacy of ILK antisense on *PTEN* negative glioblastoma U87MG tumor Xenografts

Although the small molecule ILK inhibitor is of interest, and *in vivo* studies assessing the activity of the small molecule inhibitor QLT0267 in murine models of glioblastoma are ongoing, we report here on the *in vivo* efficacy studies on ILKAS. Prior to initiating *in vivo* studies on *PTEN* negative glioblastoma tumors, we examined by immunohistochemistry the expression of PTEN and phospho-(Ser473)AKT in tumors generated following subcutaneous injection of the 3 glioblastoma cell lines in this study (Fig. 3.5). Tumors grown in Rag-2M mice were derived from the *PTEN* negative glioblastoma cell lines U87MG and U251 and the *PTEN* positive cell line SF-188. Similar to the Western blot analysis (Fig. 3.1A), PTEN staining (orange-red stain) was clearly seen in the *PTEN* positive SF-188 tumor section (Fig. 3.5A) but not in the *PTEN* negative U87MG (Fig. 3.5B) or U251 tumor sections (Fig. 3.5C).

Figure 3.5

Immunohistochemistry of SF-188, U87MG and U251 tumors generated in Rag-2M mice stained for PTEN (orange-red stain) and phosphorylation of PKB/AKT-Ser473 (orange-red stain) expression. PTEN expression was seen in the PTEN positive cell line SF-188 *(A),* and not seen in U87MG *(B)* or U251 *(C)* glioblastoma cells. PKB/AKT phosphorylation at Ser473 cannot be seen in thePTEN positive SF-188 glioblastoma cell line *(D)* but is seen in the PTEN negative glioblastoma cell lines U87MG *(E)* and U251 *(F).* IgG controls for PTEN *(G)* and phospho-PKB/AKT *(H)* IgG controls are shown above. Magnification 200X.

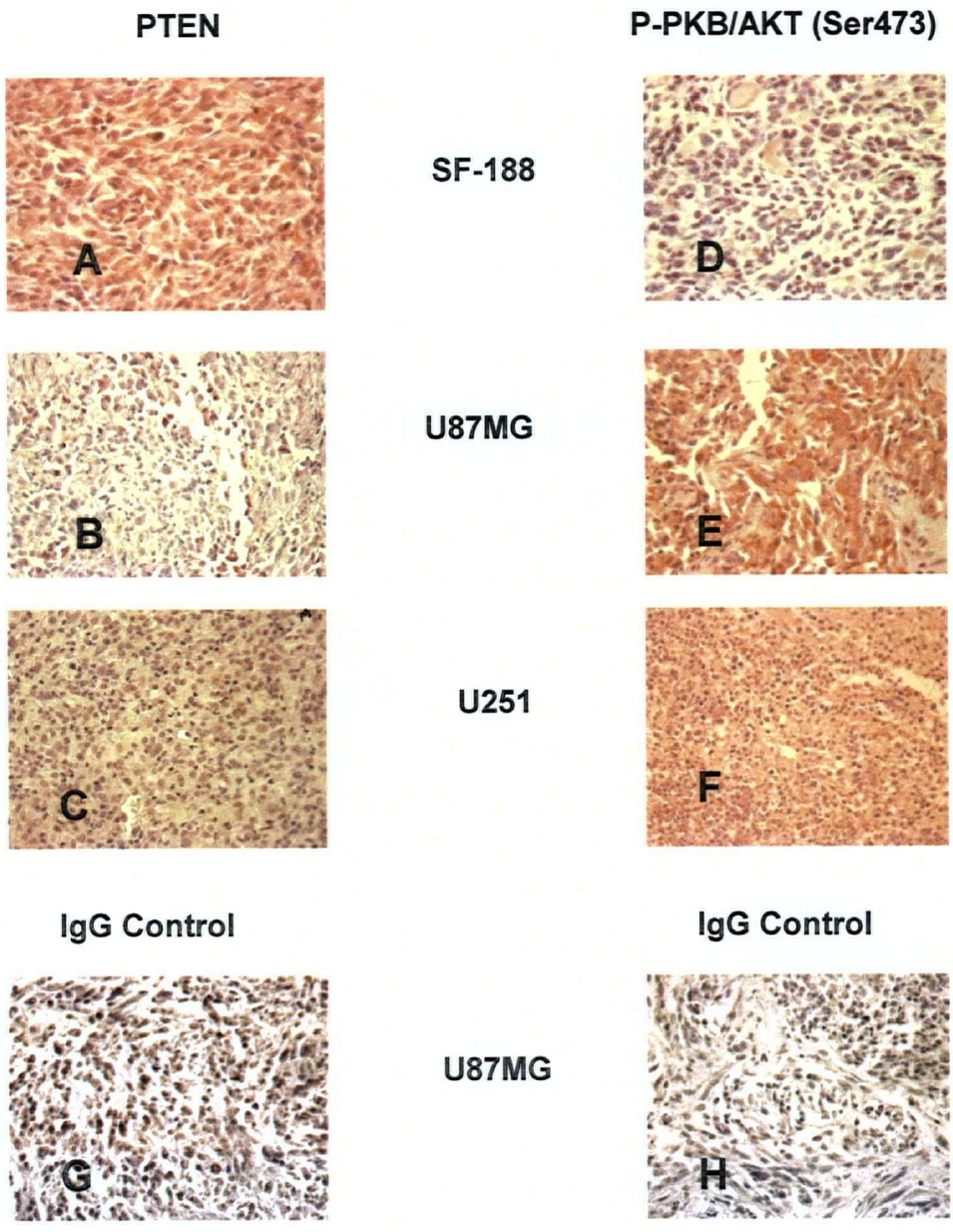

In addition, AKT phosphorylation staining specific for Ser473 was observed in the *PTEN* negative tumors U87MG (Fig. 3.5E) and U251 (Fig. 3.5F), but very little was observed in the *PTEN* positive SF-188 tumor section (Fig. 3.5D). This suggests that PTEN and PKB/AKT expression levels are consistent when comparing the *in vitro* and the *in vivo* results. Figs. 3.5G & H are representative negative IgG controls.

The antitumor effects of the ILK antisense were tested in Rag-2M mice bearing established (~100mg) subcutaneous (s.c.) xenografts of U87MG (*PTEN* negative) glioblastoma tumors. Saline treated control tumors grew reproducibly to an average size of 0.32 cm^3 (Fig. 3.6A). Treatment (qdx5 every week for 3 weeks) with a scrambled antisense (SCRAM 2) did not cause any significant change in tumor growth rate when compared to the saline control. When comparing the control animals to the ILKAS treated animals, the tumor size in the ILKAS treated group was significantly lower ($p<0.05$) at all measured time points. None of the mice treated with the ILKAS displayed signs of toxicity, and the ILKAS dose used was consistent with previous studies from our laboratory using antisense therapeutics [155-156]. To confirm the activity of ILKAS *in vivo*, western blots were carried out on harvested tumors from control and treated mice where tumors were harvested at the end of the 3 week treatment period (Fig. 3.6B). ILK protein levels were decreased in ILKAS treated mice (5 mg/kg) in contrast to untreated control tumors which showed no decrease in ILK protein levels. Mice treated with scrambled ODNs (5 mg/kg) exhibited no loss of ILK protein. To further evaluate ILKAS mediated therapeutic activity, ILK protein suppression and AKT phosphorylation were assessed using immunohistochemistry. Sections derived from isolated U87MG tumors were stained for ILK and phospho-AKT at Ser473 (Fig. 3.7).

Figure 3.6

(A) Representative study of tumor growth delay by ILKAS in Rag-2M mice bearing established U87MG xenograft tumors. ILKAS or a SCRAM control sequence were injected subcutaneously into Rag-2M miceand the resulting tumor growth curves were compared to saline treated control animals over a 3 week period. Bars: pretreatment (horizontal hatched bars),week 1 (grey bars), week 2 (black bars), week 3 (white bars). The tumor inoculation and treatment schedules are described in "Materials and Methods." All data are expressed as mean ±SE (n=6 mice/group) $p \leq 0.05$ for treatment groups compared with controls (saline) and these are indicated with an *. *(B)* Western blotting analysis of ILK and actin protein levels of harvested tumors from untreated, SCRAM2 and ILKAS treated Rag-2M mice were quantitated by densitometry. ILK and actin protein levels are normalized to untreated control tumors and values are shown below.

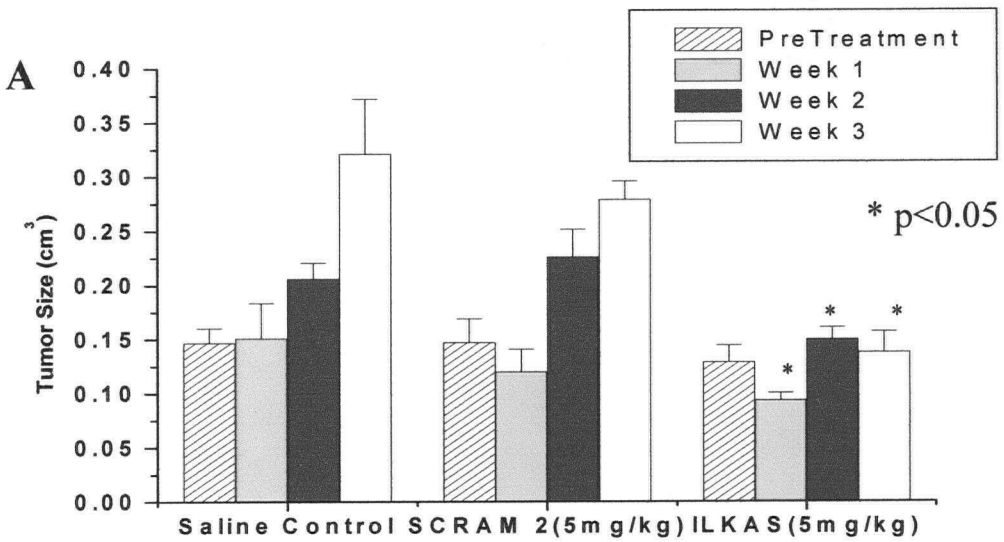

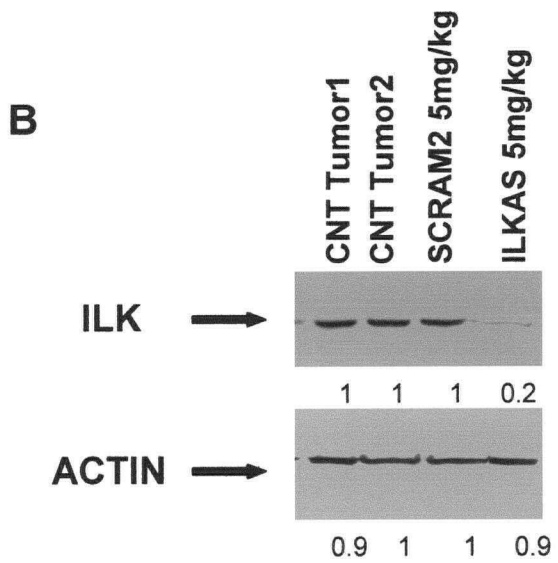

Figure 3.7

In vivo ILKAS affects on ILK and PKB/AKT-Ser473 expression in U87MG tumors. Immunohistochemistry of U87MG tumor tissue from Rag-2M mice day 41 post-inoculation. Untreated tumors stained for ILK and PKB/AKT-Ser473 expression *(B-E)* show heavy staining (brown) compared to treated ILKAS tumors stained for ILK and PKB/AKT-Ser473 expression *(C-F).* ILKAS *(A)* and phospho-PKB/AKT *(D)* IgG controls are shown above. Magnification 100X.

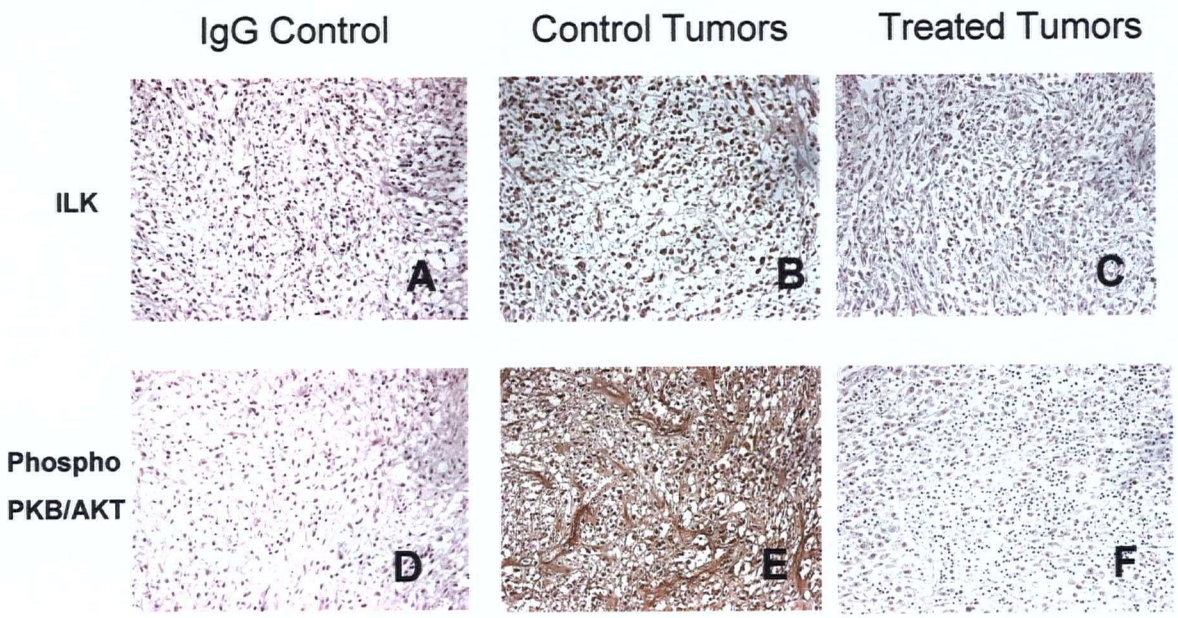

U87MG control tumors (saline treated) showed staining for ILK and PKB/AKT phosphorylated at Ser473 (Fig. 3.7B and 3.7E respectively). U87MG tumors obtained from ILKAS treated animals revealed a significant loss of ILK and phospho-(Ser473)AKT staining (Fig. 3.7C and 3.7F respectively). Figs 3.7A & D are representative IgG controls. These results indicate that the ILKAS used in these studies can mediate in vivo decreased tumor growth rates, decreased ILK expression and decreased phospho-(Ser473)AKT.

3.4. Discussion

PTEN mutation in glioblastomas has been shown to influence the PI3-kinase pathway [130] and more specifically PKB/AKT levels and activity [144], VEGF levels [128], cellular invasion [157] and cell cycle regulation [158]. Similarly, integrin-linked kinase has been shown to regulate PKB/AKT [100] in a PI3-kinase dependent manner [126]. This ILK regulated pathway affects cellular invasion [106] and cell cycle regulation [92]. Despite the parallel in cellular regulation between PTEN and ILK and the subsequent downstream PKB/AKT activity in glioblastomas, the role of ILK in glioblastoma cells has not been well described. The present study sought to characterize the role of integrin-linked kinase in glioblastoma cells *in vitro* and the potential for modulating constitutive ILK protein expression and activity by treatment with an ILK targeted antisense sequence. Preliminary results with a small molecule inhibitor of ILK are also provided. The *in vivo* data suggest ILK suppression, induced by treatment with antisense targeting ILK causes a tumor growth delay; It is possible that this approach will be sufficient to stabilize diseases but will not be able to promote tumor regression based on these results with well-established tumors (Fig. 3.6A). Consistent with other studies from this

laboratory [123][159], it is anticipated that molecularly targeted drugs need to be combined with other agents in order to obtain optimal therapeutic results such as tumor regression. The use of ILKAS for treatment of the brain cancer glioblastoma multiforme may for example, be most effective in combination with conventional drugs used in treating this disease (e.g. Temozolimide) or with other drugs targeting parallel pathways capable of compensating for ILK inhibition. Our approach involves targeting cell signaling pathways known to be involved in the progression of brain cancer and targeting via small molecule inhibitors or antisense in drug combinations that would ideally be synergistic. To this end, previous studies have shown that PD153035, an inhibitor of the highly expressed EGFR in glioblastomas, in combination with a small molecule inhibitor targeting ILK yielded a synergistic interaction and resulted in increased cell death [123]. However, in our previous study and in the current study it is important to note that in dealing with molecularly targeted drugs alone or in combination, it is critical to assess many therapeutic endpoints, particularly in defining drug efficacy and drug interactions which appear to be synergistic. Our lab is currently pursuing how to translate drug efficacy and drug interactions measured on the basis of cell based screening assays to preclinical studies of drug combinations and, eventually, to clinical trials. The later point is obviously critical, since use of the antisense against ILK may only result in patients with stable disease and this effect may not be sufficient to warrant further clinical development as a single agent. Yet the same drug may show substantial therapeutic effects in a combination setting. Regardless of how ILK inhibition is achieved, it is clear that it is an important therapeutic target and strategies assessing ILK inhibitors require serious consideration.

Integrin-linked kinase has been shown to be important in oncogenesis and is a principal mediator of cell signaling activity within the PI3- kinase cell signaling pathway. Integrin-linked

kinase has been associated with cell proliferation in ovarian cancer cells [160], ILK expression has also been shown to increase with prostate tumor grade [110], and is a potential diagnostic marker for Ewing's sarcoma and primitive ectodermal tumors [108]. It is clear that ILK plays a major role in cancer progression and glioblastomas are part of ILK's oncogenic repertoire.

CHAPTER 4

COMBINED INHIBITION OF THE PI3K/AKT AND RAS/MAPK PATHWAYS RESULTS IN SYNERGISTIC EFFECTS IN GLIOBLASTOMA CELLS*

4.1. Introduction

Two key cell signaling molecules have been implicated in glioblastoma multiforme (GBM) pathogenesis (due to their mutation, gene amplification or overexpression); the epidermal growth factor receptor, (EGFR) [161] and the gene for phosphatase and tensin homologue (*PTEN*) [150]. *EGFR* mutation can result in increased levels of p21-Ras, leading to constitutive activation of the Ras/MAPK pathway, which is functionally important in glioma proliferation. Mutations of *PTEN* in glioblastomas have been observed in as few as 15% to as many as 70% of cases [162-164]; and loss of this tumor suppressor gene has been shown to result in high levels of PKB/AKT activation in GBM [151].

Integrin-linked kinase (ILK) is a serine/threonine kinase that is regulated in a PI3K dependent manner and can phosphorylate PKB/AKT *in vitro* [126]. Conditional knock-out of ILK with the Cre-Lox system indicated ILK is vital in PKB/AKT activation [100]. GW5074 is an inhibitor of Raf-1, such that Raf-1 cannot phosphorylate and thereby activate, MEK [165]. Similarly, U0126 inhibits MEK preventing MAPK phosphorylation [166-167]. This activity halts further signal transduction along the Ras/MAPK pathway. ILK antisense (ILKAS) can inhibit ILK protein production and should therefore reduce ILK activity. This will in turn reduce phosphorylation and hence activation of PKB/AKT and further signaling along the PI3K/Akt pathway.

* A version of this chapter has been provisionally accepted. Edwards, L., Thiessen, B., Hu, Y., Dragowska, WH., Hu, Y., Yeung, JHF., Dedhar, S., Bally, M. (2005) Combined Inhibition of the PI3K/Akt and Ras/MAPK pathways results in synergistic effects in glioblastoma cells. Mol Can Ther. All work presented here is my work with indicated contributions.

Since the Ras/MAPK and PI3K/AKT pathways have both been implicated in glioblastoma progression [168], it would be anticipated that therapies that target both of these cell signaling pathways may lead to an effective treatment option.

Drug combinations are not new to GBM treatment, but drug combinations which yield specific drug effects, i.e synergism, additivity or potentiation through the use of small molecule inhibitors and/or antisense for the treatment of glioblastoma multiforme to our knowledge have not been studied extensively. This study sought to investigate such drug interactions with ILK as a primary target for combination therapy of GBM.

4.2. Hypothesis

Targeting ILK *in vitro* and *in vivo* leads to cell cycle arrest, cell death and tumor growth delay. Although the inhibition of ILK has led to stable disease *in vivo*, combination molecular targeting involving ILK and another cell signaling target known to be involved in glioblastoma progression, should improve upon a mono-therapeutic approach, especially when synergy is achieved with a drug combination of interest.

The research objectives are the following:

(1) To evaluate anticancer targeting of the PI3-kinase regulated ILK alone and in combination therapy.

(2) To determine if combinations targeting specific cell signaling pathways involved in glioblastoma multiforme can result in a synergistic effect.

(3) To determine whether ILK in combination is more effective than a mono-therapeutic approach

4.3. Results

Disruption of the PI3K/AKT pathway was achieved by using an ILK targeted antisense oligonucleotide sequence (ILKAS), which was transfected into SF-188 cells. Results, shown in Figure 4.1A, indicate that ILKAS transfection resulted in knock-down of ILK protein and decreased PKB/AKT phosphorylation on Ser-473, but not Thr-308 (Fig. 4.1A, lanes 3 and 4). Transfection with the reverse ILK antisense (RILK) did not decrease ILK or phospho-PKB/AKT protein levels (Fig. 4.1A, lane 3), nor did the vector control affect ILK or phospho-PKB/AKT levels (Fig. 4.1A, lane 2). These data demonstrate, *in vitro*, that the selected ILK targeted antisense can suppress ILK protein levels and decrease phospho-PKB/AKT activity. Treatment of SF-188 and U87MG cells with ILKAS, at doses ranging from 1 to 10 μM, decreased cell viability (Fig. 4.1B). At the highest concentrations tested (8 and 10 μM), the data suggested >80% decrease in cell viability. To determine whether the cytotoxic/cytostatic effects of ILKAS against glioblastoma cells could be enhanced when used in combination with GW5074, the effects of which have been previously described [165], a fixed-ratio of this combination (ILKAS/GW5074=1:2 mol:mol) was analyzed at and above the IC_{50} values of these individual agents. The Chou & Talalay median-effect method [116][169] was used to determine drug efficacy and the nature of the drug interaction. The dose-effect plot for U87MG cells, provided in Fig. 4.1C, showed that the combination of ILKAS (1-8 μM) with GW5074 (2-16 μM) exhibited an enhanced drug combination effect (decreased cell viability-labeled "effect", on the y-axis) relative to ILKAS and GW5074 used alone. The interactions were judged to be synergistic, with combination index (CI) values less than 0.25 (Fig. 4.1D). Similarly, the dose-effect plot and CI values for SF-188

Figure 4.1

Effects of ILK antisense (ILKAS) and the Raf-1 inhibitor GW5074 on SF-188 and U87MG glioblastoma cells. *(A),* Immunoblot analysis of SF-188 cells transfected with the indicated antisense, vector or untreated control. Equivalent amounts of protein (30μg/lane determined by Bradford assay) were resolved by 12% SDS-polyacrylamide gels. Cells were harvested 12-14 h post-transfection *(B),* Cell viability of SF-188 and U87MG glioblastoma cells treated with ILKAS (1-10 μM) was determined by the colorimetric (3-[4,5-Dimethylthiazol-2-yl]-2,5-diphenyl-tetrazolium bromide) MTT assay. *(C-F),* Dose effect and combination index plots to determine drug efficacy and interaction between ILKAS and GW5074. All assays were performed in triplicate at least two times. MTT data were obtained following treatment of cells with the indicated agents alone or in combination. Effective concentrations were analyzed using the CalcuSyn software (Biosoft, Freguson, MO) Cells were analyzed 24 h post-drug treatment. *(G),* Colony forming assay showing U87MG glioblastoma cells treated with ILKAS (5μM), GW5074 (15μM) as single agents or in combination (ILKAS 1μM/GW5074 2μM). All data are expressed as a mean ±SEM 6-well plates (three wells/condition) * $p<0.05$.

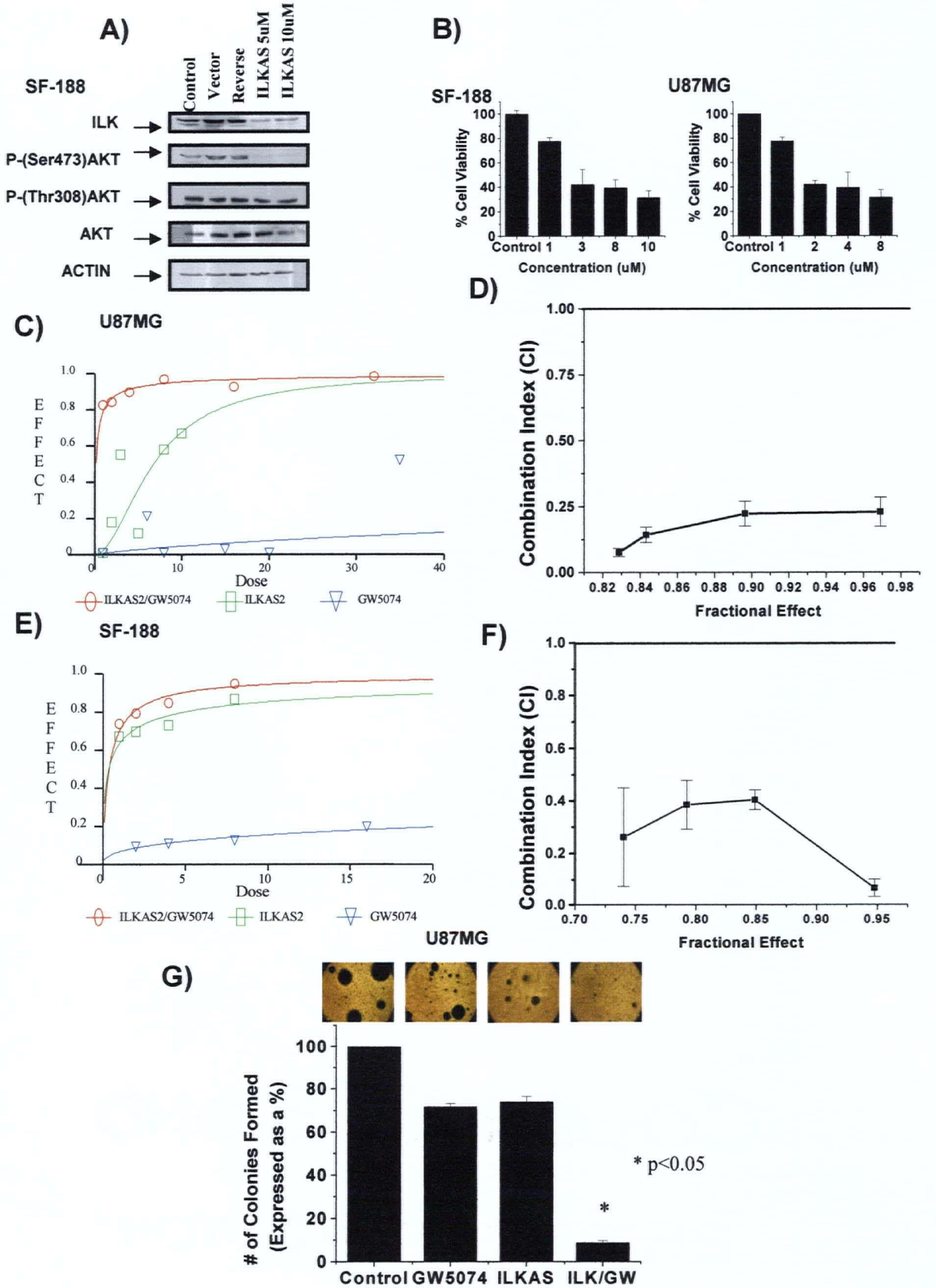
A)
SF-188
Control
Vector
Reverse
ILKAS 5uM
ILKAS 10uM
ILK
P-(Ser473)AKT
P-(Thr308)AKT
AKT
ACTIN
B)
SF-188
U87MG
% Cell Viability
Control 1 3 8 10
Concentration (uM)
Control 1 2 4 8
Concentration (uM)
C)
U87MG
EFFECT
Dose
ILKAS2/GW5074
ILKAS2
GW5074
D)
Combination Index (CI)
Fractional Effect
E)
SF-188
EFFECT
Dose
ILKAS2/GW5074
ILKAS2
GW5074
F)
Combination Index (CI)
Fractional Effect
G)
U87MG
# of Colonies Formed (Expressed as a %)
Control GW5074 ILKAS ILK/GW
* p<0.05

cells (Figs. 4.1E and 4.1F, respectively) indicate that the combination of ILKAS (1-8 μM) and GW5074 (2-16 μM) also resulted in synergy, with CI values less than 0.4 (Fig. 4.1F).

The data summarized thus far suggest a greater than additive effect on U87MG and SF-188 glioblastoma cells treated with ILKAS in combination with GW5074. These results were assessed on the basis of a MTT assay endpoint. It was important confirm that these effects would also occur when a different assay endpoint was used. A clonogenic assay was, therefore, used to determine the impact of the drugs, alone and in combination, against U87MG cells. U87MG cells were treated with ILKAS, GW5074 or the combination of the two and subsequent examination of clonogenic survival was analyzed (Fig. 4.1G). In these studies, the ILKAS added at a dose of 5 μM resulted in a 22% reduction in colony formation (3^{rd} bar graph Fig. 4.1G). GW5074, when added alone, resulted in approximately 25% colony formation inhibition when added at 15 μM (2^{nd} bar graph, Fig 1G). Addition of both ILKAS and GW5074 at a fixed drug ratio (1 μM-ILKAS/2 μM-GW5074) that was shown to be synergistic when measured using the Chou and Talalay median effect method [169] engendered a 92% reduction in colony formation (4^{th} bar graph Fig. 4.1G) . These results are consistent with the dose reduction effects associated when using agents that interact synergistically to achieve a defined effect level. In order to further evaluate the effect of this combination, apoptosis induction was assayed by measuring Annexin-V labeling of externalized phosphatidylserine (PS). The combination added at synergistic fixed-ratio doses was used and the effects achieved.

Figure 4.2

Apoptosis assessment in ILKAS and combination treated cells. *(A),* SF-188 glioblastoma cells were isolated and exposed to 2μM GW5074 ± 1μM ILKAS or left untreated for a minimum of 8hrs, where Camptothecin was used as a positive control for Annexin V-FITC and PI staining. The induction of apoptosis was determined by flow cytometric analysis of Annexin V-FITC and PI-staining. Cells in the lower right quadrant indicate Annexin-positive, early apoptotic cells. The cells in the upper right quadrant indicate Annexin-positive/PI-positive, late apoptotic cells. *(B),* SF-188 cells were treated with 2μM GW5074 ± 1μM ILKAS or left untreated and harvested and the percentage of cells with sub G_1/G_0 (apoptotic/necrotic) DNA content was measured by flow cytometric analysis of propidium iodide (PI) staining for 20,000 events. The percentages indicate dead cells. *(C),* Nuclear morphology of SF-188 cells treated with 2μM GW5074 ± 1μM ILKAS or left untreated following stained with DAPI and cytospun preparations. Arrows indicate where cell fragmentation, DNA condensation and apoptotic morphology is in response to treatment. Cells were viewed under fluorescence microscopy at 100X magnification.

A)

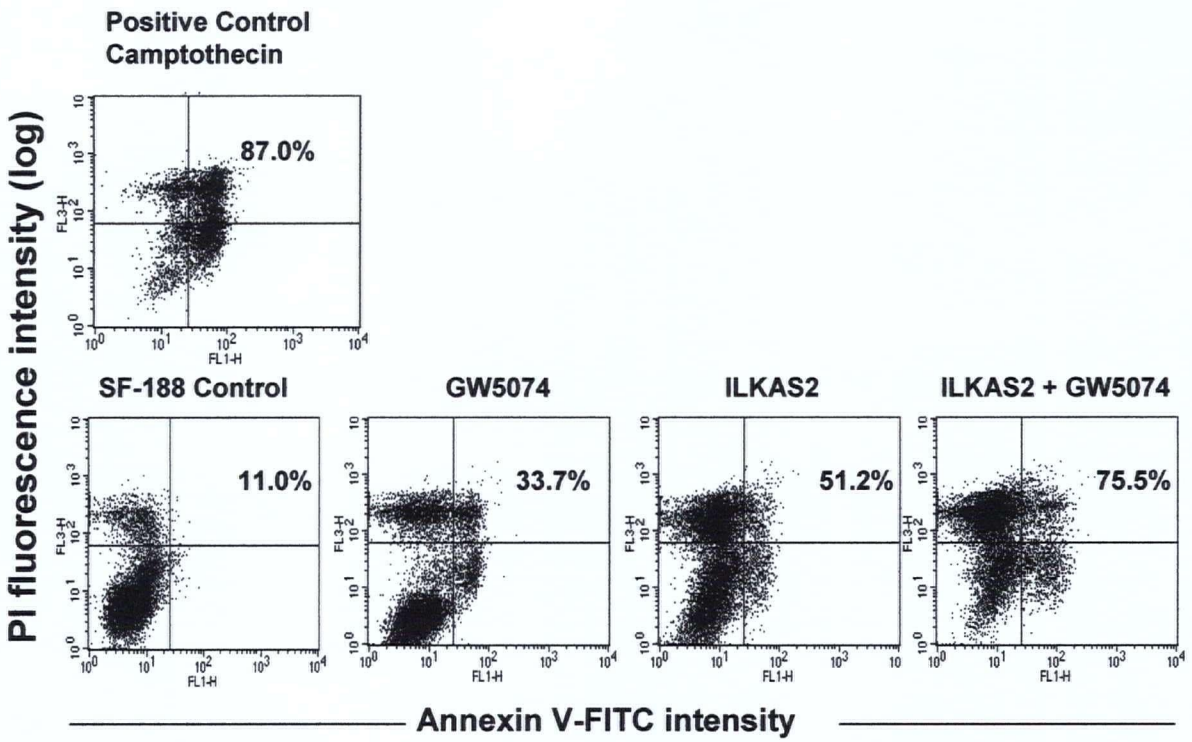
Positive Control
Camptothecin
87.0%
SF-188 Control
11.0%
GW5074
33.7%
ILKAS2
51.2%
ILKAS2 + GW5074
75.5%
PI fluorescence intensity (log)
Annexin V-FITC intensity

B)

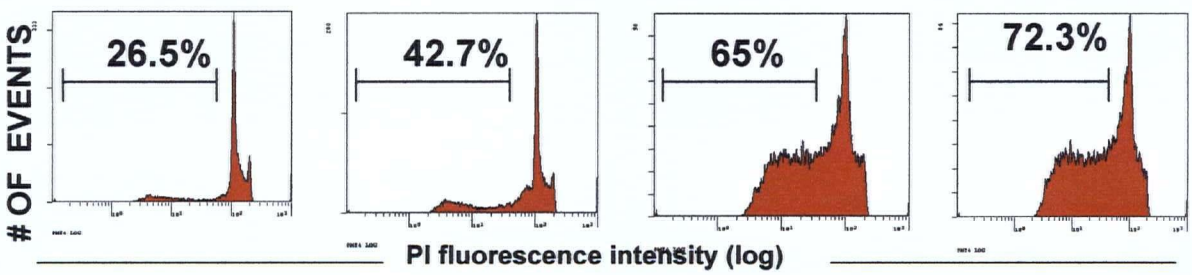
26.5%
42.7%
65%
72.3%
OF EVENTS
PI fluorescence intensity (log)

C)

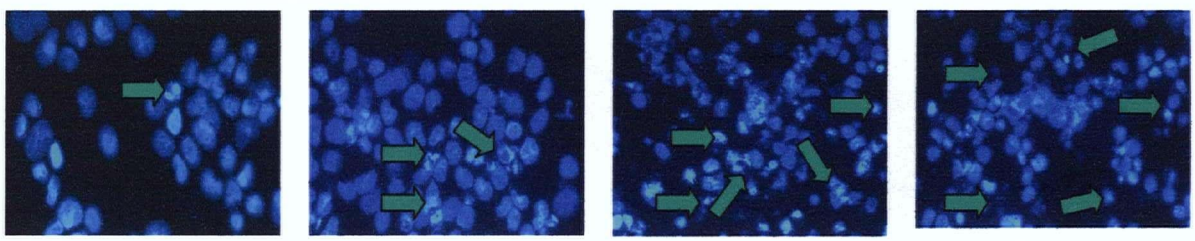

were compared to those measured with the single agents added at higher concentrations (Fig. 4.2). SF-188 glioblastoma cells were treated with the single agent ILKAS at 5 μM or the single agent GW5074 at15 μM in comparison to the drug combination of ILKAS at 1μM and GW5074 at 2 μM. Results for SF-188 are summarized in Figure 4.2. Annexin V-FITC staining (Fig. 4.2A), PI profile (Fig. 4.2B) and DAPI staining data (Fig. 4.2C). Camptothecin, a known inducer of apoptosis, was used as a positive control and untreated cells served as the negative control (Fig. 4.2A). Results of studies assessing SF-188 cells treated with ILKAS and/or GW5074 indicated that there were very few PI negative and Annexin-V positive cells in the control cultures (Fig 4.2A). Camptothecin treated cells exhibited 87.0% Annexin V labeling. Cells treated with ILKAS in combination with GW5074 showed a substantial amount of apoptosis observed by Annexin-V labeling. Cells treated with the combined drugs exhibited 75.5% Annexin-V labeling versus 51.2% and 33.7% measured for cells treated with the single agents ILKAS or GW5074, respectively. To further characterize the effects of ILKAS and GW5074 on glioblastoma cells, PI was used to stain nuclear DNA. Cells undergoing apoptosis and necrosis were identified as a population with reduced DNA content (the sub G_1/G_0 population). The sub G_1/G_0 cell population of SF-188 cells treated with the ILKAS/GW5074 (1:2 μM) combination was significantly higher than that observed when treating cells with ILKAS (5 μM) or GW5074 (15 μM) alone. This effect was achieved at a lower combined concentration than the single agents (Fig. 4.2B), a result that is again consistent with data suggesting that this might be a synergistic combination. To confirm whether transfection of glioblastoma cells with ILKAS alone and in combination with GW5074 resulted in apoptotic cell death, we examined the morphological changes of SF-188 cells by DAPI staining (Fig.

4.2C). No nuclear fragmentation or chromatin condensation in SF-188 control cultures was observed. Substantially more cells with fragmented nuclei and condensed chromatin, indicative of late apoptosis, were observed in cultures treated with ILKAS and the ILKAS/GW5074 combination (Fig. 4.2C see arrows). Having assessed the effects of targeting ILK in combination with the Raf-1 inhibitor GW5074, a relatively infrequently used inhibitor, we wanted to determine if a synergistic interaction could be achieved further downstream within the Ras/MAPK pathway with a- well known small molecule inhibitor, U0126 which targets MEK. Synergistic interactions were seen with ILKAS in combination with U0126 in U251MG and SF-188 glioblastoma cells (see Fig. 4.3). The dose-effect plot of U251MG cells in Fig. 3A showed that the combination of ILKAS (1-4 μM) with U0126 (10-40 μM) exhibited an enhanced drug combination effect (decreased cell viability-labeled "effect", on the y-axis) relative to ILKAS and U0126 used alone. Data analysis indicated combination index (CI) values ranging from 0.5 to less than 0.1 (Fig. 4.3B). The dose effect plot for SF-188 cells treated with ILKAS in combination with U0126 (Fig. 4.3C) in the same fixed ratio as U251MG glioblastoma cells also result in strong synergy (CI values were below 0.4) (Fig 4.3D). As a control, a combination of RILK and GW5074 and a combination of RILK and U0126 were used at the same concentrations as that of the ILKAS and GW5074 or U0126 in combination. For these combinations the CI values exceeded 10, suggesting that combination with the control antisense sequences actually inhibited any measured therapeutic effects due to GW5074 or U0126.In order to determine if ILKAS and U0126 were inhibiting their specific targets in the PI3K/AKT and the Ras//MAPK pathways at the same concentrations at which synergistic combination effects were seen, ILK, PKB/AKT, and MAPK levels/activity were assessed by western blot analysis in SF-188 and U251MG glioblastoma cells.

Figure 4.3

Dose effect and combination index plots to determine drug efficacy and interaction between ILKAS and U0126. MTT data were obtained following treatment of cells with the indicated agents alone or in combination. Effective concentrations were analyzed using the CalcuSyn software (Biosoft, Freguson, MO). *(A),* U251MG and *(C),* SF-188 cells were exposed to a range of ILKAS (1-10μM) and U0126 (10-100μM) concentrations alone and in combination at a fixed mole to mole ratio (i.e. 1:10) for 36 hrs. The results are visualized as a dose-effect curve and a combination index (CI)/fraction affected plot as described in figure 4.1. *(E-F),* Disruption of cell signaling pathways by single agent and combination therapy. SF-188 *(E)* and U251MG *(F)* cells respectively, were incubated in the presence or absence of 4μM ILKAS ± 40μM of U0126 Equivalent amounts of protein (30μg/lane determined by Bradford assay). Note EGF was added exogenously 12 h prior to drug treatment.

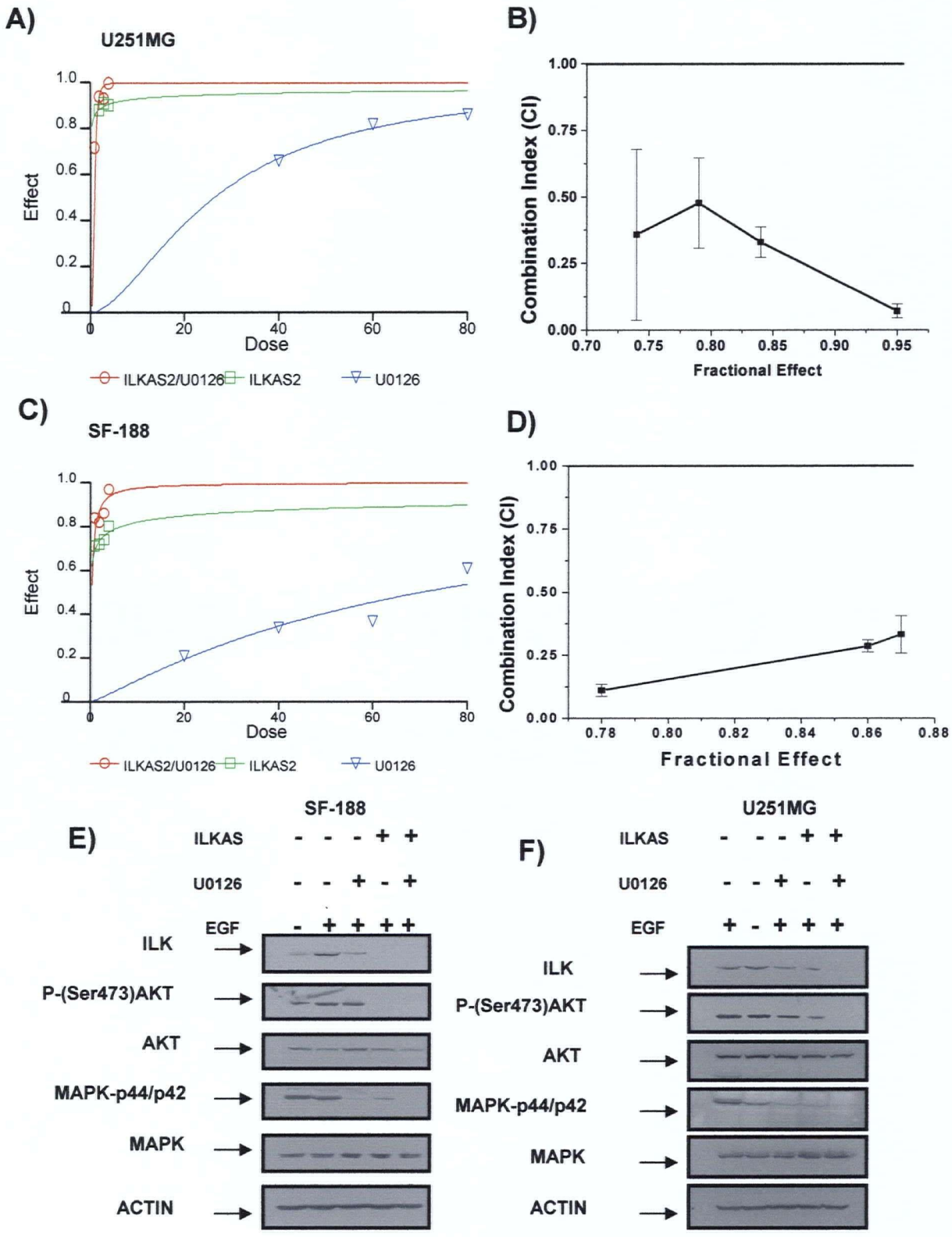
A)
U251MG
Effect
Dose
ILKAS2/U0126
ILKAS2
U0126
B)
Combination Index (CI)
Fractional Effect
C)
SF-188
Effect
Dose
ILKAS2/U0126
ILKAS2
U0126
D)
Combination Index (CI)
Fractional Effect
E)
SF-188
ILKAS
U0126
EGF
ILK
P-(Ser473)AKT
AKT
MAPK-p44/p42
MAPK
ACTIN
F)
U251MG
ILKAS
U0126
EGF
ILK
P-(Ser473)AKT
AKT
MAPK-p44/p42
MAPK
ACTIN

These studies were completed using cells cultured in the presence of epidermal growth factor (EGF) added exogenously to determine if the effects of this mitogen could be abrogated by drug treatment. The results of these studies have been summarized in Figures 4.3E and F. SF-188 cells transfected with ILKAS alone resulted in loss of ILK protein (lane 4 Fig. 4.3E). When the ILKAS was used in combination with the MEK inhibitor U0126, U0126 did not interfere with ILKAS targeting as judged by ILK protein inhibition measured in the presence of U0126 (lane 5 Fig. 4.3E). Transfection of ILKAS alone or in combination with U0126 also resulted in decreased phosphorylation of PKB/AKT Ser473 (lanes 4 and 5 Fig. 4.3E). Interestingly, ILKAS also resulted in decreased MAPKp44/p42 phosphorylation (lane 4 Fig. 4.3E) even though the ILKAS targets the PI3K/AKT pathway. SF-188 cells exposed to the MEK inhibitor U0126 in the presence and absence of ILKAS resulted in loss of MAPKp44/p42 phosphorylation (lanes 3 and 5 Fig. 4.3E). Total Akt and MAPK levels were unaffected by the ILKAS/U0126 combination. Similar results were seen for the glioblastoma cell line U251MG (Fig. 4.3F). Loss of ILK and decreased phosphorylation of PKB/AKT were seen following ILKAS transfection and this was also observed when ILKAS was used in combination with U0126 (lanes 4 and 5 Fig. 4.3F). In addition, ILKAS resulted in loss of MAPKp44/p42 phosphorylation (lane 3 Fig. 4.3F). Treatment of U251MG cells with U0126 resulted in MAPKp44/p42 loss. Total AKT and MAPK levels were unaffected as measured relative to actin levels as a loading control. Treatment of U251MG cells with U0126 and ILKAS alone and in combination promoted apoptosis (Fig. 4.4). The percentage of PI negative and Annexin-V positive cells in single agent treated cultures was 98.3% and 57.8% for U0126 and ILKAS, respectively.

Figure 4.4

(A), Apoptosis assessment in ILKAS and combination treated cells. U251MG glioblastoma cells were isolated and exposed to 40μM U0126 ± 4μM ILKAS or left untreated for a minimum of 24 h, where Camptothecin was used as a positive control for Annexin V-FITC and PI staining. The induction of apoptosis was determined by flow cytometric analysis of Annexin V-FITC and PI-staining. Cells were harvested 24-36 h later for analysis. Cells in the lower right quadrant indicate Annexin-positive, early apoptotic cells. Y axis indicates PI fluorescence intensity, the X axis indicates Annexin V-FITC intensity. The cells in the upper right quadrant indicate Annexin-positive/PI-positive, late apoptotic cells. *(B),* U251MG cells were treated with 40μM U0126 ± 4μM ILKAS or left untreated and harvested and the percentage of cells with sub G_1/G_0 (apoptotic/necrotic) DNA content was measured by flow cytometric analysis of propidium iodide (PI) staining for 20,000 events. Y axis indicates # of events and X axis indicates PI fluorescence. The percentages indicate dead cells. *(C),* Nuclear morphology of U87MG cells treated with 40μM U0126 ± 4μM ILKAS or left untreated were stained with DAPI and cytospun preparations were obtained. Arrows indicate where cell fragmentation, DNA condensation and apoptotic morphology is in response to treatment. Cells were viewed under fluorescence microscopy at 200X magnification.

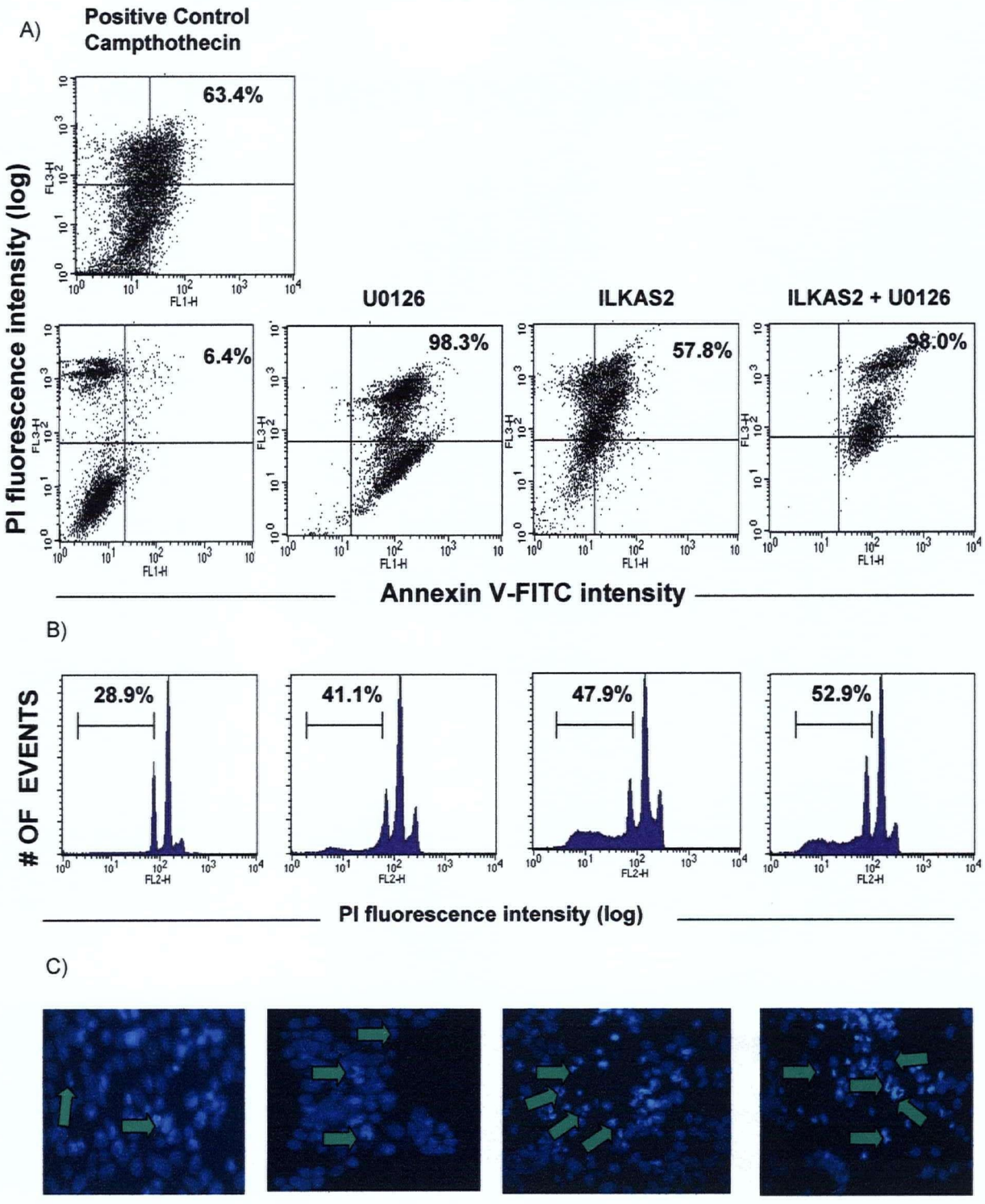
A)
Positive Control
Campthothecin
63.4%
6.4%
U0126
98.3%
ILKAS2
57.8%
ILKAS2 + U0126
98.0%
PI fluorescence intensity (log)
Annexin V-FITC intensity
B)
28.9%
41.1%
47.9%
52.9%
OF EVENTS
PI fluorescence intensity (log)
C)

There was a high proportion (98.0%) of cells expressing phosphatidyl serine (PS) in cells treated with the combination of ILKAS and U0126 (Fig. 4.4A). Please note that this effect level was achieved at a drug concentration of the agents which were 1.75 and 2.5 fold lower then that used for single agents ILKAS and U0126, respectively. Also note that in U251MG cultures treated with ILKAS and U0126 in combination (Fig. 4.4A) there were more double positive (Annexin V-FITC, PI stained) cells than in either of the single agent treated U251MG cells. This is consistent with faster progression to late stage cell death with the combination. Despite using lower drug doses, similar levels of Annexin-V positive labeling were obtained. In addition, PI analysis indicates that there was an increase in the number of cells with sub G_1/G_0 DNA content when the cells were treated with the drugs in combination (Fig. 4.4B). Analysis of DAPI stained U251MG cultures confirm the presence of cells with fragmented nuclei and condensed chromatin in single agent treated samples and the combination treated samples (Fig. 4.4C).

4.4. Discussion

The present study examines the role of drug combinations selected to affect distinct aberrant cell signaling pathways known to play a role in glioblastoma cell proliferation and survival. These in *vitro* studies provide a rationale for the preclinical development of targeted drug combinations in animal models of glioblastoma multiforme and hopefully clinical testing of an effective combination of drugs affecting these pathways. We have demonstrated that treatment of U87MG, U251MG and SF-188 glioblastoma cells with ILKAS can decrease ILK protein levels and downstream phosphorylation of the cell survival protein PKB/AKT at Ser473, the site specifically phosphorylated by ILK. This ILKAS specific effect and the associated decrease in the PKB/AKT cell survival activity likely led to increased cell death in this cell population treated with the selected ILKAS. Furthermore, when ILKAS was combined with the MEK inhibitor U0126 the measured therapeutic effects were judged to be synergistic. Synergistic interactions, in this context, means that the therapeutic effects can be achieved at a much lower concentration of the ILKAS and U0126 when used in combination as compared to doses required to achieve the same effect level when used as single agents. The concentrations used in this study were 4 μM ILKAS and 40 μM U0126 and at these concentrations the therapeutic activity, as determined by the percentage of apoptosis, were equal or greater to that achieved using 7 μM ILKAS or 100 μM U0126 singly. This dose reduction, due to drug combination synergism, has potential advantages clinically as optimal therapy may be achieved at lower dose levels and, perhaps with reduced toxicity [170].

It has been reported that there is low expression of EGFR associated with glioma cells *in vitro* [171], which may result in a lower activity of the Ras/MAPK pathway. To combat this problem we stimulated treated and untreated cells with EGF to increase EGFR expression

and/or activation prior to assessing the effects of the targeted agents. It has also been reported that EGFR is upregulated in malignant glioma [172] and this could be due to the 3-D arrangement of the tumor *in vivo* which may engender EGFR expression due to poor tumor perfusion and associated stress effects of starvation and hypoxia. This would not be seen in a monolayer culture. The monolayer culture condition may therefore limit the ability of GW5074 to act effectively due to artificially reduced EGFR expression and subsequent low Ras/MAPK pathway activity. An indirect method to address this relied on plating the glioblastoma cells in soft agar (Fig. 1G), in anticipation that EGFR expression would be enhanced. Although enhanced EGFR expression was not demonstrated, our results suggest that the therapeutic effects of the drugs alone and in combination were comparable to results generated using the MTT assay.

The activity of ILKAS not only had an affect on the PI3K/AKT pathway but also on the Ras/MAPK pathway in which phospho-MAPK activity was decreased (see Figs 3E and 3F). This was not unexpected as other groups have shown that inhibition of the PI3K pathway can result in a decrease in the activity of Ras/MAPK pathway [173]. Regardless, the in *vitro* data does suggest that the combination of ILKAS and U0126 or GW5074 can result in more than additive effects. The flow cytometry and DAPI staining results support this conclusion. There was equal or greater cell death when ILKAS and U0126 or GW5074 were used in combination and this effect was seen at lower concentrations than required to see the same effect when using either of the agents alone (Figs. 2A-C, 4A-C). It is hoped that the *in vitro* cell based screening assays can be used to confirm whether agents targeting specific cell signaling pathways act in concert and, perhaps, synergistically. Such data will help preclinical investigators to rationally choose agents for combination studies in animal models. At the moment, one of the most

significant challenges that we are attempting to address concern the translation of interesting *in vitro* drug combination effects into meaningful *in vivo* treatment strategies. To this end, our lab is developing strategies which will define combination products (a single dosage form that is comprised of two or more active agents), taking into consideration the pharmacodynamic properties of the individual agents as well as toxicity endpoints established for the individual agents in preclinical animal models.

CHAPTER 5

SUPPRESSION OF VEGF SECRETION AND ASSOCIATED CHANGES IN THE TUMOR MICRO-ENVIRONMENT BY SELECTIVE INHIBITION OF INTEGRIN-LINKED KINASE (ILK) IN GLIOBLASTOMA MULTIFORME *

5.1. Introduction

Conventional chemotherapeutic agents are ultimately a trade-off between therapeutic response and toxicity, and while novel approaches such as siRNA are in the making, the success of Gleevec™ (STI571) initally defined the prototype for selective kinase inhibition, however has since been found to be not as specific. Consequently, there has been a concerted effort into producing a new class of selective molecular targeted agent. Although some of the initial results have been encouraging, the perceived therapeutic expectations have not yet been fully realized. Targets, which impact cell growth, proliferation and apoptotic pathways are certainly important but, direct effects on the cancer cell often do not consider how therapy influences the tumor micro-environment. The tumor micro-environment is represented by a collage of attributes encompassing variations in pH, blood vessel density, hypoxic and perfused regions. This, in addition to the mixed tumor cell and host cell populations that typify tumor heterogeneity, make it easy to understand why cancer has been so difficult to treat effectively. Hypoxia inducible factor 1 alpha (HIF-1α) and vascular endothelial growth factor (VEGF) are key factors that are known to affect the tumor micro-environment and can be induced in response to hypoxia which in turn, can lead to angiogenesis. Thus the environmental crisis triggered by hypoxia can be mitigated by cellular pathways designed to promote cell survival. The tumor micro-environment

---

*

A version of this chapter has been submitted for publication. Edwards, L., Woo, J., Huxam, L., Verreault, M., Chiu, G., Raijput, A., Kyle, A., Karle, J., Raijput, A., Dragowska, WH., Yapp, D., Yan, H., Minchinton, A., Huntsman, D., Daynard, T., Thiessen, B., Dedhar, S., Bally, MB. (2005) Suppression of VEGF secretion and associated changes in the tumor micro-environment by selective inhibition of Integrin-linked kinase (ILK) in glioblastoma multiforme All work presented here is my work with indicated contributions.

allows the cancerous process to progress (promoting cell survival and adaptation) as well as enhancing the likelihood of metastatic spread (due to pro-stimulatory angiogenic factors) while at the same time creating conditions that foster development of resistance to traditional chemotherapeutic treatment [174-176].

It has been argued that targeting the tumor micro-environment may be an effective treatment option [177] due to the relatively simple nature of processes governing the micro-environment compared to the cellular processes that contribute to a tumor cell's ability to adapt to the environment that it is exposed to [178]. Approaches to targeting the tumor micro-environment have involved direct targeting of factors such as VEGF through antibodies that bind VEGF and/or small molecules that inhibit VEGF signaling through the VEGF receptor. Here we propose an alternative approach that considers central pathways within cells that lead to multiple effects, including inhibition of tumor cell proliferation, induction of apoptosis as well as inhibition of VEGF secretion. Targeted anticancer agents that achieve such effects will be particularly attractive when used in combination with conventional treatment modalities such as radiation or cytotoxic chemotherapy.

Integrin-linked kinase can be used as an example target that is capable of producing pleiotropic effects. It has been shown that a key molecular marker of hypoxia in the tumor micro-environment, HIF-1α, is upregulated in a PI-3 kinase dependent manner and can be stimulated through the activity of PKB/AKT which in turn activates VEGF [179-180]. Integrin-linked kinase (ILK) can stimulate VEGF expression by stimulating HIF-1α via a PI-3 kinase dependent stimulation of PKB/AKT [128]. ILK has also been shown to stimulate cell growth and cell cycle progression [69] and inhibit apoptosis [76]. Recently, we and others have shown the regulatory role of ILK in glioblastoma progression [149][181]. Loss of the tumor suppressor

PTEN; which has been shown to be as high as 80% [129] in glioblastomas, results in constitutive activation of ILK leading to tumor progression. Here we demonstrate that targeting ILK with small molecule inhibitors, inhibits, cell proliferation and cell survival leading to cell death *in vitro* as well as facilitating decreases in HIF-1α and VEGF expression. *In vivo* therapeutic effects of these novel agents correlate to drug mediated decreases in hypoxia and angiogenesis.

5.2. Hypothesis

ILK inhibition has been associated with inhibiting cell proliferation and increasing apoptosis in cancer. Evidence of ILK mediating micro-environmental effects such as angiogenesis through the regulation of VEGF in cancer, led to investigating the possibility of targeting ILK to examine the effects on the tumor micro-environment. Given ILKs role in regulating angiongenesis, inhibition of ILK should result in decreased angiogenesis (in addition to inhibition of cell proliferation and promotion of cell death.).

The research objectives are the following:

(1) To evaluate two small molecule inhibitors QLT0254 and QLT0267 for their ability to inhibit cell proliferation, increase apoptosis and decrease angiogenesis.

(2) To determine if these ILK inhibitors are potential anti-cancer agents.

(3) To verify that ILK is a viable therapeutic cancer target.

5.3. Results

5.3.1. QLT0254 and QLT0267 Reduces Glioblastoma Cell Viability

SF-188 (*PTEN* positive) U251MG (*PTEN* negative), and U87MG (*PTEN* negative) glioblastoma cells were treated with increasing concentrations of the ILK inhibitor QLT0254 [182] or QLT0267 [183] for 48 hrs and an MTT assay was used to determine cell viability. As shown in Table 5.1, treatment with either ILK inhibitor for 48 hrs reduced MTT labeling, indicative of cell cytotoxicity and/or cell cytostasis of all cell lines tested. The values from the MTT assay were analyzed by the software program Calcusyn to determine the IC_{50} values for the individual agents and these ranged from 6.7-38 μM for QLT0267 and 27-58 μM for QLT0254).

5.3.2. QLT0254 and QLT0267 inhibit PKB/Akt cell survival activity in Selected Glioblastoma cells

Several studies have shown that transfection of *PTEN* or a dominant negative *ILK* or an antisense targeting ILK affects the phosphorylation and activation of PKB/AKT at serine 473, a well known cell survival signaling protein [90][159]. Therefore we investigated if two small molecule inhibitors of ILK from the K15792 class of the pharmacophor family (Fig. 5.1A), QLT0254 and QLT0267, could decrease phosphorylation of PKB/AKT.

Table 5.1: IC_{50} values of QLT0254 and QLT0267 for the viability of glioblatoma cancer cell lines.

Cell Line	ILK Inhibitor	IC_{50} (μM) ±SD
SF-188	**QLT0267**	**6.7 ± 0.7**
SF-188	**QLT0254**	**51 ± 11.2**
U87MG	**QLT0267**	**23 ± 1.5**
U87MG	**QLT0254**	**27 ± 1.3**
U251MG	**QLT0267**	**38 ± 2.2**
U251MG	**QLT0254**	**58 ± 8.5**

Note cells were plated in 96-well plates and treated with QLT0254 or QLT0267 for 48 hours. Cell viability was determined using the MTT assay and subsequently analyzed by Calcusyn to estimate the IC_{50} values. Each point is the mean for 6 replicate wells and is reprentative of two independent experiments performed.

The results are summarized in Figs. 5.1(B-D). In all glioblastoma cells exposed to QLT0267 there was complete loss of phospho-PKB/AKT at Ser473 at the highest concentration tested 50 μM (Figs. 5.1B-D top panels). In the case of SF-188 and U87MG glioblastoma cells significant loss of phospho-PKB/AKT at Ser473 was noted at concentrations of 5 μM (Figs. 5.1B and 1D top panels). SF-188 cells treated with QLT0254 exhibited partial loss of phospho-PKB/AKT at Ser473 at 50 μM (Fig. 5.1B, bottom panel), U251MG (Fig. 5.1C, bottom panel) and U87MG (Fig. 5.1D, bottom panel). Note that treatment with the ILK inhibitors (QLT0254 and QLT0267) did not effect ILK protein expression. Total PKB/AKT was also unaffected by the inhibitors and actin was used as a loading control.

Figure 5.1

Structure of the K15792 class of the pharmacophor family *(A)* which were used to synthesize QLT0254 and QLT0267 ILK inhibitors. The effects of QLT0254 and QLT0267 on the phosphorylation of the cell survival protein PKB/Akt in *(B-D)* Glioblastoma SF-188 *(B),* U251 *(C)* and U87MG *(D)* cells (2 x 106). The cells were plated on 100 mm dishes and incubated with either QLT0267 (top row) or QLT0254 (bottom row) at drug concentrations of 0,5,20,50 μM for 48 h. Protein lysates were prepared and 30 μg of each lysate was resolved by electrophoresis, transferred to membranes, and probed with the indicated antibodies.

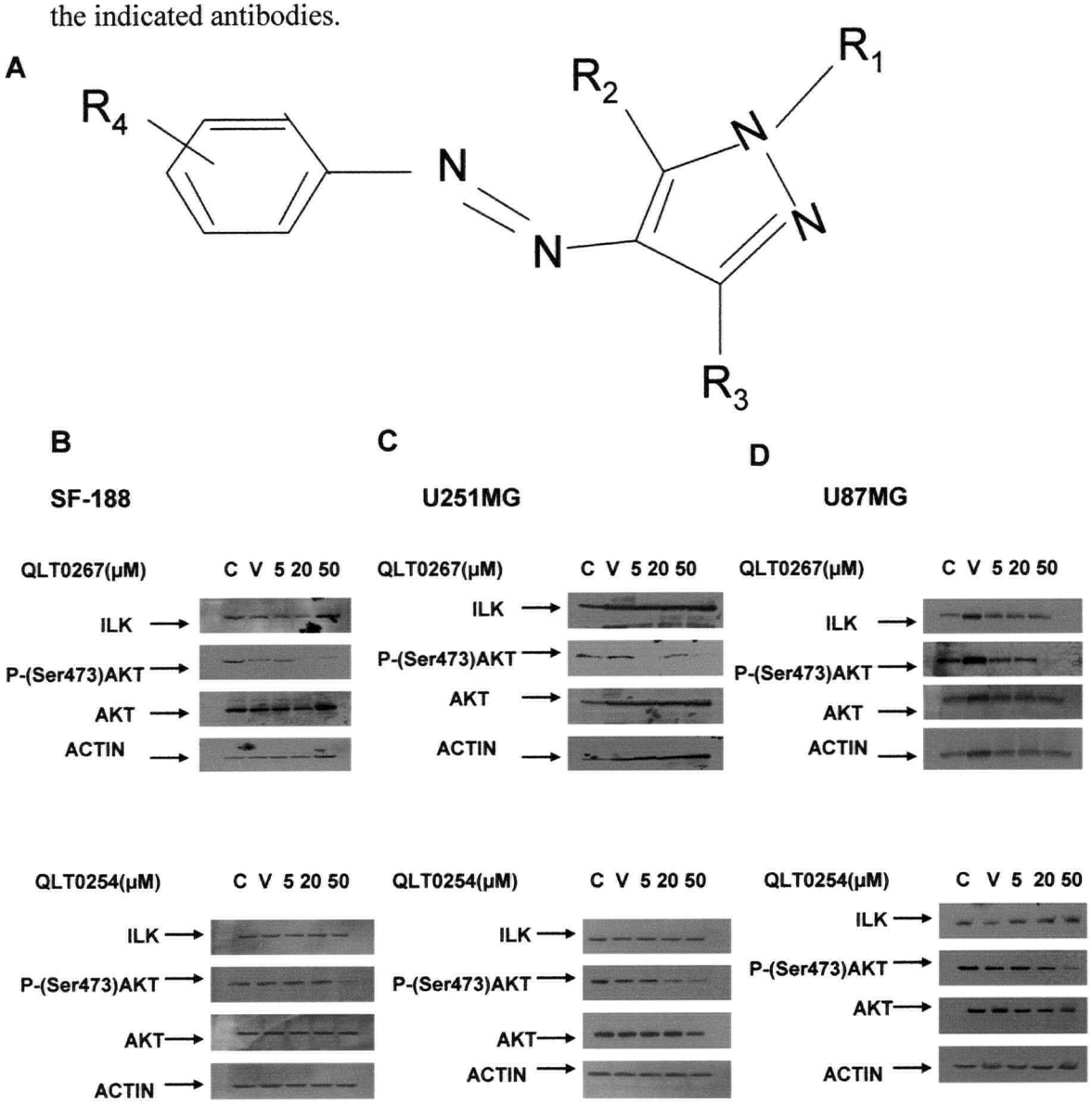

5.3.3. Effect of the QLT0254 and QLT0267 on Cell Cycle Regulation in the Selected Glioblastoma cell lines

To determine the possible cell cycle effects of ILK inhibition in U251MG, SF-188 and U87MG cells, the cells were treated with QLT0254 or QLT0267 at concentrations ranging from 0-50 μM for a maximum of 24 h. Propidium iodide (PI) staining of glioblastoma DNA cell content was assessed by flow cytometry as described in the Materials and Methods. The results, shown in Figure 5.2, indicated that the glioblastoma cells treated with QLT0254 or QLT0267 (Figs. 5.2A and 2B) exhibited a strong, dose dependent, G_2/M cell cycle block. For example, in U87MG cells 10%, 29% and 44% of the cells appeared in G_2/M following treatment with QLT0254 at 5, 20 and 50 μM (Fig. 5.2A left column and 2B top panel), respectively. Similar results were observed for PI stained U87MG cells treated with QLT0267 (Fig. 5.2A middle column). Treated SF-188 glioblastoma cells also showed a dose dependent increase in G_2/M cell cycle block [40%, 45% and 68% of cells in the G_2/M phase following exposure to QLT0254 at 5, 20 and 50 μM (Fig. 5.2B middle panel), respectively]. U251MG cells treated with QLT0254 exhibited a high secondary peak by flow anlaysis of PI stained cells (Fig. 5.2A right column) and U251MG cells treated with QLT0267 showed 14%, 25% and 35% of cells in the G_2/M phase, when treated with these drug concentrations (Fig. 5.2B bottom panel). These data indicate that the mechanism of action of the ILK inhibitors is comparable for the glioblastoma cell lines evaluated. Regardless of *PTEN* status, untreated and PTE (vehicle) treated cells responded in a comparable fashion when evaluated using this method. These results were interpreted by Visia Dragowska

Induction of Apoptosis following treatment with QLT0254 and QLT0267

To assess whether ILK inhibition by QLT0254 and QLT0267 could induce apoptosis and subsequent cell death, the activity of caspase-3 and -7 were assessed via a fluorescence assay. The different cell lines were exposed to 20 μM QLT0254 or QLT0267, drug concentrations that were typically < the IC_{50} (see Table 5.1). Since cell cycle arrest was observed within one day following treatment with QLT0254 and QLT0267, apoptosis was assessed following longer incubation times (e.g. 72 h). Representative data for SF-188 and U251MG cell lines treated with QLT0267 and the U87MG cell line treated with QLT0254 are provided in Fig. 5.2C. Caspase activity increased for SF-188 (Fig. 5.2C, far left), U251MG (Fig. 5.2C, middle) and U87MG (Fig. 5.2C, far right) following exposure to the ILK inhibitors. No significant changes in caspase activity were observed for cells treated with PTE (vehicle control) or when using the ILK inhibitors at 5 μM. These data suggest that QLT0254 and QLT0267 can induce caspase activation.

To assess cell death following drug exposure cellular DNA of treated glioblastoma cells was stained with -4',6-diamidino-2-phenylindole (DAPI). Cells were exposed to QLT0254 or QLT0267 for 72 h. Cell fragmentation and loss of DAPI staining within the cells was observed (Fig. 5.2D, micrographs) and cell death was recorded and expressed as a fold increase, relative to cell death found in untreated control glioblastoma cells.(Fig. 5.2D bar graphs). SF-188 cells treated with QLT0267 exhibited an increase of 25-fold in the measure of apoptosis (Fig. 5.2D, far left bar graph). Similarly, U251MG cells treated with QLT0267 exhibited an increase in apoptosis of 17-fold (Fig. 5.2D, middle bar graph). At least a 10-fold increase was observed in

U87MG treated with QLT0254 (Fig. 5.2D, far right bar graph). Glioblastoma cells treated with the PTE vehicle alone did not exhibit significant differences when compared to the control cells

Figure 5.2

In vitro assessment of cell cycle *(A-B),* caspase induction *(C)* and apoptosis *(D)* following treatment with the ILK inhibitors QLT0254 and QLT0267.. (A) Cells were plated onto 100 mm culture dishes and incubated with QLT0254 or QLT0267 at the indicated concentrations for 48 h. Fluorescence activated cell sorter (FACS) analysis of propidium iodide stained cells was used to determine cell cycle characteristics. These data revealed a G_2/M cell cycle block for representative glioblastoma cell lines U87MG and U251MG regardless of the ILK inhibitor used. *(B)* A breakdown of the cell cycle phases indicates a dose-dependent G_2/M block for U87MG (B top panel), SF-188 (B middle panel) and U251 (B bottom panel). *(C)* Caspase activation was seen in SF-188 (C left panel-254), U251 (C middle panel-267) and U87MG (c right panel-254) with increasing concentrations of ILK inhibitors incubated with glioblastoma cells for 72 h. Each point is the mean ±SE for 6 replicates and is reprentative of two independent experiments performed. Data is expressed relative to PTE treated control cells. *(D)* Glioblastoma cells were plated onto 100 mm culture dishes and untreated or incubated with PTE (vehicle), or 20 μM of QLT0254 or QLT0267 for 72 h and then stained with DAPI (see photo micrographs). Morphological features of cellular apoptosis were observed with a fluorescence microscope. Fold increase was determined by looking at five random fields for each condition and the observations were collected in a blinded fashion. The results are the mean ±SE of data obtained from five randomly chosen fields.

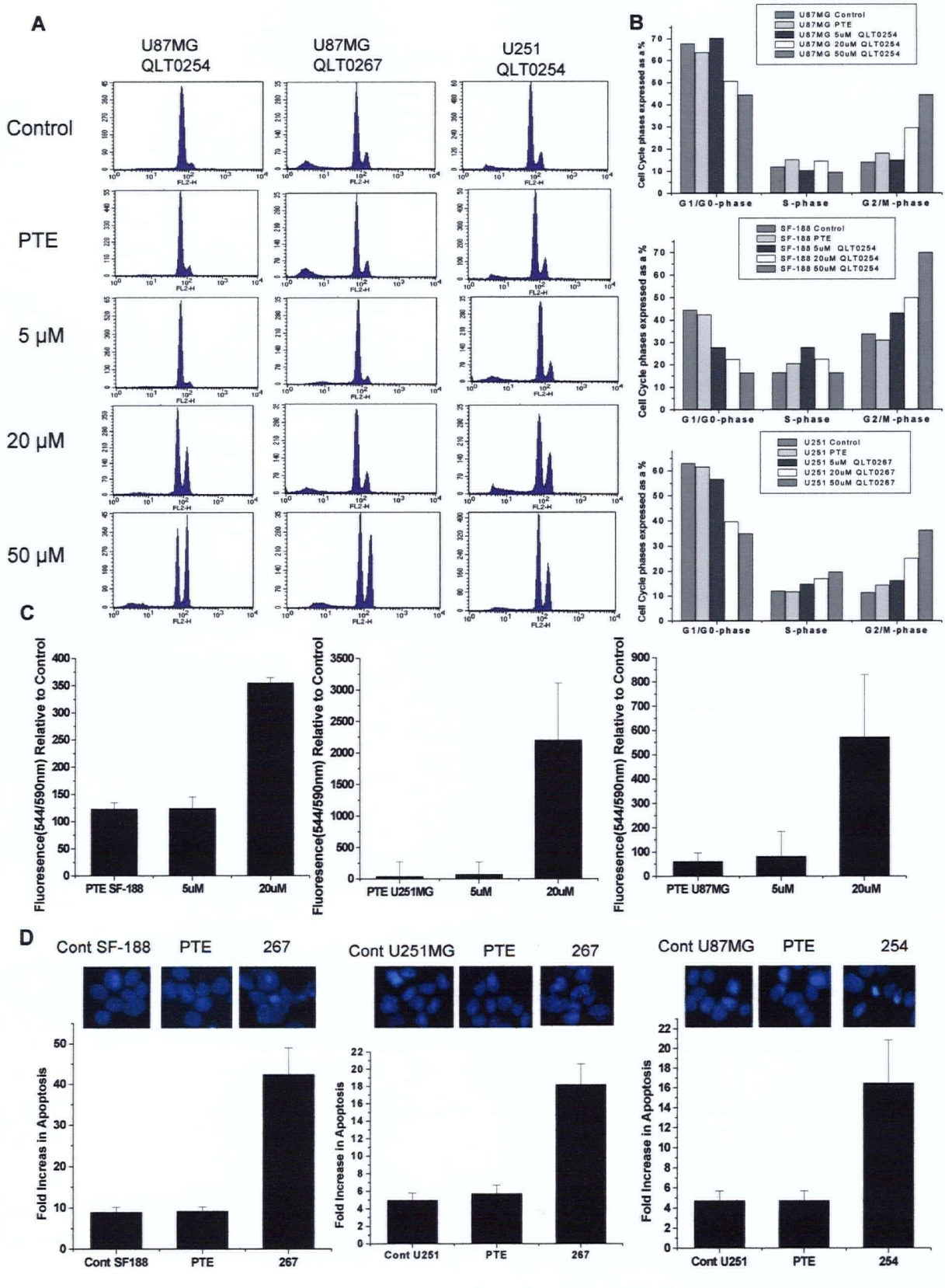
A
U87MG QLT0254
U87MG QLT0267
U251 QLT0254
Control
PTE
5 µM
20 µM
50 µM
FL2-H
B
U87MG Control
U87MG PTE
U87MG 5uM QLT0254
U87MG 20uM QLT0254
U87MG 50uM QLT0254
SF-188 Control
SF-188 PTE
SF-188 5uM QLT0254
SF-188 20uM QLT0254
SF-188 50uM QLT0254
U251 Control
U251 PTE
U251 5uM QLT0267
U251 20uM QLT0267
U251 50uM QLT0267
Cell Cycle phases expressed as a %
G1/G0-phase
S-phase
G2/M-phase
C
Fluoresence(544/590nm) Relative to Control
PTE SF-188
5uM
20uM
PTE U251MG
PTE U87MG
D
Cont SF-188
PTE
267
Cont U251MG
Cont U87MG
254
Fold Increas in Apoptosis
Fold Increase in Apoptosis
Cont SF188
Cont U251

5.3.4. Regulation of VEGF Secretion by ILK in U87.23 Glioblastoma cells

It has been shown that vascular endothelial growth factor (VEGF) in glioblastomas is regulated in a phosphatidylinositol 3'-kinase (PI3K) dependent manner [184][185]. To determine if ILK inhibition could inhibit VEGF secretion, we used *PTEN* negative U87MG glioblastoma cells, transfected with an ecdysone-inducible [152] wild-type-*PTEN* retroviral construct (designated here as U87.23). The ecdysone-inducible expression system allows the expression of the *PTEN* gene in the presence of muristirone A. A concentration of 0.5 μM of muristirone A allows for the full expression of *PTEN* (Fig. 5.3, gel). An ELISA assay was used to assess secreted VEGF levels in these cells exposed to muristirone A or the ILK inhibitors and these data are summarized in Fig. 5.3. Uninduced U87.23 glioblastoma cells (*PTEN* negative) showed high secreted VEGF protein levels (Fig. 5.3 histogram). Upon induction of PTEN by exposure to 0.5 μM muristirone A, secreted VEGF levels decreased 3-fold. Exposure of uninduced U87.23 glioblastoma cells to the ILK inhibitors QLT0254 or QLT0267 also engendered significant decreases in secreted VEGF levels. In addition, exposure of U87.23 glioblastoma cells to LY294002 which affects PI3K also resulted in a similar decrease in VEGF secretion. This experiment was done by Gigi Chiu.

Figure 5.3

ILK inhibition results in suppression of VEGF secretion. U87.23 cells were seeded into 60 mm dishes at a density of 2 x 106 cells/dish and incubated in regular media for 24 h. After 24 h, PTEN was induced or QLT0254, QLT0267 (20 μM), LY294002 (20 μM) was added. 24 h later supernatant were collected and VEGF protein levels were determined by ELISA. The graph is the product of experiments done four times on four separate occasions and the data represent the mean ±SEM.

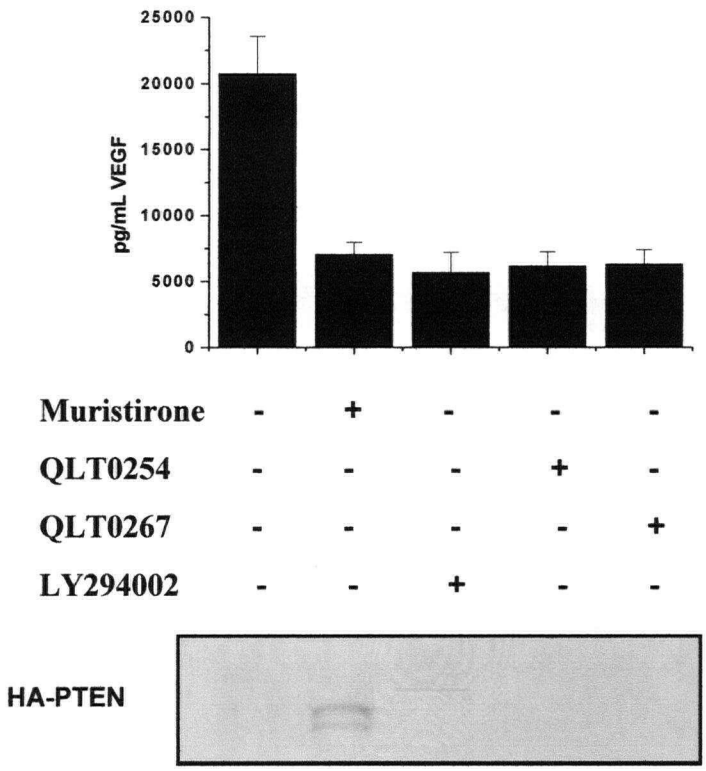

5.3.5. Antitumor efficacy of QLT0254 and QLT0267 on PTEN negative glioblastoma U87MG tumor Xenografts

We tested the antitumor effects of the ILK inhibitors QLT0254 and QLT0267 in Rag-2M mice bearing subcutaneous (s.c.) xenografts derived following injection of U87MG glioblastoma cells. Mice were treated with either saline, QLT0254 or QLT0267 or the vehicle PEG300/Ethanol/Tween 80/citrate (63:29:7.8:0.2 w/v/w/w) (PTE); The drugs were given orally at 200 mg/kg (qdx7 every week for 3 weeks) and PTE was administered at a dose equivalent to that used in the formulated drug product. Treatment commenced 32 days after initial tumor injection when the tumor size was measurable. Saline or vehicle alone treated animals exhibited tumors that grew reproducibly to an average size 0.55cm^3. Treatment with vehicle alone did not cause any significant change in tumor growth rate when compared to the saline control (Fig. 5.4, inset). Comparing the saline treated animals to the QLT0254 and QLT0267 treated animals, the tumor size in the ILK inhibitor treated groups were significantly smaller. On day 14 for example, tumors from mice treated with QLT0267 (309 mm^3 versus 131 mm^3) difference = 178 mm^3, 95% CI = 48 mm^3 to 308 mm^3; P<0.01 post-treatment. Significant decreases in tumor volume were noted on day 16 for tumors in treated mice compared to controls (Fig. 5.4). Animals treated with QLT0267 exhibited mean tumor volume of 213 mm^3 compared to tumors from control animals which were on average 549 mm^3 (difference = 336 mm^3, 95% CI = 66 to 606 mm^3; P<0.012). Similar results were seen with QLT0254 treatment where QLT0254 treated animals had a mean tumor volume of 232 mm^3 compared to tumors from control animals with an average tumor volume of 549 mm^3 (232 mm^3 versus 549 mm^3, difference = 317 mm^3, 95% CI = 66 to 568 mm^3: P<0.012). Animals treated with PTE (vehicle) gave similar results to the

saline treatment group with a mean tumor volume of 530 mm^3 compared to QLT0254 treated tumors with an average tumor volume of 232 mm^3 (232 mm^3 versus 530 mm^3, difference = 298 mm^3, 95% CI = 205 to 391 mm^3; P <.001) or QLT0267 treated tumors with a mean tumor volume of 213 mm^3. (213 mm^3 versus 530 mm^3, difference = 317 mm^3, 95% CI= 186 to 448 mm^3; P<.001). Neither ILK inhibitor was able to eliminate tumor growth, rather the dose administered caused a delay in tumor growth. None of the mice treated with either ILK inhibitor displayed signs of toxicity in general and, specifically, the 200 mg/kg dose given QD resulted in less than 5% body weight loss.

Figure 5.4

A comparison of tumor volume among the three treatment groups and control The entire course of treatment is also shown (inset). Rag-2M mice bearing U87MG xenograft tumors were orally dosed with either saline, PTE (vehicle) or QLT0254 or QLT0267 at 200 mg/kg, QD x 7 for 3 weeks. The symbols represent the values determined for each animal (n=6) receiving the indicated treatment, and the horizontal bars indicate the mean tumor volumes. * $P < 0.012$ for control versus QLT0254 and QLT267 and **$P < 0.01$ for PTE vehicle versus QLT0254 and QLT0267; statistical significance was determined using the one-way ANOVA tukey test.

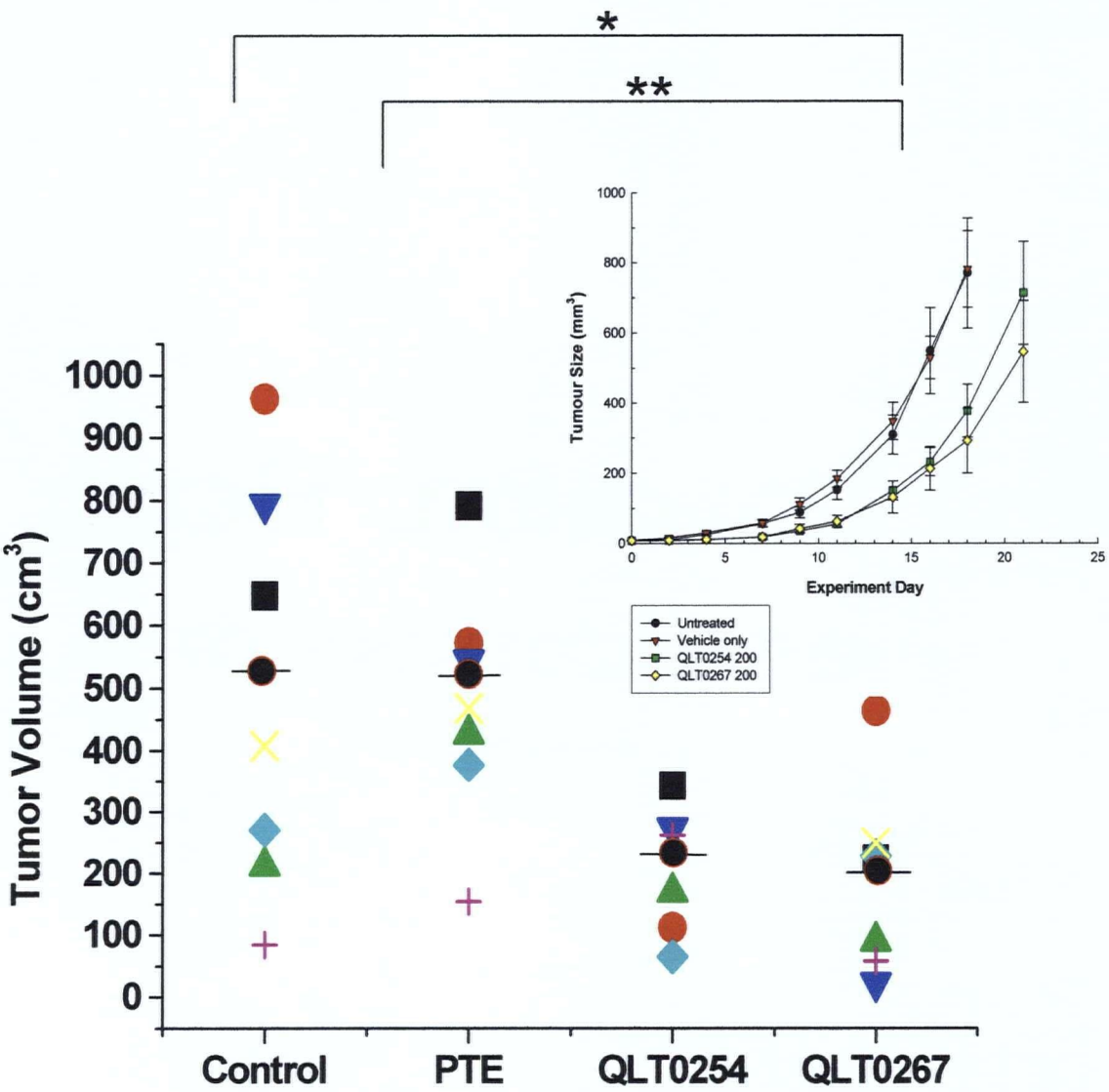

5.3.6. Effect of QLT0254 and QLT0267 on Apoptosis *in vivo*

Glioma tumor tissue was harvested two days after the final treatment from U87MG tumor bearing mice treated with either saline, QLT0254 or QLT0267. TUNEL staining of sections derived from these tumors were used to assess apoptosis (Fig. 5.5A). TUNEL staining was not as prominent in tumors from saline treated animals compared to these tumors from animals treated with QLT0254 and QLT0267 (Fig. 5.5A middle and far right photomicrographs, before and after counter staining with hematoxylin respectively). Semi-quantitative analysis of TUNEL positive cells indicated a significant proportion of DNA fragmentation in tumors from QLT0267 treated animals compared to saline control (Fig. 5.5B). An increase in TUNEL positive cells was also observed in tumors from animals treated with QLT0254, but this difference was not statistically significant. A second approach to evaluate the activity of the ILK inhibitors *in vivo* involved assessing the fraction of BrdUrd labeled cells (a measure of cell proliferation) within the U87MG tumors as judged by labeling of sections using an anti-BrdUrd antibody (see Materials and Methods) (Fig. 5.5C, inset, blue arrows show BrdUrd labeling in black). Analysis of this BrdUrd labeling revealed that tumors from animals treated with QLT0267 exhibited significant ($p<0.01$) decreases cell proliferation compared to saline control treated animals. Tumors from animals treated with QLT0254 also exhibited decreased BrdUrd labeling, albeit not a statistically significant decrease.

Figure 5.5

(A) Tumor tissue taken from U87MG xenografts from indicated groups tissue was assessed for cell death by TUNEL (A top photomicrograph) two days after final treatment. To discriminate apoptosis from necrosis, tissue was counterstained with hemotoxylin (bottom panel). *(B)* Quantification and percentage of TUNEL-positive tumor tissue was done by examining at five random fields for each condition, the results are the mean ±SE of data obtained from five randomly chosen fields and the observer was blinded to the study groups. TUNEL reveals a significant increase in apoptosis in QLT0267 treated tumors compared to control. *(C)* BrdUrd was injected in U87MG xenograft bearing mice prior to tumor harvesting. Inset shows BrdUrd labeling as represented by black dots (arrows), and is measure of cell proliferation. These data suggest an inverse correlation with TUNEL positive staining (n=6).

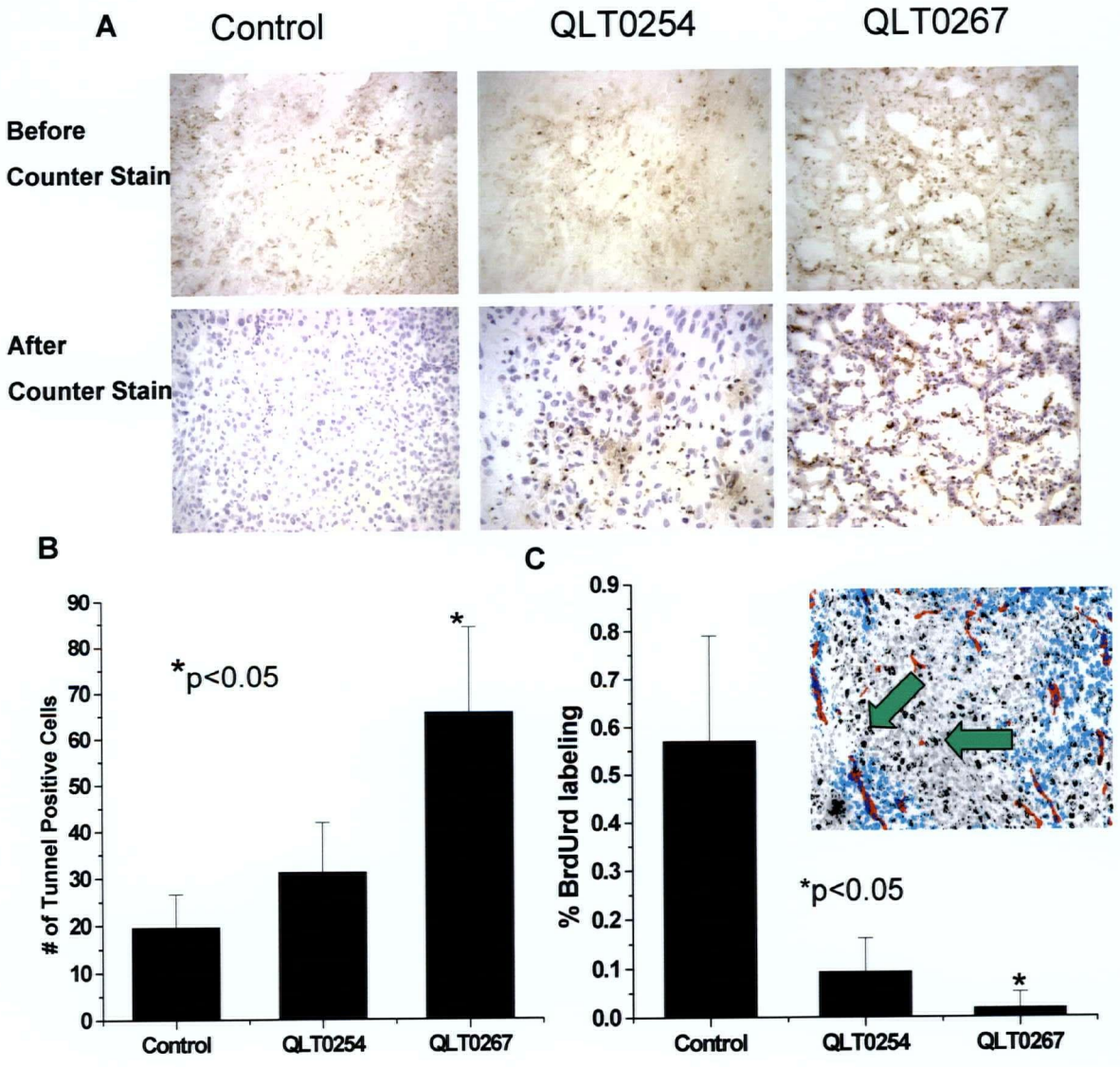

5.3.7. Analysis of Hypoxia and Vascularization in Glioblastoma Tumors

Hypoxia was detected using the nitroimidazole EF5 [136] which is metabolized and bound in viable hypoxic cells only. CD31 staining and Hoechst33342 was used to evaluate tumor vasculature. Serial sections were generated from tumor tissue harvested from U87MG tumor bearing mice treated with either saline, QLT0254 or QLT0267. The sections were stained with ELK3-51-CY3 antibody (anti-EF5-CY3 used to stain for cell labeled with EF5) or CD31 (tumor vascular endothelial cells) or Hoechst33342 (as a perfusion marker). Representative photomicrographs are shown in Fig. 5.6A. Control tumors from saline treated mice show a substantial amount of CD31 staining (shown in red) and Hoechst33342 staining (shown in blue). There is also significant EF5 labeling, indicative of hypoxia in these control tumors (Fig. 5.6A) It is notable that intense EF5 labeling was most frequently observed in regions that show reduced Hoechst33342 labeling. Tumors from QLT0254 treated animals also showed significant CD31 staining and Hoescht33342 staining, hypoxia as measured by the presence of EF5 was not detectable. This is consistent with the Hoescht33342 labeling data which suggest all regions within the tumor were well perfused. (Fig. 5.6A). Tumors from QLT0267 treated animals showed CD31 staining comparable to controls but, reduced Hoechst33342 labeling. In these tumors, Hoechst33342 appears primarily localized to the periphery of the section. Hypoxia was observed in the tumors from QLT0267 treated animals and the level of staining was similar to that seen in control tumors. Semi- quantitative analysis of EF5 staining in sections from animals treated with saline, QLT0254 and QLT0267 indicate a significant decrease in hypoxia in tumors from QLT0254 treated animals (Fig. 5.6B); 0.5% versus 8.7% difference = 8.2%, 95% CI = 3.2% to 13.2%; $P<0.027$. Staining and cryosectioning were done with the aid of Maite Verreault, Jessica Karle, Janet Woo and Lynsey Huxam.

Suppression of HIF-1α, VEGF expression by ILK inhibition Ex vivo

To further verify that ILK inhibition affects VEGF protein *in vivo* we assessed by an ELISA VEGF levels in U87MG tumor lysate prepared from tumors isolated from Rag-2M mice treated with QLT0254 or QLT0267 or saline. As shown in Figure 6C, higher VEGF levels were measured in saline treated animals versus animals treated with the ILK inhibitors. A 50% decrease in measurable VEGF was observed in tumors obtained from animals treated with QLT0254 or QLT0267 at 200 mg/kg. These data are consistent with the *in vitro* data shown in Table 5.3 and clearly indicate that the ILK inhibitors used here inhibit VEGF production.

It is known that GBM undergoes molecular changes caused by hypoxia [186-189] including the induction of VEGF [190]. Therefore, tumor lysates were also used for western blot analysis of HIF-1α and VEGF, where actin was used as a loading control (Fig. 5.6C, gel). Western blot analysis revealed that both HIF-1α and VEGF both decreased in tumor lysates prepared from tumors obtained from mice treated with the ILK inhibitors. These data support the ELISA results (see histogram) and suggests ILK inhibition can result in decreased HIF-1α as well as VEGF expression or ILK decreases oxygen consumption.

Tissue Microarray Analysis (TMA) of Microenvironmental Markers, ILK and phospho-PKB/AKT

The expression of HIF-1α and VEGF were also analyzed by immunohistochemistry. To show that ILK protein was not affected by the ILK inhibitors, a TMA was prepared for ILK staining of the three treatment groups: saline, QLT0254 and QLT0267 treated animals. TMA allows us to investigate tumors from the entire treatment groups where different tumor samples could be

stained with the same antibody, under the same conditions at the same time. These results provided supplemental information to support our tumor ELISA and western blot analysis. ILK staining suggested a uniform stain throughout control and ILK inhibitor treated tumors. This was expected given ILK inhibitors should inhibit ILK kinase activity and should not affect ILK protein levels. HIF-1α staining appeared to be less in tumors from animals treated with the ILK inhibitor as compared to control tumors (Fig. 5.6D). A semi-quantitative scoring of HIF-1α TMA indicated a significant ($P<0.036$) decrease in QLT0267 treated sections compared to control (Fig. 5.6D). Consistent with our ELISA and western analysis VEGF staining of the TMA suggested a decrease in VEGF levels in tumor tissue obtained from animals treated with QLT0254 and QLT0267 as compared to saline treated controls. TMA preparation and staining was done with the aid of Ashish Rajput.

Figure 5.6

(A) Examination of hypoxia in glioblastoma xenografts. Representative serial sections of U87MG xenograft tumors stained with PECAM/CD31 antibody (left photomicrographs) or Hoescht33342 (middle photomicrographs) or with anti-EF5-CY3 antibody (right photomicrographs). Frozen tumor sections taken from tumors obtained from saline treated (control-top) or QLT0254 (middle) or QLT0267 (bottom) treated animals show CD31 (red), Hoescht33342 (blue) and EF5 (orange/yellow-gold) which staining; the latter is used to assess the hypoxic fraction of the tumor. *(B)* Quantitative analysis of EF5 labeling reveals QLT0254 treated tumors show a significant decrease in hypoxia compared to control tumors (8.7% versus 0.5%) difference = 8.2%, 95% CI = 3.2% to 13.2%; $P<0.027$. *(C)* Suppression of HIF-1α and VEGF by QLT0254 and QLT0267. Tumor lysates were collected from saline treated, QLT0254 (200 mg/kg) or QLT0267 (200 mg/kg) treated animals. VEGF protein levels were determined by ELISA after normalization by Bradford assay. The graph is the mean (±SE) of three experiments done 3 times with 3 separately produced tumor lysates (top graph). Western analysis using tumor lysate showed decreased HIF-1α and VEGF protein levels in tumors obtained from treated as compared to control animals (gel). *(D)* Scoring of HIF-1α staining in control and QLT0254 and QLT0267 treated tumors. Scoring of all tissues were performed by a pathologist blinded to the treatment groups. Strong staining score 3 to 4, moderate staining score 2, weak staining score 0 to 1. Magnification 400X.

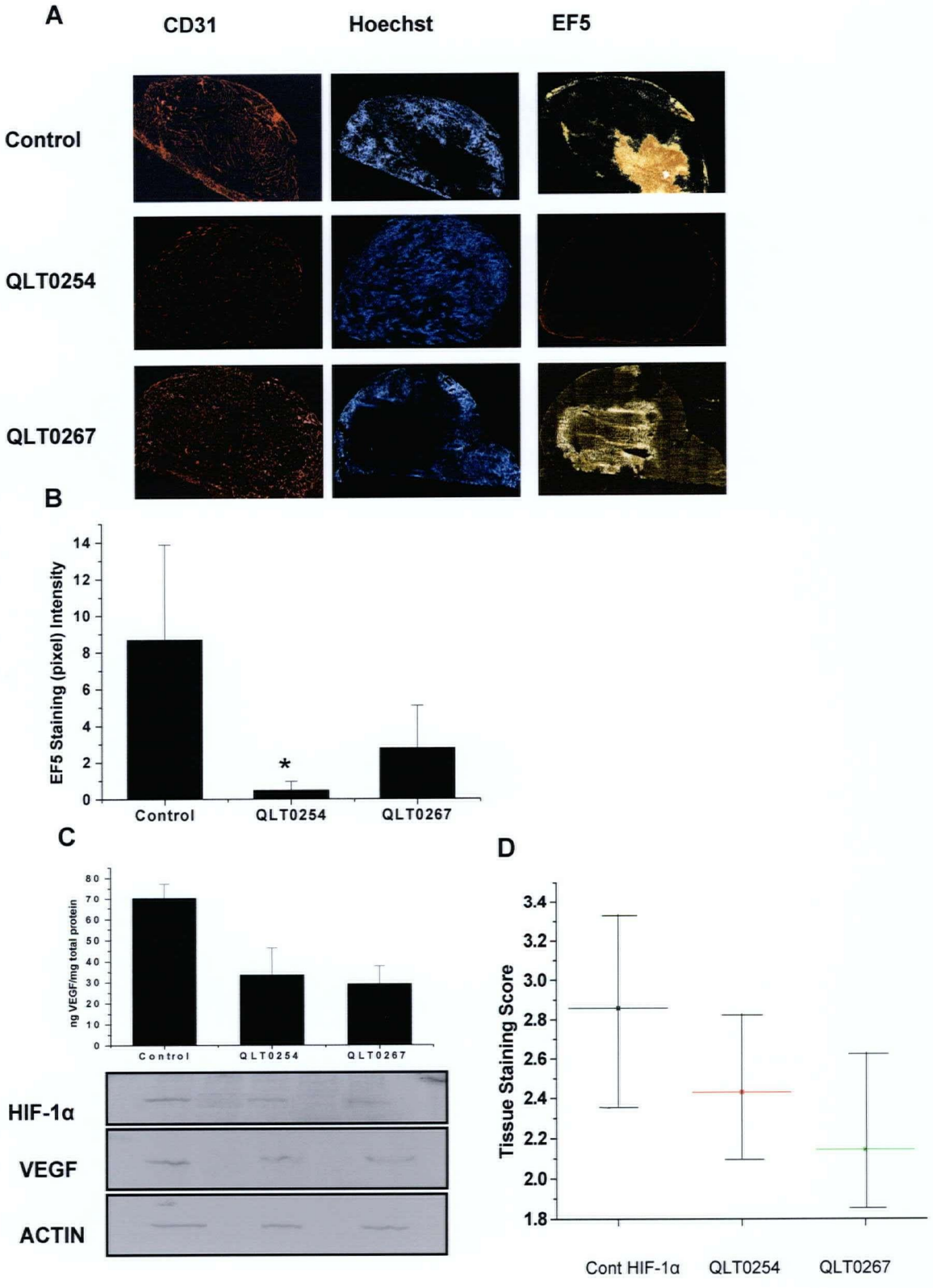
A
CD31
Hoechst
EF5
Control
QLT0254
QLT0267
B
EF5 Staining (pixel) Intensity
14
12
10
8
6
4
2
0
*
Control
QLT0254
QLT0267
C
ng VEGF/mg total protein
80
70
60
50
40
30
20
10
0
Control
QLT0254
QLT0267
HIF-1α
VEGF
ACTIN
D
Tissue Staining Score
3.4
3.2
3.0
2.8
2.6
2.4
2.2
2.0
1.8
Cont HIF-1α
QLT0254
QLT0267

5.3.8. The Effects of QLT0254 and QLT0267 Treatment on the Tumor Micro-evironment

The results thus far suggest that the selected ILK inhibitors delay tumor growth, a result that is supported by immunohistochemistry data showing an increase in apoptosis and a decrease in tumor cell proliferation. In addition, further analysis of tumors from treated animals suggest that ILK inhibition is associated with decreases in VEGF levels. The remaining evaluations therefore, focused on establishing whether these changes had an impact on tumor micro-environment as assessed by vascular density and vascular perfusion.

It should be noted that the micro-environment of glioblastomas with respect to hypoxia and human-vascularization has been characterized previously [136][185]. These reports, however, do not address how the microenvironment changes following treatment. Since therapeutic outcomes may be influenced by tumor micro-environmental factors [191-192] we believed it was important to evaluate the effects of ILK inhibition on the micro-environment. These studies characterized by qualitative and quantitative analysis of the tumor vasculature using image analysis are described in the Materials and Methods section. The tumor vascular endothelium was stained with CD31 (Fig. 5.7A enlarged box, red stained regions as indicated by purple arrow). Tumor sections obtained from U87MG isolated from animals, treated with saline (Fig. 5.7A), QLT0254 (Fig. 5.7B) or QLT0267 (Fig. 5.7C). Representative images are shown and semi-quantitative analysis of all images is summarized in Fig. 5.7D. CD31 staining results indicate that microvessels decrease with QLT0267 compared to saline treated control tumors (Fig. 5.7D). These data are summarized in Fig. 5.7D, and these analysis suggest that there is a significant decrease in tumor blood vessel density in tumors from animals treated with QLT0267. (6.8% versus 3.2%, mean difference = 3.6%, 95% CI = 0.5 to 6.7; P <0.028).

However, saline treated (n=6) or QLT0254 treated tumors (n=6) showed no differences. These data are consistent with what Yau and colleagues have shown in pancreatic tumors from animals treated with QLT0254 [182]. CD31/Hoechst33342; an indicator of perfused blood vessels (Fig. 7A enlarged box, shown by costains of red and blue indicated by the green arrow); indicated that tumors from animals treated with QLT0267 (n=6) had less than half the number of CD31/Hoechst 33342 functional blood vessels when compared to tumors treated with QLT0254 (n=6) and saline treated tumors (83% versus 35%, difference = 48%, 95% CI = 13% to 83%; $P<0.01$). These data are summarized in Fig. 5.7E.

Figure 5.7

Analysis of vascularization of U87MG tumors isolated from treated mice. *A-C.* Images of frozen tumor tissue sections from representative saline treated *(A)*, QLT0254 *(B)* and QLT0267 *(C)* U87MG tumor bearing mice which wer perfused *in vivo* with Hoechst33342 (shown in light blue) and subsequently stained with PECAM/CD31 (shown in red) antibody. *(D)* Percentage of CD31-stained (purple arrow) tumor tissue as measured by pixel intensity. Columns, mean (n=6 tumors ±SD). Total CD31-stained vessels is significant in QLT0267 treated animals compared to control. (6.8% versus 3.2) difference = 3.6%, 95% confidence interval [CI] = 0.4 to 6.8%, $P<0.028$. *(E)* Percentage of CD31 positive and Hoechst33342 perfused blood vessels (green arrow) as measured by pixel intensity. (mean n=6 tumors ±SD). Total CD31/Hoechst33342 is significantly lower in tumors from QLT0267 treated animals compared to control. (83% versus 35%) difference = 48%, 95% CI = 13% to 83%; $P<0.01$. Scale bar 150 μm.

.

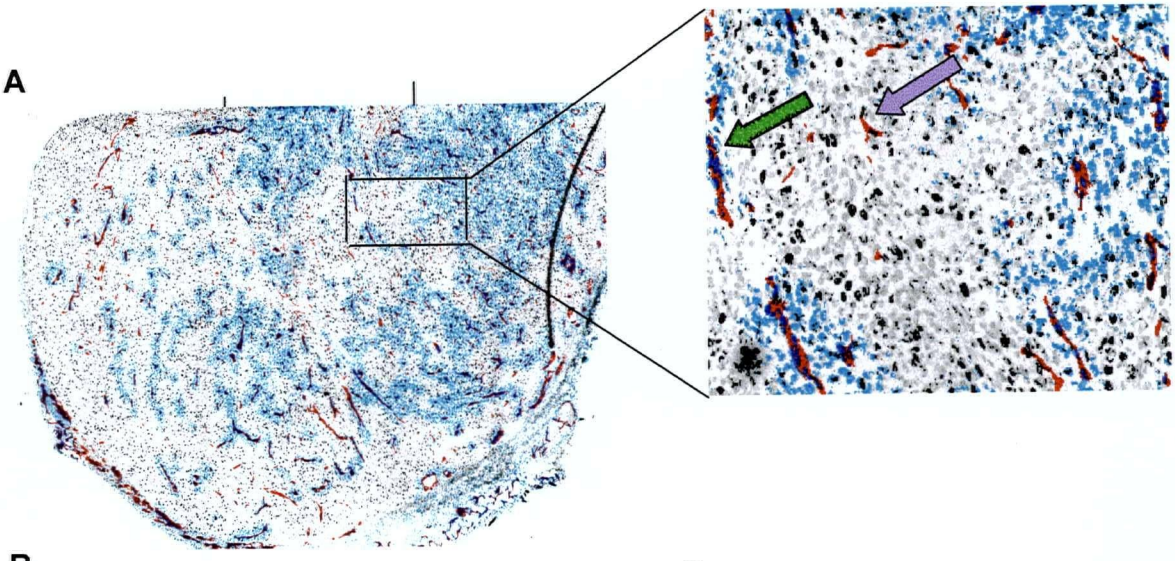
A

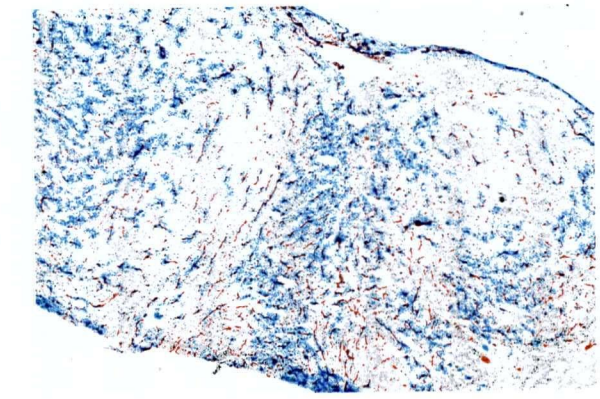
B

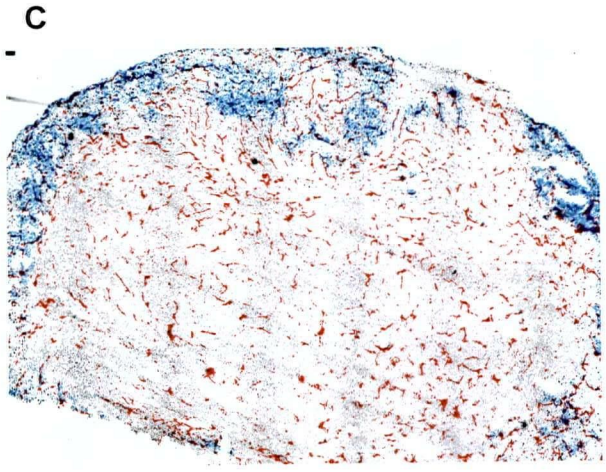
C

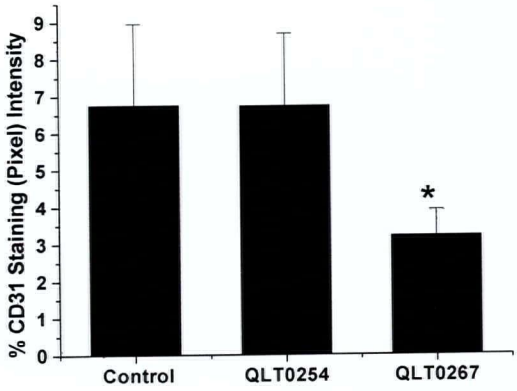
D
% CD31 Staining (Pixel) Intensity
0
1
2
3
4
5
6
7
8
9
*
Control
QLT0254
QLT0267

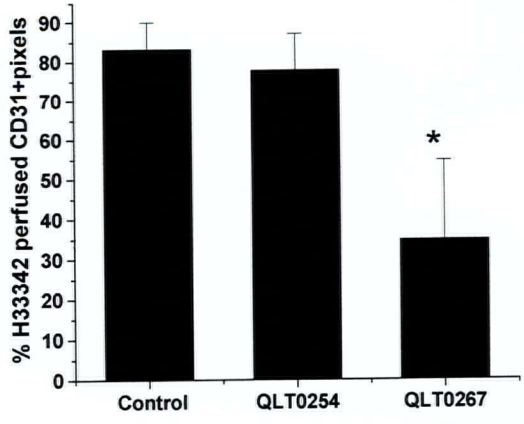
E
% H33342 perfused CD31+pixels
0
10
20
30
40
50
60
70
80
90
*
Control
QLT0254
QLT0267

5.4. Discussion

Integrin-linked kinase (ILK) in addition to regulating cell proliferation [93] and apoptosis [102] has been shown to regulate HIF-1α and VEGF in prostate cancer [128]. Both HIF-1α and VEGF are important factors that influence the development of angiogenic processes in response to hypoxia. Given that hypoxia and angiogenesis have been associated with glioblastomas [193-194], the potential of agents targeting ILK is clear: to inhibit cell growth and proliferation, to induce apoptosis and to inhibit VEGF secretion and associated angiogenic effects. Further, if ILK inhibition can inhibit production of HIF-1α that occurs in response to hypoxia, the inhibitors of ILK should provide multiple therapeutic effects via targeting a key regulatory kinase. This study gives a comprehensive assessment of the impact of targeting ILK, a kinase involved in a variety of cell signaling activities that are fundamental to cancer. In addition, the development of oral bio-available small molecule inhibitors targeting ILK is a novel approach to the treatment of cancers in which *PTEN* mutation or ILK expression are important. This is exemplified by a large proportion of glioblastomas.

QLT0254 and QLT0267 treatment was associated with inhibition of *in vitro* growth of several glioblastoma cell lines, however, this was achieved at high concentrations and these compounds may not be the generation of ILK inhibitor for clinical application, but do support the rationale for targeted therapy of GBM. These agents also mediated *in vivo* tumor growth delay when tumor bearing animals were treated orally at a dose of 200 mg/kg per/day. Although encouraging, these data are not sufficient in defining a potential cancer drug. Importantly, however, the efficacy of ILK inhibition was extended beyond these endpoints. In particular we investigated BrdUrd labeling to look at cell proliferation, EF5 labeling to examine hypoxia, and

Hoechst33342 to examine perfused blood vessels in U87MG glioblastoma tumors obtained from treated Rag-2M mice. Tumors can be imaged for these markers within the same tumor section and the staining quantified with image analysis software. It should be noted that the rationale for looking at the tumor micro-environment is important, however, the subcutaneous model used may not entirely reflect the intracranial model which would improve the analysis of tumor microenvironmental effects. This analysis gives a much more complete assessment of drug effects. Through this analysis it was determined that ILK inhibition by QLT0267 is associated with a decrease in CD31 staining, indicative of a decrease in microvessel density (Fig. 5.7D), and a decrease in Hoechst33342/CD31 staining, indicative of a decrease functional blood vessels (Fig. 5.7E). QLT0267 acts as an anti-vascular agent as well as a cytotoxic/cytostatic drug. QLT0267 treatment was not associated with significant changes in hypoxia as detected by EF5 labeling. This is not surprising if one assumes that decreasing tumor vasculature would maintain if not induce formation of hypoxic regions. Surprisingly, QLT0254 did not affect micro-vessel density or functional blood vessels, yet this inhibitor did affect significant reductions in hypoxia. Since blood vessel perfusion or microvessel density were not affected, reduced hypoxia must be explained by other results. An assessment of Fig. 5.6A, middle photomicrograph, suggest that total Hoechst33342 staining is enhanced. This may be indicative of enhanced perfusion, that is not detected when measuring CD31/Hoechst positive regions.

Perhaps most interesting, both inhibitors resulted in suppression of the angiogenic factor VEGF from cells and loss of VEGF and HIF-1α protein in tumor tissue (Figs. 5.3 and 5.6A). The *in vitro* data suggest that decreased VEGF secretion mediated by the inhibitors is comparable to decreases associated with induction of normal PTEN levels. The fact that both inhibitors are able to inhibit PKB/AKT, VEGF secretion, as well as HIF-1α and VEGF protein levels in

tumors, indicate a similar mechanism of action. Yet the effects on tumor hypoxia seem to differentiate the two drugs. When considering the data as a whole it does appear that QLT0267 is a superior drug in terms of decreasing cell proliferation (Fig. 5.5E), apoptosis (Fig. 5.5D) and tumor growth delay (Fig. 5.4). Whether this translates into clinically meaningful effects in patients can only be determined in the clinical setting. Regardless, this study highlights the benefit of analyzing multiple endpoints and the therapeutic potential of using a targeted agent that inhibits a kinase within a central pathway known to effect cell survival, cell proliferation and angiogenesis as well as metastasis. Analyzing several molecular end points such as tumor activity (e.g. cell proliferation, apoptosis), and drug induced changes in tumor micro-environment will improve the veracity of treatment approaches based on rational drug targets.

CHAPTER 6

SUMMARIZING DISCUSSION

6.1. Introduction

The treatment of brain cancer, particularly high grade gliomas such as glioblastoma multiforme has not significantly altered disease progression as judged by quality of life or overall survival due to resistance to treatment and lethality of these cancers [195-196]. The past two decades have not seen an improvement in quality of life or survival. In 1990 the life expectancy of a patient with GBM would not exceed 12 months from diagnosis [197]. In 2005 the expected survival time is still 12 months [198]. This thesis tested the hypothesis that Integrin-linked kinase (ILK) plays a key role in the progression of GBM and that inhibition or suppression of ILK would lead to a therapeutic effect. The studies were pursued in light of our basic understanding that effective chemotherapy of cancer requires the use of drug combinations, thus the studies assessed strategies that targeted ILK in combination with other agents (e.g. other targeted agents or conventional chemotherapy). The pre-clinical data obtained provides strong evidence that ILK is not only a relevant cancer target, but strategies targeting ILK merit futher investigation to demonstrate safety and efficacy in patients.

The importance of cell signaling pathways in determining cancer progression has led to the investigation of several targets in glioblastomas, agents targeting growth factor receptors, such as epidermal growth factor receptor (EGFR), platelet derived growth factor receptor (PDGFR), as well as the intracellular target Ras which have been evaluated in patients. More recently, other targets have emerged that may prove to be important molecular targets in GBM e.g. Rac [199]. The loss of *PTEN* in glioblastomas is well known and it is clear that this loss leads to the subsequent downstream activation of PKB/AKT. The results summarized in Chapter

3 are the first to document in detail ILK as an intermediate in PTEN regulation and PKB/AKT activation in glioblastoma cancer cells. This study also detailed the use of an antisense oligonucleotide to target ILK in glioblastoma cancer cell lines leading to decreased phosphorylation of PKB/AKT and tumor growth delay. In addition, Chapter 3 confirms the relationship between PTEN, ILK and PKB/AKT through the use of an inducible PTEN promoter. The strategy targeting ILK with antisense oligonucleotides clearly suggested that ILK suppression promotes a tumor growth delay in pre-clinical animal models, but not tumor eradication (Chapter 3). This result was confirmed when using small molecular inhibitors of ILK, as summarized in Chapter 5. ILK inhibition by either antisense or small molecule inhibitor result in a cell cycle arrest *in vitro*, over time this may lead to an apoptotic event, however, *in vivo*, decreased cell proliferation is more prevalent than apoptosis and may be responsible for a tumor growth delay effect.

ILK is thus a prime candidate to be used in a combination approach to achieve optimal treatment of GBM. The studies performed here with ILK as one target within a combination was focused on identification of agents that interacted in a manner that achieves additive or synergistic effects. The rationale behind the combination studies was to look for pathways that were dysregulated in glioblastomas and to seek out other targets in addition to ILK that may be critical to cancer cell survival in the context that inhibition of one pathway may be necessary, but not sufficient, to achieve optimal therapeutic effects. Given that EGFR is overexpressed in glioblastomas, targeting the EGFR in combination with agents that target ILK could potentially provide ideal therapeutic effects. Evidence to support this was provided in Chapters 1 where the EGFR inhibitor PD153035 resulted in synergy, as measured by an *in vitro* assay. Since EGFR expression results in activation of downstream targets which could be highly overexpressed as

well, targeting of the downstream targets Raf-1 and MEK in combination with ILK should also result in drug combination synergy. These results, summarized in Chapter 4, demonstrate combinations of ILK targeting (using antisense oligonucleotides) with small molecule inhibitors for the treatment of glioma resulted in synergy *in vitro*. Drug combinations that appear strongly synergistic can be defined on the basis of a cell based screening assay, however it is critical to demonstrate that the combinations are effective *in vivo* [170]. The ultimate test in glioma patient populations is beyond the scope of this thesis, but it is in patients where the efficacy of these combinations needs to be shown.

To exemplify how such combinations could be defined for patients preliminary studies provided here show that the drug combination of Gleevec™ and the ILK inhibitor QLT0267 result in a synergistic combination as judged by a cell based assay. Although the drug combination showed synergy over Fa values between 0.2 and 0.45 (Fig. 6.1), these data provide the indication of drug combination interactions that support further studies. In a U87MG xenograft tumor model, this combination appeared to cause a decrease in the viable but hypoxic tumor cell population and using this as a therapeutic endpoint suggested that the effects were greater than that which could be achieved with these agents administered separately. These results are summarized in Figure 6.2, where EF5 positive cells (Chapter 5) were assessed using a flow cytometric procedure. Interestingly, an analysis of tumor volume with this combination (summarized in Fig. 6.3) indicated that there was no synergistic effect at the dose used. These preliminary data highlight an important problem with combination studies.

Figure 6.1

Representative plot showing a synergistic effect of an ILK inhibitor (QLT0267) and Gleevec™ in U87MG glioblastoma cells exposed for 48 h. Note that each data point (square boxes shown in black) moving from left to right is an increasing ratio of the drug combination of ILKAS and Gleevec™. The data points that fall below the dotted horizontal line which represents the CI value 1 indicates a synergistic relationship. Please refer to Chapter 2 for detail on drug combination analysis.

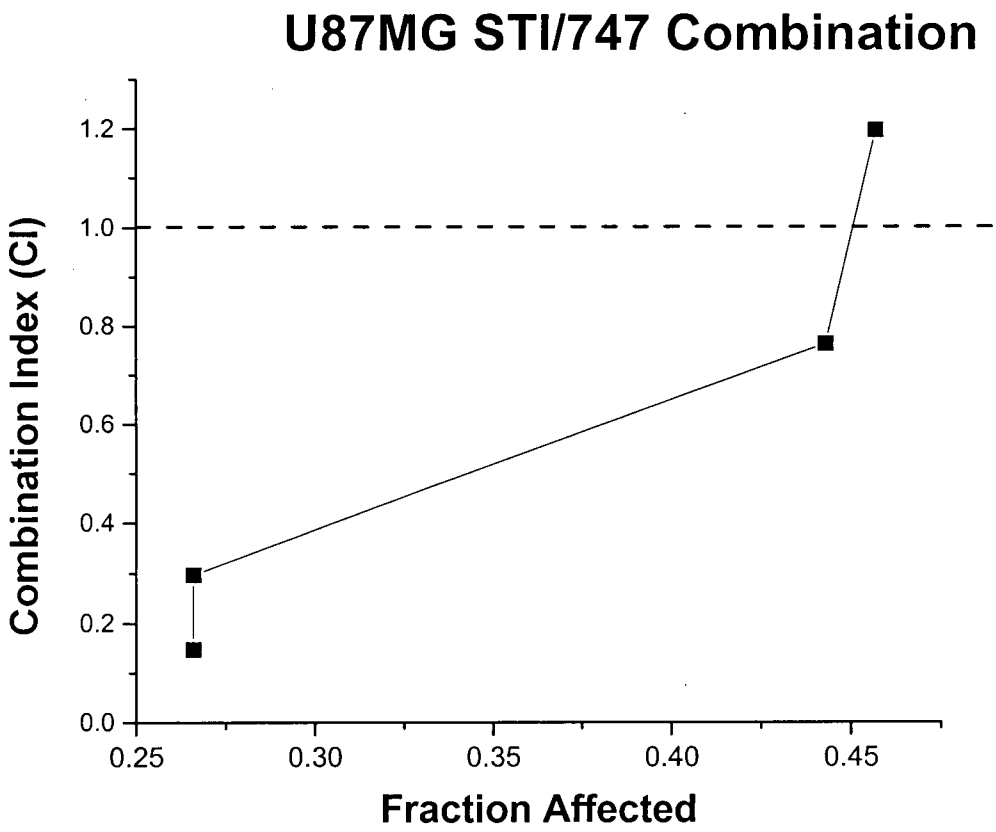

It is essential that multiple therapeutic endpoints are considered when analyzing drug combinations if statements regarding synergistic interactions are to be made. The work presented here gives insight into using various assays to determine if a desired drug combination is in fact a synergistic interaction (Chapter 4). Characterization of a drug combination or a single drug for that matter with multiple endpoints will provide important information on the viability of a cancer target and a more realistic picture of the clinical utility of the selected drug. In the analysis of the ILK inhibitors QLT0254 and QLT0267, endpoints included cell viability assays against multiple glioblastoma cell lines, as well as assessments of cell death, colony formation and modulation in the activation of molecular markers (Chapter 5). When developing the *in vivo* studies to support further development of these ILK inhibitors, endpoints considering tumor growth rates were combined with endpoints derived from image analysis, to assess drug mediated changes. The objective of such studies was to investigate effects of ILK inhibition on hypoxia and angiogenesis in addition to measures of apoptosis and cell proliferation (Chapter 5). These data suggest that these agents can produce multiple effects on glioblastoma tumor progression, effects that are consistent with the role of ILK singaling in cell proliferation and regulation of VEGF secretion.

Figure 6.2

Glioblastoma Tumor Hypoxia Decreases with ILK inhibition in Combination with Gleevec™ Rag-2M mice bearing U87MG xenograft tumors were treated with saline, antisense targeting ILK (ILKAS), Gleevec™ or the combination of Gleevec™ and ILKAS. To measure hypoxia Rag-2M mice with U87MG xenograft tumors were injected with EF5 which labels hypoxic cells 3 h prior to tumor harvesting of the treated groups and the saline treated group. Tumors (n=4) were disaggregated and flow cytommetry was used to visualize and quantify hypoxic tumor cells to non-hypoxic tumor cells. The combination of ILKAS and Gleevec™ suggests a synergy in decreasing tumor hypoxia compared to using either ILKAS or Gleevec™ alone.

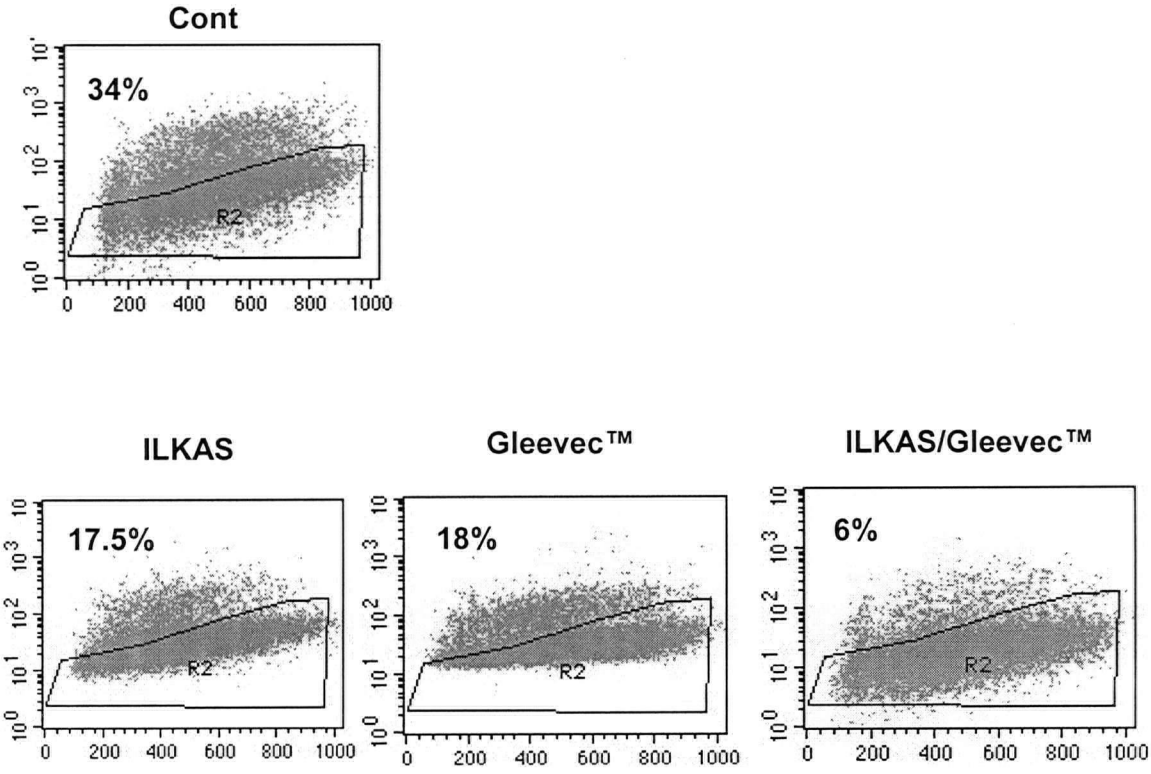

Figure 6.3

Effect of Gleevec™ and ILKAS on Rag-2M mice bearing U87MG xenograft tumors (n=5). Subcutaneous xenografts were established by injecting 5 X 10^6 U87MG glioblastoma cells. Mice received saline, ILKAS (20 mg/kg) or Gleevec™ (100 mg/kg) or the combination of ILKAS and Gleevec™ (20/100 mg/kg) for 14 days. Graph shows day 52 post tumor cell inoculation. Average mean tumor volume is shown with circle with line through the middle. Control = 764 mm^3, ILKAS = 652 mm^3, Gleevec™ = 480 mm^3 and ILKAS/Gleevec™ = 480 mm^3.

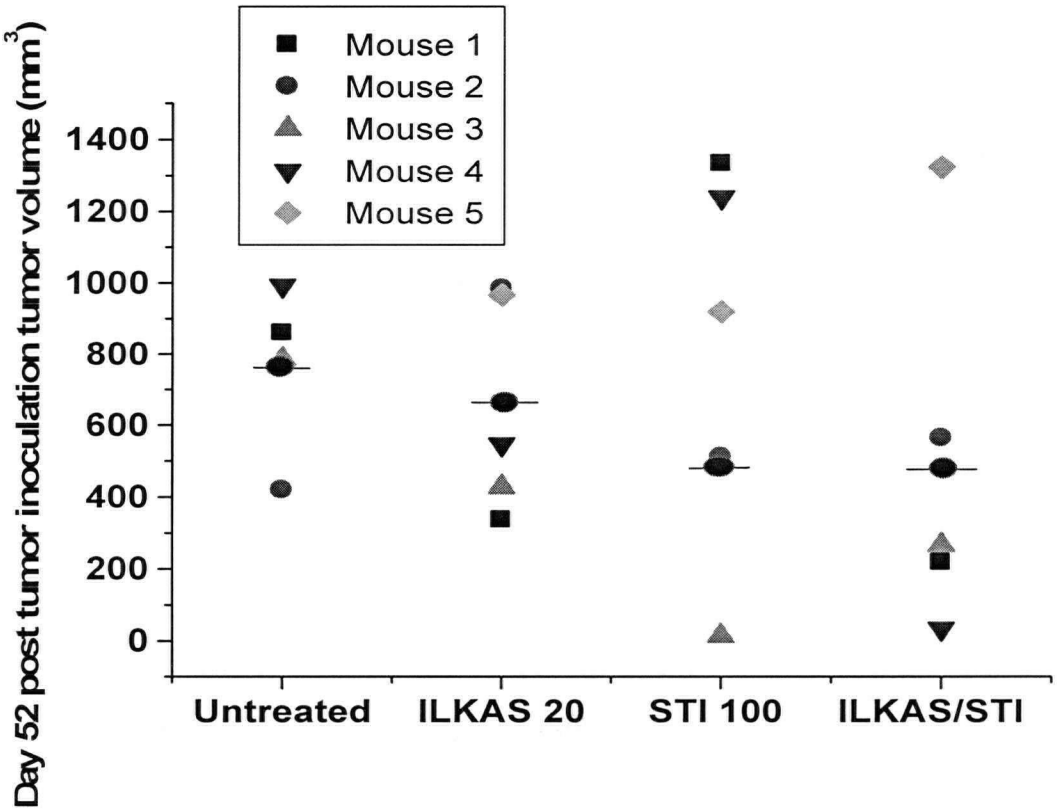

The ILK inhibitors QLT0254 and QLT0267 both resulted in inhibition of PKB/AKT activity, decreased cell viability, a dose dependent cell cycle arrest in the G_2/M phase of the cell cycle and caspase induction on all the glioblastoma cell lines tested. Further, both resulted in decreasing tumor size relative to control and vehicle control tumors (greater than 50% on day 16 post treatment). However, an examination of tumor micro-environment effects showed distinct differences. QLT0267 appeared to have anti-vascular effects with decreased micro-vessel density as determined by CD31 staining and a decrease in perfused blood vessels as measured by Hoechst33342 used to visualize perfused blood vessels (Chapter 5). In contrast, QLT0254 did not show any significant decrease in micro-vessel density or perfused blood vessels relative to saline treated tumors. Interestingly, QLT0254 significantly decreased hypoxia, whereas QLT0267 showed a decrease in hypoxia when compared to the effects of QLT0254. This would suggest that QLT0254 may be a useful chemo or radio-sensitizing agent and, although less potent as judged by cell based assay, this may be the most appropriate agent to develop in a combination setting. The benefit of assessing various endpoints allowed the elucidation of separate roles for these ILK inhibitors that would not have been uncovered with drug studies where tumor size was the only measured endpoint.

The rationale for the development of cancer drugs that target cell signaling pathways known to be critical to GBM progression is solid, however, it is unlikely that heterogenous cell populations consisting of cells with multiple dysregulated pathways will be effectively managed by an agent targeting one pathway. Thus it is the understanding that agents targeting ILK will be most useful in combination with other drugs. It is also important to note that there will also be an advantage to using agents that target pathways that control multiple processes. Although, single and combination studies have shown promise. It is believed that *in vitro* and *in vivo*

analysis using several therapeutic endponts along with established dose-response relationships are required to fully characterize combination effects. This is particularly true in light of the work from Chou and Talalay [119-120][169-120] and others that indicate that a synergistic drug combination at one dose level may not exhibit synergy at other dose levels. This indicates that there may be a finite dosage "window" to which optimum therapeutic effect (in the form of an additive or synergistic interaction) may be achieved. With this in mind the question for future investigation is how to translate interesting results obtained for drug combinations collected in pre-clinical models to the clinical setting.

This thesis has shown that ILK is involved in GBM progression and is a relevant cancer target. The therapeutic effects achieved through ILK targeting can be enhanced by defining combinations that yield synergistic interaction. ILK inhibitors combined with other agents that target appropriate cell signaling pathways involved glioblastoma progression/maintenance are of particular interest. Several molecular and therapeutic endpoints beyond tumor growth aid in the interpretation of a relevant cancer target and are useful in determining the therapeutic potential of these targeted agents. It is hoped that the data provided in this thesis, along with the associated publications that arose from this research, provide compelling evidence in support of developing treatment strategies that involve use of one agent that targets ILK.

References

1) Ohgaki, H., Dessen, P., Jourde, B., Hortsmann, S., Nishikawa, T., Di Patre, P-L., Burkhard, C., Schuller, D., Probst-Hensch, NM., Maiorka, PC., Baeza, N., Pisani, P., Yonekawa, Y., Yasargil, MG., Lutolf, UM., Kleihues, P. (2004) Genetic Pathways to Glioblastomas. Can Res 64:6892-6899.

2) Mcallister, LD., Ward, JH., Schulman, SF., DeAngelis, LM. (2002) Practical Neuro-oncology: A guide to patient care. pp. 3. Butterworth-Heinenmann, Boston.

3) Kaye, AH., Laws, ER. (1995) Historical perspective. In Brain tumors (ed. A.H. Kaye and E.R. Laws, Jr.), pp. 3-8. Churchill Livingston, New York

4) Kleihues, P., Cavenee, WK. (2000) World Health Organization classification of tumors of the nervous system. IARC/WHO, Lyon

5) Maher, EA., Furnari, FB., Bachoo, RM., Rowitch, DH., Louis, DN.,Cavenee, WK., DePinho, RA. (2001) Malignant glioma: genetics and biology of a grave matter. Gene & Dev 15, 1311-1333.

6) Huang, H., Colella, S., Kurrer, M., Yonekawa, Y., Kleihues, P., Ohgaki, H. (2000) Gene expression profiling of low-grade diffuse astrocytomas by cDNA arrays. Cancer Res 60, 6868-6874.

7) Knudson, AG jr. (1971) Mutation and cancer: statistical study of retinoblastoma. PNAS 68, 820.

8) Schenkein, I., Bueker, ED., Helson, L., Axelrod, F., Dancis, J. (1974) Increased nerve stimulating activity in disseminated neurofibromatosis. N Eng J Med 290, 613.

9) Cohnheim, J. (1889) Lectures on General Pathology. Translated from 2nd German edn by A.B. Mckee p. 746 London; The New Sydenham Society.

10) Friede, RL. (1973) Dating the development of human cerebellum. Acta Neuropath (Berl.) 23, 48.

11) Willis, RA. (1967). Pathology of Tumors, 4th edn. London; Butterworth.

12) Kleihues, P., Burger, P C., Scheithauer, BW. (1993) Histological Typing of Tumors of the Central Nervous System. World Health Organization Springer; Berlin).

13) Burger, P C., Scheithauer, BW. (1994) Tumors of the Central Nervous System (Armed Forces Institute of Pathology, Washington, DC).

14) Lewis, PD. (1968) Mitotic activity in the primate subependymal layer and the genesis of gliomas. Nature 217(132): 974-5.

15) Lantos, PL., Cox, DJ. (1976) The origin of experimental brain tumours: a sequential study. Experientia 32(11): 1467-8.

16) Vik, NA., Lin, MJ., Bigner, DD. (1977) The role of the subependymal plate in glial tumorigenesis. Acta Neuropathol (Berl) 40(1):63-71.

17) De la Monte, SM. (1989) Uniform lineage of oligodendrogliomas. Am J Path 135: 529-540.

18) Nobel, M., Gutowski, N., Bevan, K., Engel, U., Linskey, M., Urenjak, J., Bhakoo, K., Williams, S. From rodent glial precursor cell to human glial

neoplasia in the oligodendrocyte-type-2 astrocyte lineage. (1995) Glia 15(3): 222-30.

19) Hermanson, M., Funa, K., Koopmann, J., Maintz, D., Waha, A., Westermark, B., Heldin, CD., Wiestler, OD., Louis, DN., von Deimling, A., Nister, M. (1996) Association of loss of heterozygosity on chromosome 17p with high platelet-derived growth factor alpha receptor expression in human malignant gliomas. Can Res 56(1): 164-171.

20) Sanai, N., Alvarez-Buylla, A., Berger, MS. (2005) Neural Stem Cells and the Origin of Glioma. 353(8): 811-822.

21) Sanai, N., Tramontin, AD., Quinones-Hinojosa, A., Barbaro, NM., Gupta, N., Kunwar, S., Lawton, MT., McDermott, MW., Parsa, AT., Manuel-Garcia Verdugo, J., Berger, MS., Alvarez-Buylla, A. (2004) Unique astrocyte ribbon in adult human brain contains neural stem cells but lacks chain migration. Nature 427: 740-744.

22) Shoshan, Y., Nishiyama, A., Chang, A., Mork, S., Barnett, GH., Cowell, JK., Trapp, BD., Staugaitis, SM. (1999) Expression of oligodendrocyte progenitor cell

antigens by gliomas: implications for the histogenesis of brain tumors. PNAS 96: 10361-10366.

23) Lantos, PL., Pilkington, GJ. (1979) The development of experimental brain tumors. A sequential light and electron microscope study of the subependymal plate. I. Early lesions (abnormal cell clusters). Acta neruopath. (Berl.), 45, 167.

24) Todarao, GJ., Huebner, RJ. (1972) The viral oncogene hypothesis: new evidence. PNAS 69, 1009.

25) Richardson, EP. (1970) Progressive multifocal leucoencephalopathy. In: Handbook of Clinical Neurology (eds. PJ Vinken and TW Bruyn), vol. 9, p. 485. Amsterdam: North Holland.

26) Walker, DL., Padgett, BL., Zurhein, GM., Albert, AE., Marsh, RF. (1973) Human papovavirus (JC): induction of brain tumors in hamsters. J Cell Sci 181, 674.

27) Barbanti-Brodano, G., Silini, E., Mottes, M., Milinesi, G., Pagani, M., Reshligan, P., Cerna, G., Corrallini, A. (1987) DNA probes to evaluate the possible association of papovaviruses with human tumors. In: Monoclonals and

DNA Probes in Diagnostic and Preventative Medicine. New York, Raven Press pp. 147-155.

28) Billingham, RW., Boswell T. (1953) Studies on the problem of corneal honografts. Proc R Soc Lond B Biol Sci 141: 392–406.

29) Barker, CF., Billingham, RE. (1977) Immunologically privileged sites. Adv Immunol 25:1–54.

30) Barker, RA., Widner, H. (2004) Immune Problems in Central Nervous System Cell Therapy. NeurRx 1:472-481.

31) Farver, E. (1976). Putative precursor lesions: summary and some analytical considerations. Can Res 36, 2703.

32) Jondal, M., Spina, C., Targan, S. (1978) Human spontaneous killer cells selective for tumor derived target cells. Nature 272, 62.

33) Stupp, R., Mason, WP., van den Bent, MJ., Weller, M., Fischer, B., Taphoorn, MJB., Berlanger, K., Brandes, AA., Marosi, C., Bogdahn, U., Curschmann, J.,

Janzer, RC., Ludwin, SK., Gorlia, T., Allgeier, A., Lacombe, D., Cairncross, JG., Eisenhauer, E., Mirimanoff, RO. (2005) Radiotherapy plus Concomitant and Adjuvant Temozolomide for Glioblastoma. NEJM 352:987-996.

34) Kilic, T., Alberta, JA., Zdunek, PR., Acar, M., Iannarelli, P., O'Reilly, T., Buchdunger, E., Black, PM., Stiles, CD.(2000). Intracranial Inhibition of Platelet-derived Growth Factor-mediated Glioblastoma Cell Growth by an Orally Active Kinase Inhibitor of the 2-Phenylaminopyrimidine Class. Can Res 60:5143-5151.

35) Johns, HE., Cunningham, JR. (1983). The physics of radiobiology. Springfield, IL.

36) Tyrell, RM. (1991). UVA (320nm-380 nm) radiation as an oxidative stress, p. 57-83. In H. Sies (ed.), Oxidative Stress: Oxidants and Antioxidants. Academic Press, Ltd., London.

37) Tyrell, J-S., Garrett, DS., Brockie, IR., Svoboda, DL., Telser, J. (1988). Solution-state structure of the Dewar pyrimidinone photoproduct of thymidylyl-(3'-5')-thymidine. Biochemistry 27:7206-7215.

38) Ward, JF. (1988) DNA damage produced by ionizing radiation in mammalian cells:identities, mechanisms of formation and reparability. Prog Nucleic Acid Res Mol Biol 35:95-125.

39) Lett, JJ., Stacey, KA., Alexander, P. (1961). Crosslinking of dry deoxyribonucleic acids by electrons. Radiat Res 14:349-362.

40) Love, JD., Nguyen, HT., Or, A., Attri, AK., Minton, KW. (1986). UV-induced interstrand cross-linking of d(GT)n-d(CA)n is facilitated by a structural transition. J Biol Chem 261:10051-10057.

41) Marmur, J., Grossman, L. (1961). Ultraviolet light induced linking of deoxyribonucleic acid strands and its reversal by photoreactivating enzyme. Proc Natl Acad Sci USA 47:778-787.

42) Clark, JM., Beardsley, GP. (1987). Functional effects of cis-thymine glycol lesions on DNA synthesis in vitro. Biochemistry 26:5398-5403.

43) Clark, JM., Pattabiraman, N., Jarvis, W., Beardsley, GP. (1987). Modeling and molecular mechanical studies of the cis-thymine glycol radiation damage lesion on DNA. Biochemistry 26:5404-5409.

44) Chan, GL., Doetsch, PW., Haseltine, HA. (19850 Cyclobutane pyrimidine dimmers and (6-4) photoproducts block polymerization by DNA polymerase I. Biochemistry 24:5723-5728.

45) Hayes, FN., Williams, DL., Ratliff, RL., Varghese, AJ., Rupert, CS. (1971) Effect of a single thymine photodimer on the oligodeoxythymidilate-polydeoxyadenylate interaction. J Am Chem Soc 93:4940-4942.

46) Witkin, EM. (1976) Ultraviolet mutagenesis and inducible DNA repar in Escherichia coli. Bacteriol Rev 40:869-907.

47) Khan, FM. (1984). The Physics of Radiation Therapy. Baltimore, Williams and Wilkins.

48) Owen, JB., Coia, LR., Hanks, G E.(1992). Recent patterns of growth in radiation therapy facilities in the United States: a patterns of care study report. Int. J. Radiat. Oncol. Biol. Phys., *24,* 983-986.

49) Janssen, HL., Haustermans, KM., Balm, AJ., Begg, C. (2005) Hypoxia in head and neck cancer: How much, how important? Head & Neck 27(7): 622-638.

50) Fiveash, JB., Spencer, SA. (2003) Role of Radiation Therapy and Radiosurgery in Glioblastoma Multiforme. Cancer J 9(3): 222-229.

51) Durand, RE. (1994) The influence of microenvironmental factors during cancer therapy. In Vivo. 8: 691-702.

52) Olive, PL., Durand, RE. (1994) Drug and radiation resistance in spheroids: cell contact and kinetics. Cancer Metastasis Rev 13: 121-138.

53) Teicher, BA. (1994) Hypoxia and drug resistance. Cancer Metastasis Rev 13: 139-168.

54) Behin, A., Delattre, J-Y. (2004). Complications of Radiation Therapy on the Brain and Spinal Cord. Seminars in Neurology 24(4), 405-417.

55) Littman, P., Rosenstock, J., Gale, G, et al.(1984). The somnolence syndrome in leukemic children following reduced daily dose fractions of cranial radiation. Int J Radiat Oncol Biol Phys 10, 1851-1853.

56) Young, DF., Posner, JB., Chu, F., Nisce, L. (1974). Rapid-course radiation therapy of cerebral metastases: results and complications. Cancer 34, 1069-1076.

57) Hindo, WA., DeTrana, FA., Lee, MS., Hendrickson, FR. (1970). Large dose increment irradiation in treatment of cerebral metastases. Cancer 26, 138-141.

58) Armstrong, C., Ruffer, J., Corn, BW., Devriees, K., Mollman, J.(1995). Biphasic patterns of memory deficits following moderate-dose partial-brain irradiation: neuropsychologic outcome and proposed mechanisms. J Clin Oncol 13, 2263-2271.

59) Vigliani, MC., Sichez, N., Poisson, M., Delattre, JY. (1996). A prospective study of cognitive functions following conventional radiotherapy for supratentorial gliomas in yound adults: 4 year results. Int J Radiat Oncol Biol Phys 35, 527-533.

60) Levin, VA., Wilson, CB., Davis, R., Wara, WM., Pischer, TL., Irwin, L. (1979). A phase III comparison of BCNU, hydroxyurea, and radiation therapy for treatment of primary malignant gliomas. J Neurosurg 51, 526-532.

61) Gerosa, MA.,DiStefano, E., Olivia, A. (1981). VM-26 monochemotherapy trail in the treatment of recurrent supratentorial gliomas: Preliminary report. Surg Neurol 15, 128-134.

62) Eagan, RT., Creagan, ET., Biseal, HF., Layton, DD., Grover, RV, et al.(1981). Phase II study of dianhydrogalactitol based combination chemotherapy for recurrent brain tumors. Oncology 38, 4-6.

63) Gethan, EA., Walker, MD. (1977). Prognostic factors for patients with brain tumors. Natl Cancer Inst Monogr 46, 189-195.

64) LaSala, P. (1988). Advances in Neuro-Oncology: Clinical Factors Affecting Brain Tumor Chemotherapy Futura Publishing, Inc., Mount Kisco, NY pp415-432.

65) Groothuis, DR (2000) The blood-brain and blood-tumor barriers; A review of strategies for increasing drug delivery. Neuro-Oncology 2:45-59.

66) Pardridge, WM (2002) DRUG AND GENE TARGETING TO THE BRAIN WITH MOLECULAR TROJAN HORSES. Nature Rev Drug Discovery 1:131-139.

67) Pardridge, WM Brain Drug Targeting:the Future of Brain Drug Development (Cambridge Univ Press, Cambridge, 2001).

68) Brightman, MW (1977) Morphology of blood-brain interfaces. Exp Eye Res 25(Suppl) 1-25.

69) Schlageter, KE., Molnar, P., Lapin, GD., Groothuis, DR (1999) Microvessel organization and structure in experimental brain tumors: Microvessel populations with distinctive structureal and functional properties. Microvasc Res 58:312-328.

70) Demuth, R., Berens, ME (2004) Molecular mechanisms of glioma cell migration and invasion. J Neuro-Onoclogy 70:217-228.

71) Holland, EC (2000) Glioblastoma multiforme: the terminator. PNAS USA 97(12):6244-6244.

72) Brat, DS., Van Meir, EG (2004) Vaso-Occlusive and prothrombotic mechanisims associated with tumor hypoxia, necrosis, and accelerated growth in glioblastoma. Lab Invest 84(4):397-405.

73) Zagzag, D., Amirnovin, R., Greco, MA., Yee, H., Holash, J., Weigand, SJ., Zabski, S., Yancopoulos, GD., Grumet, M (2000) Vascular apoptosis and involution in gliomas precede neovascularization: a novel concept for glioma growth and angiogenesis. Lab Invest 80(6):837-849.

74) Ishii, N., Maier, D., Merlo, A., Tada, M., Sawamura, Y., Diserens, AC., Van Meir, EG (1999) Frequent co-alterations of TP53, p16/CDKN2A, p14ARF and PTEN tumor suppressor genes in human glioma cell lines. Brain Pathol 9(3):469-479.

75) Zundel, W., Schindler, C., Hass-Kogan, D., Koong, A., Kaper, F., Chen, E., Gottschalk, AR., Ryan, HE., Johnson, RS., Jefferson, AB., Stokow, D., Gaicci, AJ: Loss of PTEN facilitates HIF-1-mediated gene expression. Genes Dev 14(4);391-396.

76) Hanahan, D., Folkamn, J (1996) Patterns and emerging mechanisms of the angiogenic switch during tumorigenesis. Cell 86(3):353-364.

77) Wu, C., Keightley, SY., Leung-Hagesteijn, C., Radeva, G., Coppolino, M., Goicoechea, S., McDonald, JA., Dedhar, S. (1998) Integrin-linked protein kinase regulates fibronectin matrix assembly, E-cadherin expression, and tumorigenicity. JBC 273(1): 528-36.

78) Hannigan, GE., Leung-Hagesteijn, C., Fitz-Gibbon, L., Coppolino, MG., Radeva, G., Filmus, J., Bell, JC., Dedhar, S. (1996) Regulation of cell adhesion and anchorage-dependent growth by a new beta 1-integrin-linked protein kinase. Nature 379: 91-96.

79) Giancotti, FG & Ruoslahti, E. (1999) Integrin signaling during tumor progression. Science 285: 1028-1032.

80) Tu, Y., Huang, Y., Zhang, Z., Hua, Y., Wu, C. (2001) A new focal adhesion protein that interacts with integrin-linked kinase and regulates cell adhesion and spreading. J Cell Biol 153: 585-598.

81) Yamaji, S., Suzuki, A., Sugiyama, Y., Koide, Y., Yoshida, M., Kanamori, H., Mohri, H., Ohno, S., Ishigatsubo, Y. (2001) A novel integrin-linked kinase-binding protein, affixin, is involved in the early stage of cell-substrate interaction. J Cell Biol 153: 1251-1264.

82) Nikolopoulos, SN., Turner, CE. (2001) Integrin-linked kinase (ILK) binding to paxillin LD1 motif regulates ILK localization to focal adhesions. J Biol Chem 276: 23499-23505.

83) Yoganathan, N., Yee, A., Zhang, Z., Leung, D., Yan, J., Fazli, L., Kojic, DL., Costello, PC., Jabali, M., Dedhar, S., Sanghera, J. (2002) Integrin-linked kinase, a promising cancer therapeutic target: biochemical and biological properties. Pharmacol Ther 93(2-3): 233-42.

84) Wu, C. (2005) PINCH, N(i)ck and the ILK: network wiring at cell–matrix adhesions. Trends in Cell Biol 15(9): 460-466.

85) Guo, L., Wu, C. (2002) Regulation of fibronectin matrix deposition and cell proliferation by the PINCH-ILK-CH-ILKBP complex. FASEB J 16: 1298-1300.

86) Tu, Y., Li, F., Goicoechea, S., Wu, C. (1999) The LIM-only protein PINCH directly interacts with integrin-linked kinase and is recruited to integrin-rich sites in spreading cells. Mol Cell Biol 19(3): 2425-34.

87) Wu, C. (1999) Integrin-linked kinase and PINCH: partners in regulation of cell-extracellular matrix interaction and signal transduction. J Cell Sci 112 (Pt 24): 4485-9.

88) Wu, C. (2004) The PINCH-ILK-parvin complexes: assembly, functions and regulation. Biochim Biophys Acta 1692(2-3): 55-62.

89) Brakebusch, C., Fassler R. (2003) The integrin–actin connection, an eternal love affair. Embo J 22: 2324-2333.

90) Persad, S., Attwell, S., Gray, V., Delcommenne, M., Troussard, A., Sanghera, J., Dedhar, S. (2000) Inhibition of integrin-linked kinase (ILK) suppresses activation of protein kinase B/Akt and induces cell cycle arrest and apoptosis of PTEN-mutant prostate cancer cells. Proc Natl Acad Sci USA 97: 3207-1322.

91) Stambolic, V., Suzuki, A., de la Pompa, JL., Brothers, GM., Mirtsos, C., Sasaki, T., Ruland, J., Penninger, JM., Siderovski, DP., Mak, TW. (1998) Negative regulation of PKB/AKT-dependent cell survival by the tumor suppressor PTEN. Cell 95: 29-39.

92) D'Amico, M., Hulit, J., Amanatullah, DF., Zafonte, BT., Albanese, C., K-I., Moon, RT., Davis, R, Lisanti, MP., Shtutman, M., Zhurinsky, J., Ben-Ze'ev, A., Troussard, AA., Dedhar, S., Pestell, RG. (2000) The integrin-linked kinase regulates the cyclin D1 gene through glycogen synthase kinase 3beta and cAMP-responsive element-binding protein-dependent pathways. J Biol Chem 275: 32649-32657.

93) Radeva, G., Petrocelli, T., Behrend, E., Leung-Hagesteijn, C., Filmus, J., Slingerland, J., Dedhar, S. (1997) Overexpression of the integrin-linked kinase promotes anchorage-independent cell cycle progression. J Biol Chem 272: 13937-13944.

94) Nicholson, KM., Anderson, NG. (2002) The protein kinase B/Akt signalling pathway in human malignancy. Cell Signal 14: 381-395.

95) Lynch DK., Ellis, CA., Edwards, PA, Hiles, ID. (1999) Integrin-linked kinase regulates phosphorylation of serine 473 of protein kinase B by an indirect mechanism. Oncogene 18: 8024-8032.

96) Persad, S., Attwell, S., Gray, V., Mawji, N., Deng, JT., Leung, D., Yan, J., Sanghera, J., Walsh, MP., Dedhar, S. (2001) Regulation of Protein Kinase B/Akt-

Serine 473 Phosphorylation by Integrin-linked Kinase. J Biol Chem 276(29): 27462-27469.

97) Feng, J., Park, J., Cron, P., Hess, D., Hemmings, BA. (2004) Identification of a PKB/Akt Hydrophobic Motif Ser-473 Kinase as DNA-dependent Protein Kinase 279(39): 41189-41196.

98) Dong, LQ., Liu, F. (2005) PDK2: the missing piece in the receptor tyrosine kinase signaling pathway puzzle. Am J Physiol Endocrinol Metab 289: E187-E196.

99) Deng, JT., Sutherland, JT., Braughtigan, JL., Eto, M., Walsh, MP. (2002) Phosphorylation of the Myosin phosphatase inhibitors, CPI-17 and PHI-1, by integrin-linked kinase. Biochem J 367: 517-524.

100) Troussard, AA., Mawji, NM., Ong, C., Mui, A., St –Arnaud, R., Dedhar S. (2003) Conditional knock-out of integrin-linked kinase demonstrates an essential role in protein kinase B/Akt activation. JBC 278(25): 22374-8.

101) White, DE., Cardiff, RD., Dedhar, S., Muller, WJ. (2001) Mammary epithelial-specific expression of the integrin-linked kinase (ILK) results in the

induction of mammary gland hyperplasias and tumors in transgenic mice. Oncogene 20(48): 7064-72.

102) Attwell, S., Roskelley, C., Dedhar, S. (2000) The integrin-linked kinase (ILK) suppresses anoikis. Oncogene 19: 3811-3815.

103) Downward, J. (1998) Mechanisms and consequences of activation of protein kinase B/Akt. Curr Opin Cell Biol 10: 262-267.

104) Cardone, MH., Roy, N., Stennicke, HR et al. (1998) Regulation of cell death protease caspase-9 by phosphorylation. Science 282: 1318-1321.

105) Troussard, AA., Tan, C., Yoganathan, TN., Dedhar, S. (1999) Cell-extracellular matrix interactions stimulate the AP-1 transcription factor in an integrin-linked kinase- and glycogen synthase kinase 3-dependent manner. Mol Cell Biol 19: 7420-7427.

106) Tan, C., Costello, P., Sanghera, J., Dominguez, D., Baulida, J., de Herreros, AG., Dedhar, S. (2001) Inhibition of integrin linked kinase (ILK) suppresses beta-catenin-Lef/Tcf-dependent transcription and expression of the E-

cadherin repressor, snail, in APC-/- human colon carcinoma cells. Oncogene 20: 133-140.

107) Kieffer, N., Schmitz, M., Plancon, S., Margue, C., Huselstein, F., Grignard, G., Dippel, W., Nathan M., Giacchi, S., Scheiden, R. (2005) ILK as a potential marker gene to ascertain specific adenocarcinoma cell mRNA isolation from frozen prostate biopsy tissue sections. Int J Oncol 26(6):1549-58.

108) Chung, DH., Lee, JI., Kook, MC., Kim, JR., Kim, SH., Choi, EY., Park, SH., Song, HG. (1998) ILK (beta 1 integrin-linked protein kinase): A novel immunohistochemical marker for Ewing's sarcoma and primitive neuroectodermal tumor. Virchows Arch 433: 113-117.

109) Dai, DL., Markretsov, N., Campos, EI., Huang, C., Zhou, Y., Huntsman D., Martinka, M., Li, G. (2003) Increased expression of integrin-linked kinase is correlated with melanoma progression and poor patient survival. Clin Can Res 9(12): 4409-14.

110) Graff, JR., Deddens, JA., Konicek, BW, Colligan, BM., Hurst, BM., Carter, HW, Carter, JH. (2001) Integrin-linked kinase expression increases with prostate tumor grade. Clin Can Res 7: 1987-1991.

111) Berx, G., Van Roy, F. (2001) The E-cadherin/catenin complex: An important gatekeeper in breast cancer tumorigenesis and malignant proression. Breast Can Res 3: 289-293.

112) Marotta, A., Tan, C., Gray, V., Malik, S., Gallinger, S., Sanghera, J., Dupuis, B., Owen, D., Dedhar, S., & Salh, B. (2001) Dysregulation of integrin-linked kinase (ILK) signaling in colonic polyposis. Oncogene 20: 6250-6257.

113) Wang, SC., Makino, K., Xia, W., Kim, JS., Im, SA., Peng, H., Mok, SC., Singletary, SE., Jung, MC. (2001) DOC-2/hDab-2 inhibits ILK activity and induces anoikis in breast cancer cells through an Akt-independent pathway. Oncogene 20: 6960-6964.

114) Takada, T., Noguchi, T., Inagaki, K., Hosooka, T., Fukunaga, K., Yamao, T., Ogawa, W., Matozaki, T., Kasuga, M. (2002) Induction of apoptosis by stomach cancer-associated protein-tyrosine phosphatase-1 (SAP-1). J Biol Chem 277: 34359-34366.

115) Leung-Hagesteijn, C., Mahendra, A., Naruszewicz, I., Hannigan, GE (2001) Modulation of integrin signal transduction by ILKAP, a protein phosphatase 2C associating with the integrin-linked kinase, ILK1. EMBO J 20(9):2160-70.

116) Chou, T-C., and Talalay, P. (1983) Analysis of combined drug effects: A new look at a very old problem. Trends Pharmacol Sci 4: 450-454.

117) Greco, WR., Bravo, G., Parsons, JC. (1995) The Search for Synergy: A Critical Review from a Response Surface Perspective. The Amer Soc Pharm Exp Ther 47(2): 332-338.

118) Zhao, L., Wientjes, GM., Au, JL-S. (2004) Evaluation of Combination Chemotherapy. 10:7994-8004.

119) Chou, T-C. (1974) Relationships between inhibition constants and fractional inhibitions in enzyme-catalyzed reactions with different numbers of reactants, different reaction mechanisms, and different types of mechanisms of inhibition. Mol Pharmacol 10: 235-247.

120) Chou, T.C. (1976) Derivation and properties of Michaelis-Menten type and Hill type equeations for reference ligands. J Theoret Biol 65: 345-356.

121) Gorre, ME., Mohammed, M., Ellwood, K., Hsu, N., Paquette, R., Rao, N., Sawyers, CL. (2001) Clinical Resistance to STI-571 Cancer Therapy Caused by BCR-ABL Gene Mutation or Amplification. Science 293: 876-880.

122) Barthe, C., Cony-Makhoul, P., Melo, JV., Reiffers Francois-Xavier Mahon, J., Hochhaus, A., Kreil, S., Corbin, A., Rosee, PL., Lahaye, T., Berger, U., Cross, NCP., Linkesch, W., Druker, BJ., Hehlmann, R., Passerini, CG., Corneo, G., D'Incalci, M., Gorre, M., Shah, N., Ellwood, K., Nicoll, J., Sawyers, CL. (2001) Roots of Clinical Resistance to STI-571 Cancer Therapy. Science 21: 2163.

123) Edwards, LA., Shabbits, J., Bally, MB., Dedhar, S. (2004) Integrin-linked kinase (ILK) in combination molecular targeting: Cancer Treatment and Research, Kluwer, NY.

124) Lopez-Ilasaca, M., Crespo, P., Pellici, PG., Gutkind, JS., Wetzker, R. (1997) Linkage of G protein-coupled receptors to the MAPK signaling pathway through PI 3-kinase γ. Science 275: 394-397.

125) Nelson, JM., Fry, D. (2001) AKT, MAPK (Erk1/2), and p38 Act in Concert to Promote Apoptosis Response to ErbB Receptor Family Inhibition. JBC 276(18): 14842-14847.

126) Delecommenne, M., Tan C., Gray, V., Rue, L., Woodgett, J., Dedhar, S. (1998) Phosphoinositide-3-OH kinase-dependent regulation of glycogen synthase

kinase 3 and protein kinase B/AKT by the integrin-linked kinase. Proc Natl Acad Sci USA 95: 11211-11216.

127) Marotta, A., Parhar, K., Owen, D., Dedhar, S., Salh, B. (2003) Characterisation of integrin-linked kinase siganlling in sporadic human colon cancer. BJC 88: 1755-1762.

128) Tan C, Cruet-Hennequart S, Troussard A, Fazli L, Costello P, Sutton K, Wheeler J, Gleave M, Sanghera J, Dedhar S. (2004) Regulation of tumor angiogenesis by integrin-linked kinase (ILK) Can Cell 5(1):79-90.

129) Wang, SI., Puc, J., Li, J., Bruce, JN., Cairns, P., Sidransky, D. (1997) Somatic mutations of PTEN in glioblastoma multiforme Can Res 57: 4183-4186.

130) Choe, G., Horvath ,S., Cloughesy, TF., Crosby, K., Seligson, D., Palotie, A., Inge, L., Smith, BL., Sawyers, CL., Mischel, PS. (2003) Analysis of the Phosphatidylinositol 3'Kinase Signaling Pathway in Glioblastoma Patients in Vivo. Can Res 63:2742-2746.

131) Ermoian, RP., Furniss, CS., Lamborn, KR., Basila, D., Berger, MS., Gottschalk, AR., Nicholas, MK., Stokoe, D., Haas-Kogan, DA. (2002)

Dysregulation of PTEN and Protein Kinase B Is Associated with Glioma Histology and Patient Survival. Clin Can Res 8:1100-1106.

132) Alley, MC., Scudiero, DA., Monks, A., Hursey, ML., Czerwinski, MJ., Fine, DL., Abbott, BJ., Mayo, JG., Shoemaker, RH., Boyd, MR. (1988) Feasibility of drug screening with panels of human tumor cell lines using a microculture tetrazolium assay. Can Res 48: 589-601.

133) Xiong, Y., Zhang, H., Beach, D. (1993) Subunit rearrangement of the cyclin-dependent kinases is associated with cellular transformation. Genes Dev 7:1572-1583.

134) Parker RL, Huntsman DG, Lesack DW, et al. (2002) Assessment of interlaboratory variation in the immunohistochemical determination of estrogen receptor status using a breast cancer tissue microarray. Am J Clin Pathol 117: 723-8.

135) Liu CL, Prapong W, Natkuman Y, et al. (2002) Software tools for high-throughput analysis and archiving of immunohistochemistry staining data obtained with tissue microarrays. Am J Pathol 161: 1557-64.

136) Evans, SM., Joiner B., Jenkins, WT., Laughlin, KM., Lord, EM., Koch, CJ. (1995) Identification of hypoxia in cells and tissues of epigastric 9L rat glioma using EF5 [2-(2-nitro-1H-imidazol-l-yl)-N-(2,2,3,3,3-pentafluoropropyl) acetamide]. Br J Cancer 72: 875-882.

137) Li, DM., Sun, H. (1997) TEP1, encoded by a candidate tumor suppressor locus, is a novel protein tyrosine phosphatase regulated by transforming growth factor beta. Can Res 57: 2124-2129.

138) Li, J., Yen, C., Liaw, D., Podyspaniana, K., Bose, S., Wang, SI., Puc, J., Miliaresis, C., Rodgers, L., McCombie, R., et al. (1997) PTEN, a Putative Protein Tyrosine Phosphatase Gene Mutated in Human Brain, Breast, and Prostate Cancer. Science 275: 1943-1947.

139) Steck, PA., Pershouse, MA., Jasser, SA., Yung, WK., Lin, H., Ligon, AH., Langford, LA., Baumgard, ML., Hattier, T., Davis, T., et al. (1997) Identification of a candidate tumour suppressor gene, MMAC1, at chromosome 10q23.3 that is mutated in multiple advanced cancers. Nat Genet 15: 356-362.

140) Katso, R., Okkenhaug, K., Ahmadi, K., White, S., Timms, J., & Waterfield, MD. (2001) CELLULAR FUNCTION OF PHOSPHOINOSITIDE 3-

KINASE: Implications for Development, Immunity, Homeostasis, and Cancer Ann Rev CelL Dev Biol 17:615-675.

141) Liaw, D., Marsh, DJ., Li, J., Dahia, PL., Wang, SI., Zheng, Z., Bose, S., Call, KM., Tsou, HC., Peacocke, M., et al. (1997) Germline mutations of the PTEN gene in Cowden disease, an inherited breast and thyroid cancer syndrome. Nat Genet 16: 64-67.

142) Nelen, MR., can Staveren, WC., Peeters, EA., Hassel, MB., Gorlin, RJ., Hamm, H., Lindboe, CF., Fryns, JP., Sijmons, RH., Woods, DG., et al. (1997) Germline mutations in the PTEN/MMAC1 gene in patients with Cowden disease. Hum Mol Genet 6: 1383-1387.

143) Tsou, HC., Teng, DH., Ping, XL., Brancolini, V., Dacis, T., Hu, R., Xie, XX., Gruener, AC., Schrager, CA., Christiano, AM., et al. (1997) MMAC1 Mutations in Early-Onset. Breast Cancer Am J Hum Genet 61: 1036-1043.

144) Ermoian, RP., Furniss, CS., Lamborn, KR., Basila, D., Berger, MS., Gottschalk, AR., Nicholas, MK., Stokoe, D., Haas-Kogan, DA. (2002) Dysregulation of PTEN and Protein Kinase B Is Associated with Glioma Histology and Patient Survival. Clin Can Res 8: 1100-1106.

145) Choe, G., Horvath, S., Cloughesy, TF., Crosby, K., Seligson, D., Palotie, A., Inge, L., Smith, BL., Sawyers, CL., Mischel, PS. (2003) Analysis of the Phosphatidylinositol 3'-Kinase Signaling Pathway in Glioblastoma Patients in Vivo Can Res 63: 2742-2746.

146) Tu, Y., Li, F., Wu, C. (1998) Nck-2, a novel Src homology2/3-contatining adaptor protein that interacts with the LIM-only protein PINCH and components of growth factor receptor kinase-signaling pathways Mol Biol Cell 9: 3367-3382.

147) Novak, A., Hsu, SC., Leung-Hagesteijn, C., Radeva, G., Papkoff, J., Montesano, R., Roskelley, C., Grosschedl, R., Dedhar, S. (1998) Cell adhesion and the integrin-linked kinase regulate the LEF-1 and beta-catenin signaling pathways. Proc Natl Acad Sci USA 95: 4374-4379.

148) Ishii T, Furuoka H, Muroi Y, Nishimura M. (2003) Inactivation of integrin-linked kinase induces aberrant tau phosphorylation via sustained activation of glycogen synthase kinase 3beta in N1E-115 neuroblastoma cells. J Biol Chem 278(29): 26970-26975.

149) Obara, S., Nakata, M., Takeshima, H., Katagiri, H., Asano, T., Oka, Y., Maryuma, I., Kuratsu, J. (2004) Integrin-linked kinase regulation of the cell viability in PTEN mutant glioblastoma and in vitro inhibition by the specific COX-2 inhibitor NS-398. Can Lett 208(1): 115-122.

150) Knobbe, CB., Merlo, A., Reifenberger, G. (2002) PTEN signaling in gliomas. Neuro-Oncology 4: 196-211.

151) Haas-Koogan, DA., Shaley, N., Wong, M., Mills, G., Yount, G., Stokoe, D. (1998) PKB/Akt Activity is elevated in Glioblastoma Cell Lines due to Mutation of PTEN. Curr Biol 8: 1195-1198.

152) Stolarov, J., Chang, K., Reiner, A., Rodgers, L., Hannon, GJ., Wigler, MH., Mittal, V. (2002) Design of a retroviral-mediated ecdysone-inducible system and its application to the expression profiling of the PTEN tumor suppressor. Proc Natl. Acad Sci USA 98(23): 13043-13048.

153) Tan, C., Mui, A., Dedhar, S. (2002) Integrin-linked Kinase Regulates Inducible Nitric Oxide Synthase and Cyclooxygenase-2 Expression in an NF-κB-dependent Manner. J Biol Chem 277(5): 3109-3116.

154) Edwards, L., Thiessen, B., Yan, H., Dedhar, S., Bally, M. (2003) Inhibitory effects of an antisense oligonucleotide targeting integrin-linked kinase (ILK) and its potential use in combination therapy for the treatment of glioblastoma multiforme [abstract]. Neuro-Oncology 5(4): 300.

155) Hu, Y., Cherton-Horvat, G., Dragowska, V., Baird, S., Korneluk, RG., Durkin, JP., Mayer, LD., LaCasse, EC. (2003) Antisense Oligonucleotides Targeting XIAP Induce Apoptosis and Enhance Chemotherapeutic Activity against Human Lung Cancer Cells *in Vitro* and *in Vivo*. Clin Can Res 9: 2826-2836.

156) Waterhouse, DN., Dragowska, WH., Gelmon, KA., Mayer, LD., Bally, MB. (2004) Pharmacodynamic Behaviour of Liposomal Antisense Oligonucleiotides Targeting Her-2/neu and Vascular Endothelial Growth Factor in an Ascitic MDA435/LCC6 Human Breast Cancer Model. Can Bio & Ther 3(2): 197-204.

157) Park, M-J., Kim, M-S., Park, I-C., Kang, H-S., Yoo, H., Park, S-H, et al. (2002) PTEN Suppresses Hyaluronic Acid-induced Matrix Metalloproteinase-9 Expression in U87MG Glioblastoma Cells through Focal Adhesion Kinase Dephosphorylation. Can Res 62: 6318-6322.

158) Cheney, W., Neuteboom, STC., Vaillancourt, M-T., Ramachandra, M., Bookstein, R. (1999) Adenovirus-mediated Gene Transfer of *MMAC1/PTEN* to Glioblastoma Cells Inhibits S Phase Entry by the Recruitment of $p27^{Kip1}$ into Cyclin E/CDK2 Complexes. Can Res 59: 2318-2323.

159) Edwards, LA., Thiessen, B., Dragowska, WH., Hu, Y., Yeung, JHF., Dedhar, S., Bally, MB. Combined Inhibition of the PI3K/Akt and Ras/MAPK pathways results in synergistic effects in glioblastoma cells. Mol Can Ther (in press)

160) Cruet-Hennequart, S., Maubant, S., Luis, J., Gauduchon, P., Staedel, C., Dedhar, S. (2003) α_v integrins regulate cell proliferation through integrin-linked kinase (ILK) in ovarian cancer cells. Oncogene 22: 1688-170.

161) Sauter, G., Maeda, T., Waldman, FM., Davis, RL., Fererstein, BG. (1996) Patterns of epidermal growth factor receptor amplification in malignant gliomas. Am J Pathol 148: 1047-1053.

162) Duerr, EM., Rollbrocker, B., Hayashi, Y., et al. (1998) Cytogenetic and loss of heterozygosity studies have suggested the presence of at least one tumor

suppressor gene on chromosome 10 involved in the formation. Oncogene 16: 2259-2264.

163) Schmidt, EE., Ichimura, K., Goike, HM., Moshref, A., Liu, L., Collins VP. (1998) Mutational profile of the PTEN gene in primary human astrocytic tumors and cultivated xenografts. J Neuropathol Exp Neurol 58: 1170-1183.

164) Rasheed, BK., McLendon, RE., Parsons, R., Friedman, HS., Friedman, AH., Friedman, HS., et al. (1997) PTEN gene mutations are seen in high-grade but not in low-grade gliomas. Cancer Res 57: 4187-4190.

165) Lackey, K., Cory, M., Davis, R., et al. (2000) The discovery of potent cRaf1 kinase inhibitors. Bioorg Med Chem Lett 10: 223-226.

166) Favata, MF., Horiuchi, KY., Manos, EJ., et al. (1998) Identification of a Novel Inhibitor of Mitogen-activated Protein Kinase Kinase. J Biol Chem 273(29): 18623-18632.

167) DeSilva, DR., Jones, E A., Favata, M F., et al. (1998) Inhibition of Mitogen-Activated Protein Kinase Kinase Blocks T Cell Proliferation But Does Not Induce or Prevent Anergy. J Immun 160: 4175-4181.

168) Rajasekhar, VK., Viale, A., Socci, ND., et al. (2003) Oncogenic Ras and Akt signaling contribute to glioblastoma formation by differential recruitment of existing mRNAs to polysomes. Mol Cell 12(4): 889-901.

169) Chou, T-C., Talalay, P. (1977) A simple generalized equation for the analysis of multiple inhibitions of Michaelis-Menten kinetic systems. J Biol Chem 252: 6438-6442.

170) Chou, R., Talalay, P. (1984) Quantitative analysis of dose- effecting relationships: The combined effects of multiple drugs or enzyme inhibitors. Adv Enzyme Regul 22: 27-55.

171) Hoffmann, MK., Fodero-Tavoletti, MT., Mishima, K., et al. (2001) The protein Tyrosine Phosphatase TCPTP Suppresses the Tumorigenicity of Glioblastoma Cells Expressing a Mutant Epidermal Growth Factor Receptor. J Biol Chem 276(49): 46313-46318.

172) Heimberger, AB., Learn, CA., Archer, GE., et al. (2002) Brain Tumors in Mice are Susceptible to Blockade of Epidermal Growth Factor Receptor (EGFR)

with the Oral, Specific, EGFR-Tyrosine Kinase Inhibitor ZD1839 (Iressa). Clin Can Res 8: 3496-3502.

173) Ekstrand, AJ., James, CD., Cavenee, WK., et al. (1991) Genes for epidermal growth factor receptor, transforming growth factor alpha, and epidermal growth factor and their expression in human gliomas in vivo. Cancer Res 51(8): 2164-2172.

174) Mottram, JC. (1936) Factor of importance in radiosensitivity of tumors. Br J Radiol 9:606-614.

175) Tannock, I. (1982) Response of aerobic and hypoxic cells in a solid tumor to Adriamycin and cyclophosphamide and interaction of the drugs with radiation. Can Res 42: 4921-4926.

176) Brown, I., Giaccia, AJ. (1994) Tumor hypoxia: The picture has changed in the 1990's. Int J Rad Biol 65: 95-102.

177) Folkman, J. (1998) Antiangiogenic gene therapy. PNAS 95: 9064-9066.

178) Lee, AV. (2004) Location, location, location: regulation of breast cancer progression by the microenvironment. Breast Can Res 6: 279-280.

179) Jiang, BH., Jiang, G., Zheng, JZ., Lu, Z., Hunter, T., Vogt, PK. (2001) Phosphatidylinositol 3-kinase signaling controls levels of hypoxia-inducible factor 1. Cell Growth Differ 12: 363-369.

180) Fukuda, R., Hirota, K., Fan, F., Jung, YD., Ellis, LM., Semenza, GL. (2002) Insulin-like growth factor 1 induces hypoxia-inducible factor 1-mediated vascular endothelial cell growth factor expression, which is depedent on MAP kinase and PI-3-kinase signaling in colon cancer cells. J Biol Chem 277: 38205-38211.

181) Edwards, L., Thiessen, B., Dragowsak, WH., Daynard, T., Bally, MB, Dedhar S. (2005) Inhibition of ILK in PTEN-mutant human glioblastomas inhibits PKB/Akt activation, induces apoptosis, and delays tumor growth. Oncogene 24: 3596-3605.

182) Yau, CYF., Wheeler, JJ., Sutton, KL., Hedley, DW. (2005) Inhibition of Integrin-Linked Kinase by a Selective Small Molecule Inhibitor, QLT0254, Inhibits the PI3K/PKB/mTOR, Stat3, and FKHR Pathways and Tumor Growth,

and Enhances Gemcitabine-Induced Apoptosis in Human Orthotopic Primary Pancreatic Cancer Xenografts. Can Res 65: 1497-1504.

183) Younes, MN., Kim Seungwon, K., Yigitbasi, OG., Mandal, M., Jasser, SA., Schiff, BA., Bucana, C, El-Naggar, A., Bekele, BN., Mills, GB., Myers, JN. Integrin-Linked Kinase Is a Potential Therapeutic target for Anaplastic Thyroid Cancer (in press).

184) Pore, N., Liu, S., Haas-Kogan, DA., O'Rourke, DM, Maity, A. (2003) PTEN Mutation and Epidermal Growth Factor Receptor Activation Regulate Vascular Endothelial Growth Factor (VEGF) mRNA Expression in Human Glioblastoma Cells by Transactivating the Proximal VEGF Promoter. Can Res 63: 236-241.

185) Maity, A., Pore, N., Lee, J., Solomon, D., O'Rourke, DM. (2000). Epidermal Growth Factor Receptor Transcriptionally Up-Regulates Vascular Endothelial Growth Factor Expression in Human Gliobalstoma Cells via a Pathway involving Phosphatidylinositol 3'-Kinase and Distinct from That Induced by Hypoxia. Can Res 60: 5879-5886.

186) Brat, DS., Van Meir, EG. (2004) Vaso-Occlusive and prothrombotic mechanisims associated with tumor hypoxia, necrosis, and accelerated growth in glioblastoma. Lab Invest 84(4): 397-405.

187) Knisely, JP., Rockwell, S. (2002) Importance of hypoxia in the biology and treatment of brain tumors. Neuroimaging Clin North Am 12: 525-36.

188) Marti, HJ., Bernaudin, M., Bellail, A, et al. (2000) Hypoxia-induced vascular endothelial growth factor expression precedes neovascularization after cerebral ischemia. Am J Pathol 156: 965-76.

189) Zagzag, D., Zhong, H., Scalzitti, JM., Laughner, E., Simons, JW., Semenza, GL. (2000) Expression of hypoxia-inducible factor 1 alpha in brain tumors: association with angiogenesis, invasion, and progression. Cancer (Phila) 88: 2606-18.

190) Ziemer, L., Koch, C., Maity, A., Magarelli, D., Horan, A., Evans, S. (2001) Hypoxia and VEGF mRNA expression in human tumors. Neoplasia 6: 500-08.

191) Brown, JM. (1999) The hypoxic cell: a target for selective cancer therapy-eighteenth Bruce F. Cain Memorial Award lecture. Can Res 59: 5863-5870.

192) Shannon, AM., Bouchier-Hayes, DJ., Condron, CM., Toomey D. (2003) Tumor hypoxia, chemotherapeutic resistance and hypoxia-related therapies. Cancer Treat Rev 29: 297-307.

193) Kaur, B., Tan, C., Brat, DJ., Post, DE., Van Meir, E. (2004) Genetic and hypoxic regulation of angiogenesis in gliomas. J Neuro-Oncology 70: 229-243.

194) Rege, TA., Fears, CY., Gladson, CL. (2005) Endogenous inhibitors of angiogenesis in malignant gliomas: Nature's antiangiogenic therapy. Neuro-Oncology 7(2): 4-119.

195) Brem, H. (1990) Modern treatment of brain tumors. Maryland Med J 39: 351-354.

196) Weingart, J., Brem, H. (1992) Biology and therapy of glial tumors. Curr Opin Neurol Neurosurg 5: 808-812.

197) Avgeropoulos, NG., Batchelor, TT. (1999) New Treatment Strategies for Malignant Gliomas. The Oncologist 4(3): 209-224.

198) Heimberger, AB., Hlatlky, R., Yang, D., Weinberg, J., Gilbert, M., Sawaya, R., Aldape, K. (2005) Prognostic Effect of Epidermal Growth Factor Receptor and EGFRvIII in Glioblastoma Patients. Clin Can Res 11: 1462-1466.

199) Senger, DL., Tudan, C., Guiot, MC., Mazzoni, IE., Molenkamp, G., LeBlanc, R., Antel, J., Olivier, A., Snipes, GJ., Kaplan, DR. (2002) Suppression of Rac Activity Induces Apoptosis of Human Glioma Cells but not Normal Human Astrocytes. Can Res 62: 2131-2140.